

One-Step Abductive Multi-Target Learning with Diverse Noisy Samples and Its Application to Tumour Segmentation for Breast Cancer

Yongquan Yang¹, Fengling Li^{1,2}, Yani Wei^{1,2}, Jie Chen¹, Ning Chen³, Mohammad H. Alobaidi⁴, Hong Bu^{1,2}

1. Institute of Clinical Pathology, West China Hospital, Sichuan University, Chengdu, China

2. Department of Pathology, West China Hospital, Sichuan University, Chengdu, China

3. School of Electronics and Information, Xi'an Polytechnic University, Xi'an, China

4. Department of Civil Engineering, McGill University, Montreal, Canada

Abstract

Recent studies have demonstrated the effectiveness of the combination of machine learning and logical reasoning, including data-driven logical reasoning, knowledge driven machine learning and abductive learning, in inventing advanced technologies for different artificial intelligence applications. One-step abductive multi-target learning (OSAMTL), an approach inspired by abductive learning, via simply combining machine learning and logical reasoning in a one-step balanced multi-target learning way, has as well shown its effectiveness in handling complex noisy labels of a single noisy sample in medical histopathology whole slide image analysis (MHWSIA). However, OSAMTL is not suitable for the situation where diverse noisy samples (DiNS) are provided for a learning task. In this paper, giving definition of DiNS, we propose one-step abductive multi-target learning with DiNS (OSAMTL-DiNS) to expand the original OSAMTL to handle complex noisy labels of DiNS. Applying OSAMTL-DiNS to tumour segmentation for breast cancer in MHWSIA, we show that OSAMTL-DiNS is able to enable various state-of-the-art approaches for learning from noisy labels to achieve more rational predictions. We released a model pretrained with OSAMTL-DiNS for tumour segmentation in HE-stained pre-treatment biopsy images in breast cancer, which has been successfully applied as a pre-processing tool to extract tumour-associated stroma compartment for predicting the pathological complete response to neoadjuvant chemotherapy in breast cancer.

Key words

Abductive learning; Machine learning; Logical reasoning; Tumour segmentation for breast cancer.

1 Introduction

Perception and cognition, two instincts of human beings for information processing in problem-solving, can be respectively realized by machine learning (Wichmann et al., 2005) and logical reasoning (Rips, 1983). Usually, the paradigm for information processing of machine learning is data-driven, i.e., machine learning constructs the flow of information processing based on collected data. Whereas, the paradigm for information processing of logical reasoning is knowledge-driven, i.e., logical reasoning constructs the flow of information processing based on accumulated knowledge. In most history of artificial intelligence research, machine learning and logical reasoning have been separately developed (Zhou, 2019), due to their significant differences in the representation for the flow of information processing. In recent years, however, with the argument that human beings perform information processing in problem-solving based on the leverage of both perception and cognition, researchers have shown that more effective flows of information processing can be constructed via the combination of machine learning and logical reasoning (D’Amato et al., 2012; D. Li et al., 2020; Zhou, 2019). Existing efforts of combining machine learning and logical reasoning for advanced artificial intelligence technologies can be summarized as in data-driven logical reasoning (DDLRL) (D’Amato et al., 2012), knowledge-driven machine learning (KDML) (D. Li et al., 2020) and abductive learning (ABL) (Zhou, 2019).

DDLRL maintains logical reasoning as the dominant paradigm for information processing, in which some data-driven flows constructed by machine learning serves as intermediate components. KDML maintains machine learning as the dominant paradigm for information processing, in which some knowledge-driven flows constructed by logical reasoning serves as intermediate components. DDLRL prioritizes logical reasoning over machine learning while KDML prioritizes machine learning over logical reasoning. As a result, machine learning and logical reasoning are not fully exploited in DDLRL and KDML. To overcome this problem, ABL unifies machine learning and logic reasoning in a balanced way and targets at achieving mutual benefit between machine learning and logical reasoning in an iterative strategy.

Apart from the fact that the original paradigm of ABL has been demonstrated to be effective in some real-world applications (Dai et al., 2019; Huang et al., 2020), recent studies (Yang, Yang, Chen, et al., 2020; Yang, Yang, Yuan, et al., 2020) show approach that simply exploits the concept of unifying machine learning and logical reasoning in a balanced way from ABL is as well fairly effective in specific application. This approach is so called one-step abductive multi-target learning (OSAMTL) (Yang, Yang, Chen, et al., 2020), since it only combines machine learning and logical reasoning in a one-step balanced way without targeting at a mutual benefit in an iterative strategy. OSAMTL targets at alleviating the situation where it is often difficult for experts to manually achieve the accurate ground-truth labels, which leads to labels with complex noisy for a learning task (aka, learning from noisy labels (Frénay & Verleysen, 2014; Karimi et al., 2020; Song et al., 2022)). Based on the concept of unifying machine learning and logical reasoning in a balanced way from ABL, OSAMTL exploits multiple inaccurate targets abduced from a single noisy sample via logical reasoning to

achieve more reasonable predictions via multi-target learning. On a *H. pylori* segmentation task in medical histopathology whole slide images (Hanna et al., 2020) analysis (MHWSIA) (Yang, Yang, Chen, et al., 2020; Yang, Yang, Yuan, et al., 2020), for the first time, OSAMTL has been reported to possess potentials in handling complex noisy labels in MHWSIA. More details about existing approaches in combination of machine learning and logical reasoning can be found in section 2.1.

Since it is based on a single noisy sample, OSAMTL is naturally not suitable for the situation where diverse noisy samples (DiNS) are provided for a learning task. DiNS contain at least two types of noisy samples, where diversity exists between any two non-repeating noisy samples. Due to this property, DiNS can constitute a noisy data that have very complex noise. In this paper, formally giving definition of DiNS, we propose one-step abductive multi-target learning with DiNS (OSAMTL-DiNS) and provide analyses of OSAMTL-DiNS compared with the original OSAMTL. Being able to handle DiNS, OSAMTL-DiNS only require very inaccurately labelled (complex noisy) samples to produce a predictive model. This property forms the major advantage of OSAMTL-DiNS, since the data preparation can be much less labour-intensive though at least two types of noisy samples are needed. Thus, OSAMTL-DiNS is suitable to address some tasks in the field of medical analysis where the problem of low consistency always exists. Low consistency, here in the context of DiNS, can refer to that large is the difference between the noisy distributions of two different noisy samples prepared by experts for a same medical analysis task, which usually results in more complex noisy in data annotations. More details about DiNS and the proposed OSAMTL-DiNS can be found in section 2.2.

Quantitative evaluation of tumour in breast cancer can provide clues important to subsequent therapy of breast cancer (Pu et al., 2020; Yau et al., 2022). The key point is to achieve tumour segmentation for breast cancer (TSfBC), which is a fundamental key technique that can be leveraged to calculate the tumour-stroma ratio which has been proven to be a prognostic factor in breast cancer (de Kruijf et al., 2011). Existing deep learning (LeCun et al., 2015) enhanced approaches that can be leveraged to achieve TSfBC can be classified into two schemes: learning with noisy-free/accurate labels (Bhattacharjee et al., 2022; Priego-Torres et al., 2020, 2022) and learning with noisy/inaccurate labels (Diao et al., 2022; G. Xu et al., 2019; Y. Xu et al., 2014). The first type of scheme adopts the supervised learning paradigm. However, due to the difficulty in accurately labelling the tumour in breast cancer on whole slide images, very limited noisy-free data is often available, which will inevitably limit the generalization of the prediction model. The second type of scheme adopts the weakly supervised learning paradigm, which avoids the problem of the difficulty in obtaining noisy-free data faced by the first type of scheme. However, the popular strategy of using image patch-level labels to achieve pixel-level segmentation (Diao et al., 2022; G. Xu et al., 2019; Y. Xu et al., 2014) has the drawbacks in MHWSIA that the work load of image patch-level labelling can still be very massive due to the large size of whole slide images and the prediction results can be very coarse at high resolution.

To alleviate this situation, in this paper, we applied the proposed OSAMTL-DiNS to TSfBC in MHWSIA. As OSAMTL-DiNS only requires very inaccurately labelled

(complex noisy) samples, the difficulty in pixel-level labelling for the task of TSfBC in MHWSIA is considerably reduced. Referring to the proposed OSAMTL-DiNS, we implemented an OSAMTL-DiNS-based image semantic segmentation solution for TSfBC in MHWSIA and conducted extensive experiments to demonstrate the potentials of OSAMTL-DiNS in MHWSIA. More details about the application of OSAMTL-DiNS to TSfBC and corresponding strategies for experimental conduction can be found in section 2.3 and section 2.4.

Experiment results show that OSAMTL-DiNS is able to enable various existing approaches for learning from noisy labels (Algan & Ulusoy, 2021; Frénay & Verleysen, 2014; Sukhbaatar & Fergus, 2014), including naively learning from noisy labels, Forward, Backward (Patrini et al., 2017), Boost-Hard, Boost-Soft (Arazo et al., 2019; Reed et al., 2015), D2L (Ma et al., 2018), SCE (Wang et al., 2019), Peer (Liu & Guo, 2020), DT-Forward (Yao et al., 2020), and NCE-SCE (Ma et al., 2020), to achieve more rational predictions. We also released a model pretrained with OSAMTL-DiNS for tumour segmentation in HE-stained pre-treatment biopsy images in breast cancer, which has been successfully applied as a pre-processing tool to extract tumour-associated stroma compartment for predicting the pathological complete response to neoadjuvant chemotherapy in breast cancer (F. Li et al., 2022).

In summary, the contributions of this work are as follows:

- One-step abductive multi-target learning with diverse noisy samples (OSAMTL-DiNS) is proposed, which only require very inaccurately labelled (complex noisy) samples to produce a predictive model.
- The proposed OSAMTL-DiNS is applied to address the task of tumour segmentation for breast cancer (TSfBC) in medical histopathology whole slide image analysis (MHWSIA).
- Extensive experiments show that the proposed OSAMTL-DiNS is able to enable various existing approaches for learning from noisy labels to achieve more rational predictions in the task of TSfBC in MHWSIA, which reflects the potential effectiveness of OSAMTL-DiNS in handling complex noisy labels in MHWSIA.
- A model pretrained with OSAMTL-DiNS for tumour segmentation in HE-stained pre-treatment biopsy images in breast cancer is released and has been successfully applied as a pre-processing tool to extract tumour-associated stroma compartment for predicting the pathological complete response to neoadjuvant chemotherapy in breast cancer, which reflects the potentials of using OSAMTL-DiNS to help building basic tools for MHWSIA.

2 Material and Methods

This section is structured as follows. In section 2.1, we formalize existing methodologies for combining machine learning and logical reasoning and summarize their differences. In section 2.2, we present the methodology of the proposed OSAMTL-DiNS and corresponding summaries compared with the original OSAMTL. In section 2.3, we apply the proposed OSAMTL-DiNS to tumour segmentation for

breast cancer (TSfBC) in MHWSIA. In section 2.4, on the basis of the implemented application of OSAMTL-DiNS to TSfBC, we present the experimental strategies for conducting extensive experiments to investigate the contributions of OSAMTL-DiNS in handling complex noisy labels.

2.1 Combination of Machine Learning and Logical Reasoning

2.1.1 Preliminary

Machine learning Commonly for a machine learning task in artificial intelligence research, a collected dataset containing certain instances (x) and corresponding labels (y) for the task is provided. The objective of the task here is to estimate a predictive function f parameterized by θ ($f(\theta)$) that can map x to corresponding predictions ($f(x; \theta)$) which are as correct as possible compared with y . Formally, the objective of a machine learning task can be expressed as

$$\tilde{f}(\tilde{\theta}) = \arg \min_{f \in \Theta_f, \theta \in \Theta_\theta} ||f(x; \theta) - y||,$$

where Θ_f is the function space of f , Θ_θ is the parameter space of θ corresponding to f and $||f(x; \theta) - y||$ denotes the error between $f(x; \theta)$ and y .

Logical reasoning Commonly for a logical reasoning task in artificial intelligence research, a collected dataset containing certain instances (x) and corresponding labels (y) for the task and a collected knowledge base (kb) containing various prior knowledge or facts about the task are both provided. The objective of the task here is to search a reasoning path r that can from x and y draw conclusions ($r(< x, y >)$) consistent with some knowledge or facts in kb . Formally, the objective of a logical reasoning task can be expressed as

$$\tilde{r} = \arg \text{search}_{r \in \Theta_r} r(< x, y >) \cong kb,$$

where Θ_r is the reasoning path space of r and $r(< x, y >) \cong kb$ denotes $r(< x, y >)$ is consistent with kb .

2.1.2 Data-driven logical reasoning

Data-driven logical reasoning (DDLRL) (D'Amato et al., 2012) adapts machine learning to logical reasoning. Formally, the objective of a DDLRL task can be expressed as

$$\tilde{r} = \arg \text{search}_{r \in \Theta_r} r(< x, \tilde{f}(x; \tilde{\theta}) >) \cong kb, \quad (1)$$

where $\tilde{f}(\tilde{\theta}) = \arg \min_{f \in \Theta_f, \theta \in \Theta_\theta} ||f(x; \theta) - y||$.

2.1.3 Knowledge-driven machine learning

Knowledge-driven machine learning (KDML) (D. Li et al., 2020) adapts logical reasoning to machine learning. Formally, the objective of a task can be expressed as

$$\tilde{f}(\tilde{\theta}) = \arg \min_{f \in \Theta_f, \theta \in \Theta_\theta} ||f(\tilde{r}(< x, y >); \theta) - y||, \quad (2)$$

where $\tilde{r} = \arg \text{search}_{r \in \Theta_r} r(< x, y >) \cong kb$.

2.1.4 Abductive learning

Abductive learning (ABL) (Zhou, 2019) has two important concepts: 1) unifying machine learning and logic reasoning in a balanced way, and 2) targeting at achieving

a mutual benefit between machine learning and logical reasoning in an iterative strategy. Formally, the objective of a ABL task can be expressed as

$$\begin{cases} \tilde{r}_k = \arg \underset{r \in \Theta_r}{search} r(< x, \tilde{y}_{ml,k} >) \cong kb, \tilde{y}_{ml,k} = \tilde{f}_{k-1}(x; \tilde{\theta}_{k-1}) \\ \tilde{f}_k(\tilde{\theta}) = \arg \underset{f \in \Theta_f, \theta \in \Theta_\theta}{min} ||f(x; \theta) - \tilde{y}_{lr,k}||, \tilde{y}_{lr,k} = \tilde{r}_k(< x, \tilde{y}_{ml,k} >) \end{cases} \quad (3)$$

where $k = 1, \dots, N$ and $\tilde{f}_0(\tilde{\theta}_0)$ can be a pre-trained machine learning model.

2.1.5 One-step abductive multi-target learning

One-step abductive multi-target learning (OSAMTL) (Yang, Yang, Chen, et al., 2020) only combines machine learning and logical reasoning in a one-step balanced multi-target learning way. Formally, the objective of a OSAMTL task can be expressed as

$$\begin{cases} \tilde{r} = \arg \underset{r \in \Theta_r}{search} r(< x, y >) \cong kb \\ \tilde{f}(\tilde{\theta}) = \arg \underset{f \in \Theta_f, \theta \in \Theta_\theta}{min} ||f(x; \theta) - \tilde{y}_{lr}||, \tilde{y}_{lr} = \tilde{r}(< x, y >) = \{t_1, \dots, t_n\} \end{cases} \quad (4)$$

where y can be rough labels provided by experts or predictions of a pre-trained machine learning model, and \tilde{y}_{lr} is a set of multiple inaccurate targets which can be expressed as $\{t_1, \dots, t_n\}$.

2.1.6 Summary

From formula (1), we can note that DDLR prioritizes logical reasoning over machine learning by maintaining logical reasoning as the dominant paradigm for information processing, in which the results produced by machine learning serves as some inputs. From formula (2), we can note that KDML prioritizes machine learning over logical reasoning by maintaining machine learning as the dominant paradigm for information processing, in which the results produced by logical reasoning serves as some inputs. In the paradigms of both DDLR and KDML, machine learning and logical reasoning are not fully exploited by adapting one to the other.

From formula (3), we can note that the results produced by machine learning serve as some inputs of logical reasoning and the results produced by logical reasoning serve as the target of machine learning. This indicates that machine learning and logical reasoning are placed in equal positions in the objective of a ABL task. Iteratively, let $k = 1, \dots, N$, ABL is able to fully exploit machine learning and logical reasoning, which cannot be fulfilled by DDLR or KDML.

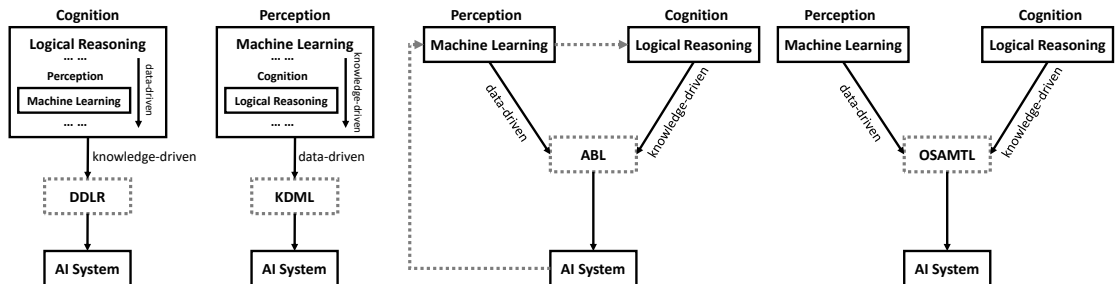


Figure. 1. Summarization for differences of DDLR, KDML, ABL and OSAMTL for the combination of machine learning and logical reasoning.

noisy sample (NLS_*) of the given diverse noisy samples (DNS) have a set of instances and a set of noisy labels respectively.

The diversity of two noisy samples ($Div_{a,b}$) can be evaluated by the differences between their instances and corresponding noisy labels. Formally, the diversity of two noisy samples can be denoted by

$$\begin{aligned} Div_{a,b} &= \text{Differentiate}(NS_a, NS_b) \\ &= \text{Differentiate}(IS_a, IS_b) * \text{Differentiate}(NLS_a, NLS_b). \end{aligned}$$

For simplicity, we define $Div_{a,b} \in [0,1]$, where 1 signifies diversity exists between NS_a and NS_b while 0 indicates the opposite.

Diverse noisy samples (DiNS) have at least two noisy samples, where diversity exists between any two non-repeating noisy samples. Due to this property, DiNS can constitute a noisy data that have very complex noise. Formally, diverse noisy samples can be defined as

$$\begin{aligned} DiNS &= \{NS_1, \dots, NS_d\} = \{\{IS_1, NLS_1\}, \dots, \{IS_d, NLS_d\}\} \\ &= \left\{ \left\{ \{I_{1,1}, \dots, I_{1,n_1}\}, \{NL_{1,1}, \dots, NL_{1,n_1}\} \right\}, \dots, \left\{ \{I_{d,1}, \dots, I_{d,n_d}\}, \{NL_{d,1}, \dots, NL_{d,n_d}\} \right\} \right\} \\ &= \left\{ \left\{ (I_{1,1}, NL_{1,1}), \dots, (I_{1,n_1}, NL_{1,n_1}) \right\}, \dots, \left\{ (I_{d,1}, NL_{d,1}), \dots, (I_{d,n_d}, NL_{d,n_d}) \right\} \right\} \\ &\quad s.t. \quad \forall a, \forall b \in \{1, \dots, d\} \text{ and } a \neq b, \exists Div_{a,b} = 1. \end{aligned}$$

Since

2.2.2 One-step abductive multi-target learning with diverse noisy samples

With the given definition of diverse noisy samples (DiNS), we propose one-step abductive multi-target learning with diverse noisy samples (OSAMTL-DiNS). OSAMTL-DiNS constitutes of four components, including input materials, one-step logical reasoning, target rearrangement and multi-target learning.

Input materials The input materials of OSAMTL-DiNS include some given diverse noisy samples ($DiNS$) and a knowledge base (KB) containing a list of domain knowledge about the true target of a specific task. Referring to the formulations of DNS presented in Section 3.1, the input materials of OSAMTL can be more specifically denoted as follows

$$\begin{aligned} DiNS &= \{NS_1, \dots, NS_d\}, \\ KB &= \{K_1, \dots, K_b\}. \end{aligned}$$

One-step abductive logical reasoning with DiNS With the given $DiNS$ and KB , the one-step logical reasoning procedure of OSAMTL-DiNS, which consists of four substeps, abduces multiple targets containing information consistent with the domain knowledge about the true target of a specific task.

The substep one extracts a list of groundings from the given set of noisy label samples that can describe the logical facts contained in the given diverse noisy samples. Formally, this grounding extract (GE) step can be expressed as

$$\begin{aligned} G &= GE(DiNS; p^{GE}) = \{GE(NS_1; p^{GE_1}), \dots, GE(NS_d; p^{GE_d})\} \\ &= \{G_1 = \{G_{1,1}, \dots, G_{1,r_1}\}, \dots, G_d = \{G_{d,1}, \dots, G_{d,r_d}\}\}. \end{aligned} \quad (5)$$

Via logical reasoning, the substep two estimates the inconsistencies between the extracted groundings G and the domain knowledge in the knowledge base KB . Formally, this reasoning (R) step can be expressed as

$$\begin{aligned} IC &= R(G, KB; p^R) = \{R(G_1, KB; p^{R_1}), \dots, R(G_d, KB; p^{R_d})\} \\ &= \{IC_1 = \{IC_{1,1}, \dots, IC_{1,i_1}\}, \dots, IC_d = \{IC_{d,1}, \dots, IC_{d,i_d}\}\}. \end{aligned} \quad (6)$$

The substep three revises the groundings of the given set of noisy label samples by logical abduction based on reducing the estimated inconsistency IC . Formally, this logical abduction (LA) step can be expressed as

$$\begin{aligned} RG &= LA(IC; p^{LA}) = \{LA(IC_1; p^{LA_1}), \dots, LA(IC_d; p^{LA_d})\} \\ &= \{\{GR_{1,1}, \dots, GR_{1,z_1}\}, \dots, \{GR_{d,1}, \dots, GR_{d,z_d}\}\} \\ &= \{RG_1(GR_{1,1}), \dots, RG_s(GR_{s,z_s})\} \quad s.t. \quad s = \sum_{i=1}^d z_i. \end{aligned} \quad (7)$$

Finally, the substep four leverages the revised groundings RG to abduce multiple targets containing information consistent with our domain knowledge about the true target for the instance sample of the given noisy samples. Formally, this target abduce (TA) step can be expressed as

$$\begin{aligned} T &= TA(\{RG\}; p^{TA}) \\ &= \left\{ TA(\{RG_{1,1}, \dots, RG_{1,e_1}\}; p^{TA_1}), \dots, \right. \\ &\quad \left. TA(\{RG_{m,1}, \dots, RG_{m,e_m}\}; p^{TA_m}) \right\} \\ &= \{T_1, \dots, T_m\} \quad s.t. \quad \{RG_{*,1}, \dots, RG_{*,e_*}\} \in RG. \end{aligned} \quad (8)$$

In the four formulas (1)-(4), each p^* denotes the hyper-parameters corresponding to the implementation of respective expression.

Target rearrangement The target rearrangement procedure of OSAMTL-DiNS rearranges the multiple targets abduced by the one-step logical reasoning with DiNS into ordered multiple targets that are corresponding to each instance sample of the given diverse noisy samples. Formally, the target rearrangement (TR) procedure of OSAMTL-DiNS can be expressed as

$$\begin{aligned} \tilde{ts} &= TR(T, p^{TR}) \\ &= \{TR(\{T_i | i \in [1, m], T_i \in T\}, p^{TR_1}), \dots, TR(\{T_i | i \in [1, m], T_i \in T\}, p^{TR_d})\} \\ &= \{\tilde{ts}_1 = \{\tilde{ts}_{1,1}, \dots, \tilde{ts}_{1,r_1}\}, \dots, \tilde{ts}_d = \{\tilde{ts}_{d,1}, \dots, \tilde{ts}_{d,r_d}\}\} \quad s.t. \quad \tilde{ts}_* \in T \text{ and } r_* > 1. \end{aligned} \quad (9)$$

Here, p^{TR} denotes the hyper-parameters corresponding to the implementation of a target rearrangement procedure.

The formula (5) reflects that each instance sample of the given diverse noisy samples (IS_*) has corresponding r number of targets ($\tilde{t}_* = \{\tilde{t}_{*,1}, \dots, \tilde{t}_{*,r_*}\}$) abduced by the one-step logical reasoning. Referring to the situation where each instance sample of the given diverse noisy samples only has one instance, the formular (5) can be deduced to imply that each instance contained in an instance sample of the given diverse noisy samples has corresponding multiple targets abduced by one-step logical reasoning. With this implication, we can rewrite the rearranged targets for an instance sample of the given diverse noisy samples as

$$\tilde{t}_* = \{\tilde{t}_{*,1}, \dots, \tilde{t}_{*,r_*}\} = \left\{ \{\tilde{t}_{(*,1),1}, \dots, \tilde{t}_{(*,1),r_*}\}, \dots, \{\tilde{t}_{(*,n_*)}, \dots, \tilde{t}_{(*,n_*)}, r_*\} \right\}. \quad (10)$$

As a result, the instances (I) contained in the given diverse noisy samples and corresponding rearranged multiple targets (\tilde{t}) can be denoted as

$$\begin{aligned} I &= \{IS_1 \cup \dots \cup IS_d\} = \left\{ \{I_{1,1}, \dots, I_{1,n_1}\} \cup \dots \cup \{I_{d,1}, \dots, I_{d,n_d}\} \right\} = \{I_1, \dots, I_n\}, \\ \tilde{t} &= \{\tilde{t}_{s_1} \cup \dots \cup \tilde{t}_{s_d}\} = \left\{ \left\{ \{\tilde{t}_{(1,1),1}, \dots, \tilde{t}_{(1,1),r_1}\}, \dots, \{\tilde{t}_{(1,n_1),1}, \dots, \tilde{t}_{(1,n_1),r_1}\} \right\} \cup \dots \cup \right. \\ &\quad \left. \left\{ \{\tilde{t}_{(d,1),1}, \dots, \tilde{t}_{(d,1),r_d}\}, \dots, \{\tilde{t}_{(d,n_d),1}, \dots, \tilde{t}_{(d,n_d),r_d}\} \right\} \right\} \\ &= \left\{ \tilde{t}_1 = \{\tilde{t}_{1,1}, \dots, \tilde{t}_{1,r_1}\}, \dots, \tilde{t}_n = \{\tilde{t}_{n,1}, \dots, \tilde{t}_{n,r_n}\} \right\}, \quad s.t. \quad n = \sum_{i=1}^d n_i. \end{aligned} \quad (11)$$

Multi-target learning The multi-target learning procedure of OSAMTL-DiNS is carried out on the basis of a specifically constructed learning model that maps input instances (I) into its corresponding target prediction (t), which can be expressed as

$$t = LM(I, \omega) = \{t_1, \dots, t_n\}. \quad (12)$$

Here, LM is short for learning model, and ω denotes the hyper-parameters corresponding to the construction of a specific learning model.

The multi-target learning procedure of OSAMTL-DiNS, which constitutes of a joint loss construction and optimization, imposes the rearranged multiple targets (\tilde{t}) upon machine learning to constrain the prediction of the learning model (t). The joint loss is constructed by estimating the error between t_* and \tilde{t}_* , which can be expressed as

$$\mathcal{L}(t, \tilde{t}; \ell) = \frac{1}{n} \sum_{j=1}^n \sum_{i=1}^{r_j} \alpha_i \ell(t_j, \tilde{t}_{j,i}) \quad s.t. \quad \sum_{i=1}^{r_j} \alpha_i = 1. \quad (13)$$

Here, ℓ denotes the hyper-parameters corresponding to the construction of the basic loss function, and α_i is the weight for estimating the loss between t_j and an abducted target ($\tilde{t}_{j,i}$) contained in \tilde{t}_j . Then, the objective can be expressed as

$$\min_t (\mathcal{L}(t, \tilde{t}; \ell); \lambda). \quad (14)$$

Here, λ denotes the hyper-parameters corresponding to the implementation of an optimization approach.

2.2.3 Summary

OSAMTL-DiNS inherits properties from OSAMTL (Yang, Yang, Chen, et al., 2020), including the difference of OSAMTL from abductive learning (ABL) (Zhou, 2019) and the distinctiveness of OSAMTL from various state-of-the-art approaches that are based on pre-assumptions about noisy-labelled instances (Arazo et al., 2019; Liu & Guo, 2020; Ma et al., 2018, 2020; Reed et al., 2015; Wang et al., 2019; Yao et al., 2020) or need premised requirements (Acuna et al., 2019; Li, J., Socher, R., & Hoi, 2020; Xiao et al., 2015) to be carried out to handle noisy labels. OSAMTL-DiNS also inherits the essence of the multi-target learning procedure of OSAMTL, which is that the multi-target learning procedure can enable the learning model to learn from a weighted summarization of multiple targets that contain information consistent to our prior knowledge about the true target of a specific task. For more details of these properties of OSAMTL-DiNS inherited from OSAMTL, readers can refer to (Yang, Yang, Chen, et al., 2020).

OSAMTL-DiNS improves OSAMTL. The one-step logical reasoning procedure of OSAMTL-DiNS abduces multiple targets using given diverse noisy samples and knowledge base, while the logical reasoning procedure of OSAMTL abduces multiple targets using given one noisy sample and knowledge base. OSAMTL-DiNS is suitable to address tasks where a knowledge base and multiple noisy samples are available and each noisy sample has a different noisy distribution in labels. From this side, OSAMTL can only handle a subset of the tasks for which OSAMTL-DiNS are suitable, since it can only handle the situation where the available noisy sample has one noisy distribution in labels. Thus OSAMTL-DiNS expands the generalization of original OSAMTL to a wider range of tasks.

Besides, OSAMTL-DiNS possesses an extra target rearrangement procedure that rearranges the multiple targets abduced by the one-step logical reasoning with DiNS into ordered multiple targets corresponding to the instances contained in the given diverse noisy samples. As a result, the instances contained in the given diverse noisy samples and corresponding rearranged multiple targets can be conveniently employed by the multi-target learning procedure of OSAMTL-DiNS.

As OSAMTL-DiNS is proposed to handle DiNS, it can produce a predictive model based on very inaccurately labelled (complex noisy) samples. This property forms the major advantage of OSAMTL-DiNS, since the data preparation can be much less expensive and less labour-tensive though at least two types of noisy samples are needed. Being able to handle DiNS, OSAMTL-DiNS is suitable to address some tasks in the field of medical analysis where the problem of low consistency always exists. Low consistency, here in the context of DiNS, can refer to that large is the difference between the noisy distributions of two different noisy samples prepared by experts for a same medical analysis task, which usually results in more complex noisy in data annotations.

2.3 OSAMTL-DiNS Applied on Tumour Segmentation for Breast Cancer

In this section, we apply OSAMTL-DiNS on tumour segmentation for breast cancer (TSfBC) in medical histopathology whole slide image analysis (MHWSIA). Firstly, in section 2.3.1 we introduce the background of TSfBC, and in section 2.3.2 we give application settings of applying OSAMTL-DiNS on TSfBC. Secondly, in sections 2.3.3-6, we implement the OSAMTL-DiNS based solution for TSfBC. Finally, in section 2.3.7 we summarize the outline of the implementation of the OSAMTL-DiNS based solution for TSfBC.

2.3.1 Tumour segmentation for breast cancer

Fig. 2 shows the illustrations for two tasks of TSfBC. The two tasks include a task that aims to segment tumour in HE-stained pre-treatment biopsy images and a task that aims to segment residual tumour in HE-stained post-treatment surgical resection images. From the illustrations presented in Fig. 3.A and Fig. 3.B, we can note that it is indeed difficulty to accurately annotate the true targets for both segmentation tasks. Referring to these illustrations and additional suggestions from pathology experts, we here claim that the tumour segmentation task in HE-stained post-treatment surgical resection images is more difficult than the tumour segmentation task in HE-stained pre-treatment biopsy images.

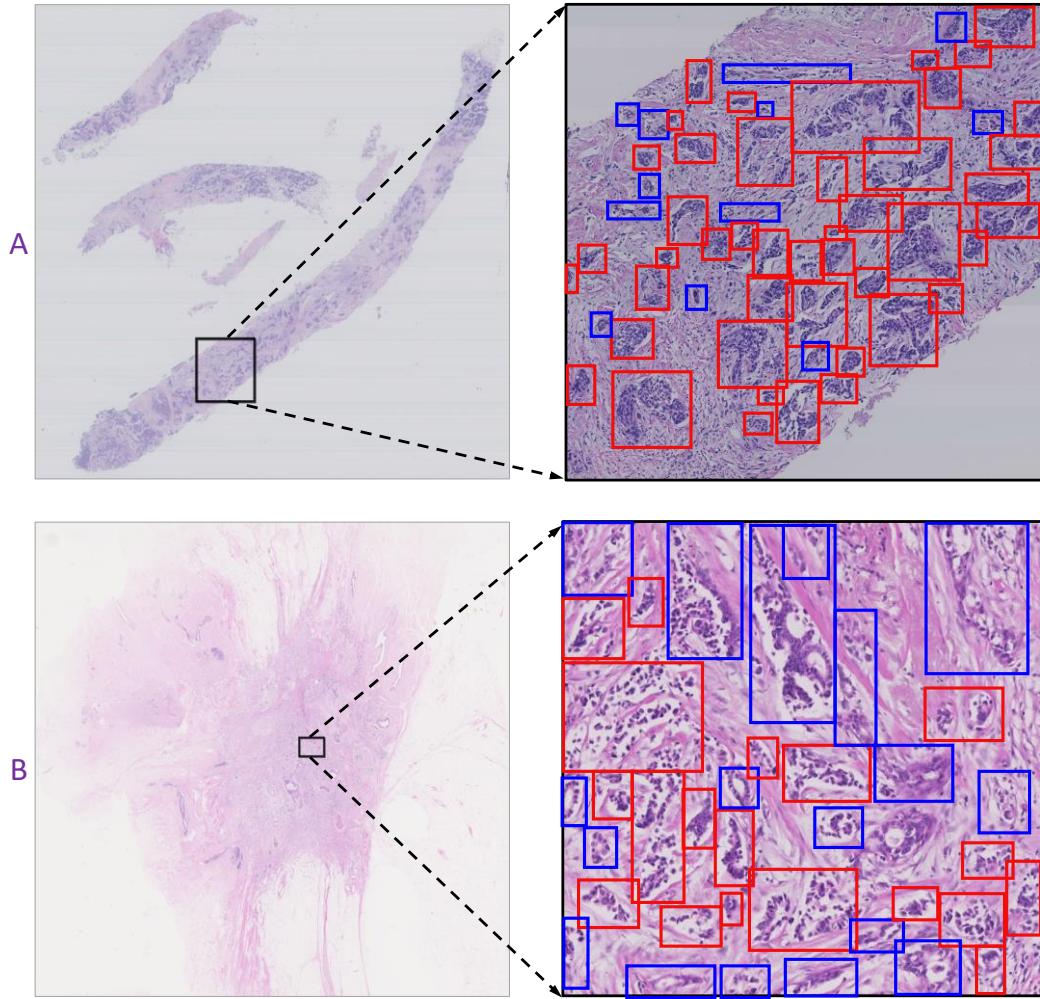


Figure. 3. Illustrations for two tumour segmentation tasks for breast cancer. A: tumour segmentation in HE-stained pre-treatment biopsy images. B: tumour segmentation in HE-stained post-treatment surgical resection images. A-Left: A $1\times$ magnification shown medical histopathology whole slide image digitalized from a HE-stained pre-treatment biopsy slide; A-Right: A $10\times$ magnification shown image patch cropped from the left whole slide image at the boxed area. B-Left: A $0.5\times$ magnification shown medical histopathology whole slide image digitalized from a HE-stained post-treatment surgical resection slide; B-Right: A $10\times$ magnification shown image patch cropped from the left whole slide image at the boxed area. Red boxes in A-Right image or B-Right image: areas that confidently contain tumour. Blue boxes in A-Right image or B-Right image: areas that possibly (not sure) contain tumour. Rest of A-Right image or B-Right image: areas that confidently do not contain tumour. Pathology experts annotated these boxes shown in A-Right image and B-Right image.

Existing deep learning (LeCun et al., 2015) enhanced approaches that can be leveraged to achieve TSfBC can be classified into two schemes: learning with noisy-free/accurate labels (Bhattacharjee et al., 2022; Priego-Torres et al., 2020, 2022) and learning with noisy/inaccurate labels (Diao et al., 2022; G. Xu et al., 2019; Y. Xu et al., 2014). The first type of scheme adopts the supervised learning paradigm. However, due to the difficulty in accurately labelling the tumour in breast cancer on whole slide images (Hanna et al., 2020), very limited noisy-free data is often available, which will inevitably limit the generalization of the prediction model. The second type of scheme adopts the weakly supervised learning paradigm, which avoids the problem of the

difficulty in obtaining noisy-free data faced by the first type of scheme. However, the popular strategy of using image patch-level labels to achieve pixel-level segmentation (Diao et al., 2022; G. Xu et al., 2019; Y. Xu et al., 2014) has the drawback in MHWSIA that the work load of image patch-level labelling can still be very massive due to the large size of whole slide images. To alleviate this situation, we apply the proposed OSAMTL-DiNS to TSfBC.

2.3.2 Application setting

On one hand, due to the difficulty to visually annotate the true target for TSfBC on HE-stained images, we asked two pathology experts to provide weak annotations: one pathology expert only aims to as accurate as possible exclude the non-true target on one data set; and another pathology expert only aims to as accurate as possible include the target on another dataset. As a result, two diverse noisy samples (DiNS) are provided for TSfBC from the vision perspective. On the other hand, existing knowledge of pathology can semantically give clear descriptions, that is a list of semantic sentences from pathological knowledge can present what is the true target for TSfBC. As a result, we also asked the two pathology experts to provide a knowledge base (KB) about the true target for TSfBC from the semantic perspective.

The noisy labels contained in visual DiNS are inaccurate but can be easily transformed into learnable target, meanwhile, the sentences contained in semantic KB are clear but cannot be easily transformed into learnable target. It is desirable to take the advantages of both visual DiNS and semantic KB into machine learning to achieve more reasonable predictions. Fortunately, the proposed OSAMTL-DiNS framework can take advantages of both visual DiNS and semantic KB by transforming visual DiNS into multiple learnable inaccurate targets containing information consistent with the knowledge of semantic KB for the true target via one-step abductive logical reasoning. Thus, on the basis of the provided visual DiNS and semantic KB, we employ OSAMTL-DiNS to address tumour segmentation in HE-stained pre-treatment biopsy images and tumour segmentation in HE-stained post-treatment surgical resection images.

2.3.3 Input materials

Diverse noisy samples The diverse noisy samples (DiNS) provided for the two tumour segmentation tasks for breast cancer are denoted as follows.

$$\begin{aligned} DNS &= \{NS_1, NS_2\} = \{\{IS_1, NLS_1\}, \{IS_2, NLS_2\}\} \\ &= \left\{ \left\{ \{I_{1,1}, \dots, I_{1,n_1}\}, \{NL_{1,1}, \dots, NL_{1,n_1}\} \right\}, \left\{ \{I_{2,1}, \dots, I_{2,n_2}\}, \{NL_{2,1}, \dots, NL_{2,n_2}\} \right\} \right\} \\ &= \left\{ \left\{ (I_{1,1}, NL_{1,1}), \dots, (I_{1,n_1}, NL_{1,n_1}) \right\}, \left\{ (I_{2,1}, NL_{2,1}), \dots, (I_{2,n_2}, NL_{2,n_2}) \right\} \right\}. \end{aligned}$$

Some examples of the provided DiNS for the two tasks are shown as Fig. 4. The noisy labels contained in the provided DiNS can significantly alleviate the mission for accurate ground-truth labels, however, these noisy labels also suffer from severe inaccuracy compared with the true target for TSfBC. From Fig. 4, we can observe that many non-tumour areas are included as tumour by the labels of NS_1 while many tumour areas are excluded as non-tumour by the labels of NS_2 .

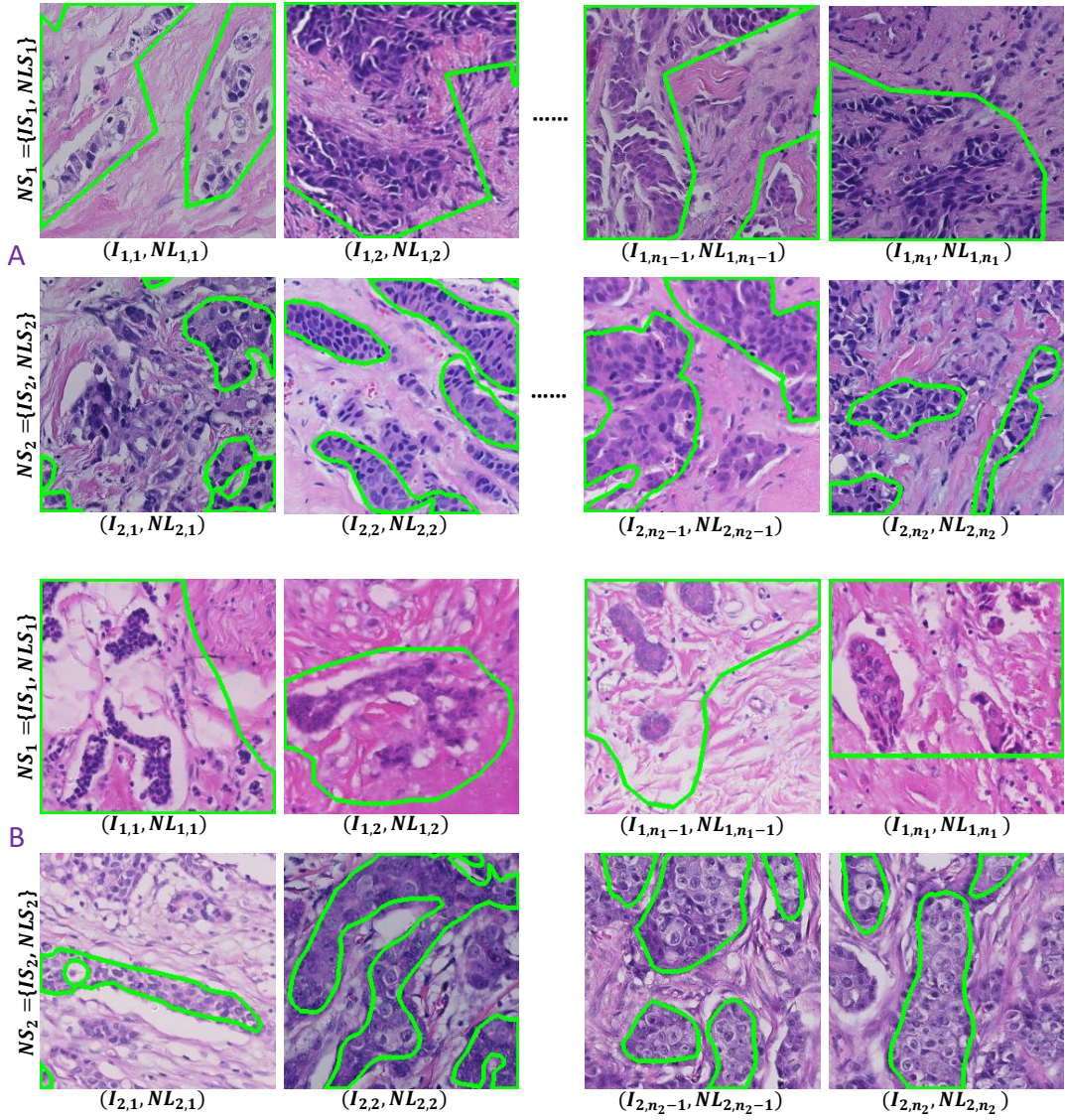


Figure. 4. Examples of diverse noisy samples provided for the two tumour segmentation tasks for breast cancer. A: diverse noisy samples for tumour segmentation in HE-stained pre-treatment biopsy images. B: diverse noisy samples for tumour segmentation in HE-stained post-treatment surgical resection images.

Knowledge base Regarding to existing knowledge of pathology, the knowledge base (KB) provided for the two tumour segmentation tasks for breast cancer are shown as Table 1.

$$KB = \{K_1, K_2, K_3, K_4, K_5, K_6\}.$$

Table 1. Knowledge provided for tumour segmentation for breast cancer

Knowledge Base
K_1 : Tumour is composed of tumour cells.
K_2 : Tumour cells may be arranged in cords, clusters, and trabeculae.
K_3 : Some tumours are characterized by predominantly solid or syncytial infiltrative pattern with little associated stroma.
K_4 : Cytoplasm of tumour cell is eosinophilic and vacuolated.
K_5 : Nuclei of tumour cell is enlarged and chromatin of tumour cell is vacuolated.
K_6 : Nuclei of tumour cell is degenerated.

2.3.4 One-step abductive logical reasoning with DiNS

Grounding Extract The Grounding Extract step takes the provided *DNS* (shown in Fig. 2) as input and produces a list of groundings that describe the logical facts of the provided DiNS. Referring to Eq. (5), we use the semantics contained in the provided *DNS* as p^{GE} to implement the Grounding Extract step, which can produce groundings as follows

$$\begin{aligned} G &= GE(DNS; \{\text{semantics contained in } DNS\}) \\ &= \left\{ \begin{aligned} &GE \left(\begin{aligned} &NS_1 = \{IS_1, NLS_1\}; \\ &\{\text{semantics contained in } NLS_1 \text{ for labeling } IS_1\} \end{aligned} \right), \\ &GE \left(\begin{aligned} &NS_2 = \{IS_2, NLS_2\}; \\ &\{\text{semantics contained in } NLS_2 \text{ for labeling } IS_2\} \end{aligned} \right) \end{aligned} \right\}, \\ &= \left\{ \begin{aligned} &G_1 = \{G_{1,1}, G_{1,2}\}, \\ &G_2 = \{G_{2,1}, G_{2,2}\} \end{aligned} \right\}. \end{aligned}$$

Details of the extracted groundings are provided in Table 2.

Table 2. Details of the extracted groundings

Extracted Groundings
$G_{1,1}$: pixels of IS_1 outside the polygons of NLS_1 are tumour negatives
$G_{1,2}$: pixels of IS_1 inside the polygons of NLS_1 are tumour positives
$G_{2,1}$: pixels of IS_2 inside the polygons of NLS_2 are tumour positives
$G_{2,2}$: pixels of IS_2 outside the polygons of NLS_2 are tumour negatives

Reasoning The Reasoning step takes the G extracted by the Grounding Extract step and the provided KB as inputs and produces a list of inconsistencies that describe the gap between the extracted groundings G and the provided KB from various perspectives. On the basis of the extracted groundings G and the provided KB , we derive two reasonings (Reasoning 1 and Reasoning 2). The validity of the two derived reasonings are respectively proved by Proof-R1 and Proof-R2 which are provided in Supplementary 1.

Reasoning 1. *If G_1 is given and KB is given, then inconsistency between the false tumour negatives covered by $G_{1,1}$ and the false tumour negatives covered by KB is low, inconsistency between the false tumour positives covered by $G_{1,2}$ and the false tumour positives covered by KB is high, inconsistency between the true tumour positives covered by $G_{1,2}$ and the true tumour positives covered by KB is low, and inconsistency between the true tumour negatives covered by $G_{1,1}$ and the true tumour negatives covered by KB is high.*

Reasoning 2. *If G_2 is given and KB is given, then inconsistency between the false tumour positives covered by $G_{2,1}$ and the false tumour positives covered by KB is low, inconsistency between the false tumour negatives covered by $G_{2,2}$ and the false tumour negatives covered by KB is high, inconsistency between the true tumour negatives covered by $G_{2,2}$ and the true tumour negatives covered by KB is low, and inconsistency*

between the true tumour positives covered by $G_{1,1}$ and the true tumour positives covered by KB is high.

Referring to Eq. (6), we use Reasoning 1 and Reasoning 2 as p^R to implement the Reasoning step, which can produce estimated inconsistencies between the extracted groundings G and the provided KB as follows

$$\begin{aligned} IC &= R(G, KB; \{Reasoning\ 1, Reasoning\ 2\}) \\ &= \{R(G_1, KB; Reasoning\ 1), R(G_2, KB; Reasoning\ 2)\} \\ &= \left\{ \begin{aligned} IC_1 &= \{IC_{1,1}, IC_{1,2}, IC_{1,3}, IC_{1,4}\}, \\ IC_2 &= \{IC_{2,1}, IC_{2,2}, IC_{2,3}, IC_{2,4}\} \end{aligned} \right\} \end{aligned}$$

Details of the estimated inconsistencies are provided in Table 3.

Table 3. Details of the estimated inconsistencies

Estimated Inconsistencies
$IC_{1,1}$: inconsistency between the false tumour negatives covered by $G_{1,1}$ and the false tumour negatives covered by KB is low
$IC_{1,2}$: inconsistency between the false tumour positives covered by $G_{1,2}$ and the false tumour positives covered by KB is high
$IC_{1,3}$: inconsistency between the true tumour positives covered by $G_{1,2}$ and the true tumour positives covered by KB is low
$IC_{1,4}$: inconsistency between the true tumour negatives covered by $G_{1,1}$ and the true tumour negatives covered by KB is high
$IC_{2,1}$: inconsistency between the false tumour positives covered by $G_{2,1}$ and the false tumour positives covered by KB is low
$IC_{2,2}$: inconsistency between the false tumour negatives covered by $G_{2,2}$ and the false tumour negatives covered by KB is high
$IC_{2,3}$: inconsistency between the true tumour negatives covered by $G_{2,2}$ and the true tumour negatives covered by KB is low
$IC_{2,4}$: inconsistency between the true tumour positives covered by $G_{2,1}$ and the true tumour positives covered by KB is high

Abduction The Abduction step takes the IC estimated by Reasoning step and the G extracted by the Grounding Extract step as inputs and produces a list of revised groundings that reduce the inconsistencies in IC . On the basis of the estimated IC and the extracted G , we derive two reasonings (Reasoning 3 and Reasoning 4). The validity of the two derived reasonings are respectively proved by Proof-R3 and Proof-R4 which are provided in Supplementary 1.

Reasoning 3. If IC_1 is given, then $G_{1,1}$ should not be revised to remain $IC_{1,1}$, $G_{1,2}$ should not be revised to remain $IC_{1,3}$, $G_{1,1}$ should be revised to reduce $IC_{1,4}$, and $G_{1,2}$ should be revised to reduce $IC_{1,2}$.

Reasoning 4. If IC_2 is given, then $G_{2,1}$ should not be revised to remain $IC_{2,1}$, then $G_{2,2}$ should not be revised to remain $IC_{2,3}$, $G_{2,1}$ should be revised to reduce $IC_{2,2}$, and $G_{2,2}$ should be revised to reduce $IC_{2,4}$.

Referring to Eq. (7), we use Reasoning 3 and Reasoning 4 as p^{LA} to implement the Abduction step, which can produce revised groundings as follows

$$\begin{aligned}
RG &= LA(\{IC\}; \{Reasoning\ 3, Reasoning\ 4\}) \\
&= \{LA(\{IC_1\}; Reasoning\ 3), \\
&\quad LA(\{IC_2\}; Reasoning\ 4)\} \\
&= \{\{GR_{1,1}, GR_{1,2}, GR_{1,3}, GR_{1,4}\}, \\
&\quad \{GR_{2,1}, GR_{2,2}, GR_{2,3}, GR_{2,4}\}\} \\
&= \{RG_1(GR_{1,1}), RG_2(GR_{1,2}), RG_3(GR_{1,3}), RG_4(GR_{1,4}), \\
&\quad RG_5(GR_{2,1}), RG_6(GR_{2,2}), RG_7(GR_{2,3}), RG_8(GR_{2,4})\}
\end{aligned}$$

Details of the grounding revisions and the revised groundings are respectively provided in Table 4 and Table 5.

Table 4. Details of the grounding revisions

Grounding Revisions
$GR_{1,1}$: $G_{1,1}$ should not be revised to remain $IC_{1,1}$
$GR_{1,2}$: $G_{1,2}$ should not be revised to remain $IC_{1,3}$
$GR_{1,3}$: $G_{1,1}$ should be revised to reduce $IC_{1,4}$
$GR_{1,4}$: $G_{1,2}$ should be revised to reduce $IC_{1,2}$
$GR_{2,1}$: $G_{2,1}$ should not be revised to remain $IC_{2,1}$
$GR_{2,2}$: $G_{2,2}$ should not be revised to remain $IC_{2,3}$
$GR_{2,3}$: $G_{2,1}$ should be revised to reduce $IC_{2,4}$
$GR_{2,4}$: $G_{2,2}$ should be revised to reduce $IC_{2,2}$

Table 5. Details of the revised groundings

Revised Groundings
$RG_1(GR_{1,1})$: $G_{1,1}$, pixels of IS_1 outside the polygons of NLS_1 are tumour negatives
$RG_2(GR_{1,2})$: $G_{1,2}$, pixels of IS_1 inside the polygons of NLS_1 are tumour positives
$RG_3(GR_{1,3})$: pixels of IS_1 outside the polygons of NLS_1 are not exactly true tumour negatives
$RG_4(GR_{1,4})$: pixels of IS_1 inside the polygons of NLS_1 are not exactly true tumour positives
$RG_5(GR_{2,1})$: $G_{2,1}$, pixels of IS_2 inside the polygons of NLS_2 are tumour positives
$RG_6(GR_{2,2})$: $G_{2,2}$, pixels of IS_2 outside the polygons of NLS_2 are tumour negatives
$RG_7(GR_{2,3})$: pixels of IS_2 inside the polygons of NLS_2 are not exactly true tumour positives
$RG_8(GR_{2,4})$: pixels of IS_2 outside the polygons of NLS_2 are not exactly true tumour negatives

Target Abduce The target abduce step takes the RG produced by the Abduction step as input and abduces a list of multiple targets to more appropriately represent the true target of tumour for breast cancer. On the basis of the input RG , we derive four reasonings (Reasoning 5, Reasoning 6, Reasoning 7 and Reasoning 8). The validity of the four derived reasonings are respectively proved by Proof-R5-9 which are provided in Supplementary 1.

Reasoning 5. If RG_1 is given and RG_2 is given, then a target (T_1) can be abduced from the union of RG_1 and RG_2 , and T_1 has a high recall of true tumour positives and a high precision of true tumour negatives.

Reasoning 6. If RG_5 is given and RG_6 is given, then a target (T_2) can be abduced from the union of RG_5 and RG_6 , and T_2 has a high precision of true tumour positives and a high recall of true tumour negatives.

Reasoning 7. If the target (T_1) abduced from the union of RG_1 and RG_2 is given, RG_3 is given and RG_4 is given, then T_1 has a low precision of true tumour positives and a low recall of true tumour negatives.

Reasoning 8. If the target (T_2) abduced from the union of RG_5 and RG_6 is given, RG_7 is given and RG_8 is given, then T_2 has a low recall of true tumour positives and a low precision of true tumour negatives.

Reasoning 9. If the target (T_1) abduced from the union of RG_1 and RG_2 is given and the target (T_2) abduced from the union of RG_5 and RG_6 is given, then a target (T_3) can be abduced by improving T_1 with T_2 , a target (T_4) can be abduced by improving T_2 with T_1 , T_3 can have a relatively higher precision of true tumour positives than T_1 and a relatively higher recall of true tumour negatives than T_1 , and T_4 can have a relatively higher recall of true tumour positives than T_2 and a relatively higher precision of true tumour negatives than T_2 .

Referring to Eq. (8), we use Reasoning 5-9 as p^{TA} to implement the Target Abduce step, which can be denoted as follows

$$\begin{aligned}
 T &= TA(RG; \{Reasoning\ 5, \dots, Reasoning\ 9\}) \\
 &= \left\{ \begin{array}{l} TA(\{RG_1, RG_2\}; Reasoning\ 5), TA(\{RG_4, RG_5\}; Reasoning\ 6), \\ TA\left(\begin{array}{c} \{RG_1, RG_2, RG_3, RG_4, RG_5, RG_6\}; \\ \{Reasoning\ 5, Reasoning\ 7, Reasoning\ 9\} \end{array}\right), \\ TA\left(\begin{array}{c} \{RG_4, RG_5, RG_6, RG_7, RG_1, RG_2\}; \\ \{Reasoning\ 6, Reasoning\ 8, Reasoning\ 9\} \end{array}\right) \end{array} \right\} \\
 &= \{T_1, T_2, T_3, T_4\}.
 \end{aligned}$$

With Reasoning 5, we generate the target T_1 by the union of RG_1 and RG_2 to keep a high recall of true tumour positives and a high precision of true tumour negatives. With Reasoning 6, we generate the target T_2 by the union of RG_4 and RG_5 to keep high precision of true tumour positives and a high recall of true tumour negatives. With Reasoning 5-9, we generate the target T_3 to keep a relatively higher precision of true tumour positives than T_1 and a relatively higher recall of true tumour negatives than T_1 . Specifically, we first employed NLS_1 to train an image semantic segmentation model and then tested it on the instance images of NLS_2 to produce T_3 . With Reasoning 6-9, we generate the target T_4 to keep a relatively higher recall of true tumour positives than T_2 and a relatively higher precision of true tumour negatives than T_2 . Specifically, we first employed NLS_2 to train an image semantic segmentation model and then tested it on the instance images of NLS_1 to produce T_4 . Some examples of the abduced multiple targets for the two tumour segmentation tasks for breast cancer illustrated in Fig. 2 are provided in Supplementary 2.

2.3.5 Target rearrangement

The target rearrangement step takes the T produced by the Target Abduce step as input and produce ordered multiple targets that are corresponding to each of the two given diverse noisy samples. On the basis of the input T , we derive two reasonings (Reasoning 10 and Reasoning 11). The validity of the two derived reasonings are respectively proved by Proof-R10 and Proof-R11 which are provided in Supplementary 1.

Reasoning 10. *If T_1 is given and T_3 is given, then T_1 and T_3 can be combined to approximate the true target for NS_1 .*

Reasoning 11. *If T_2 is given and T_4 is given, then T_2 and T_4 can be combined to approximate the true target for NS_2 .*

Referring to Eq. (9), we use Reasoning 10 and Reasoning 11 as p^{TR} to implement the Target Rearrangement step, which can produce rearranged targets as follows

$$\begin{aligned}\tilde{s} &= TR(T, \{Reasoning10, Reasoning11\}) \\ &= \{TR(\{T_1, T_3\}, Reasoning10), \\ &\quad TR(\{T_2, T_4\}, Reasoning11)\} \\ &= \{\tilde{t}s_1 = \{\tilde{t}s_{1,1}, \tilde{t}s_{1,2}\} = \{T_1, T_3\}, \tilde{t}s_2 = \{\tilde{t}s_{2,1}, \tilde{t}s_{2,2}\} = \{T_4, T_2\}\}.\end{aligned}$$

On the basis of the rearranged \tilde{s} and referring to Eq. (10)-(11), the instances (I) contained in the given DNS and their corresponding rearranged multiple targets are denoted as follows.

$$I = \{I_1, \dots, I_n\}, \quad \tilde{t} = \{\tilde{t}_1 = \{\tilde{t}_{1,1}, \tilde{t}_{1,2}\}, \dots, \tilde{t}_n = \{\tilde{t}_{n,1}, \tilde{t}_{n,2}\}\}, \quad s.t. \ n = n_1 + n_2.$$

Some examples of the rearranged multiple targets are provided in Supplementary 2.

2.3.6 Multi-target learning

Referring to Eq. (12), we employ deep convolutional neural network (DCNN) to implement the learning model (LM) that maps input instances (I) into its corresponding target predictions (t) by

$$t = LM(I, DCNN) = \{t_1, \dots, t_n\}.$$

The DCNN employed for the learning model of tumour segmentation here is a symmetric image semantic segmentation architecture that we constructed in (Yang, Yang, Chen, et al., 2020) by referring to the commonly used FCN (Shelhamer et al., 2017), which is the representative for the fully convolutional networks based solutions and has inspired various other solutions (Badrinarayanan et al., 2017; Chen et al., 2018; Falk et al., 2019; Fu et al., 2019; Zhao et al., 2017) achieving state-of-the-art performances in image semantic segmentation.

On the basis of the rearranged targets \tilde{t} and the target prediction of implemented learning model and referring to Eq. (13), we employ cross entropy (CE) to implement the multi-target learning procedure by

$$\mathcal{L}(t, \tilde{t}; CE) = \frac{1}{n} \sum_{j=1}^n (\alpha_1 CE(t_j, \tilde{t}_{j,1}) + \alpha_2 CE(t_j, \tilde{t}_{j,2})) \quad s.t. \ \alpha_1 + \alpha_2 = 1.$$

Referring to Eq. (14), we employ stochastic gradient descent (SGD) to implement the objective by

$$\min_t (\mathcal{L}(t, \tilde{t}; CE); SGD).$$

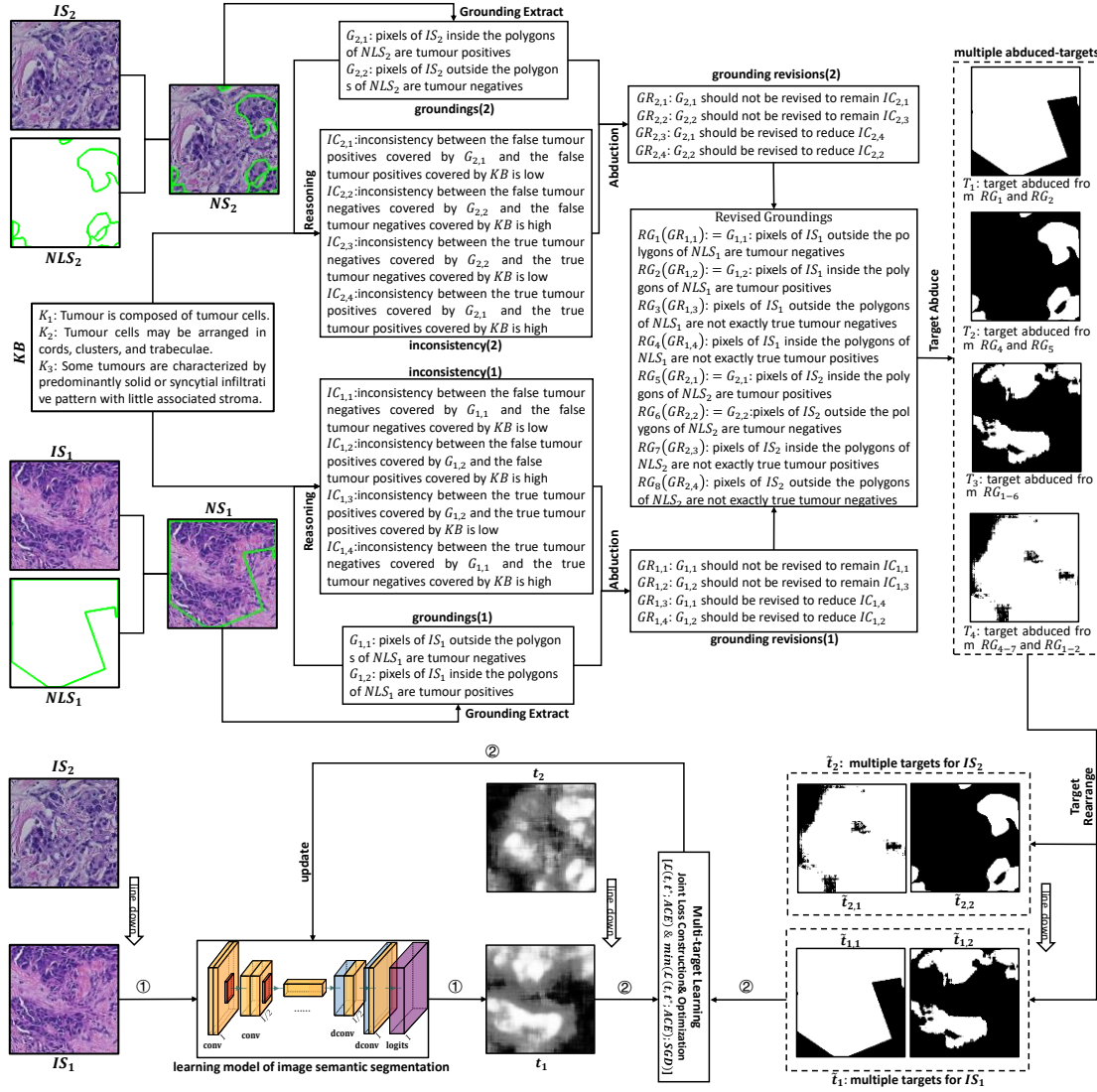


Figure. 5. The outline of the OSAMTL-DiNS solution implemented for the TSfBC in HE-stained pre-treatment biopsy images. Black lines: input materials; Green lines: one-step abductive logical reasoning with DiNS; Blue lines: target rearrangement; Red lines: multi-target learning.

2.3.7 Summary

Referring to the contents of sections 2.3.3-6, the outline of the OSAMTL-DiNS solution implemented for the TSfBC in HE-stained pre-treatment biopsy images is shown as Fig. 5. On the basis of Fig. 5, the simplified outline of the OSAMTL-DiNS solution implemented for residual TSfBC in HE-stained post-treatment surgical resection images is simplistically shown as Fig. 6.

2.4 Experimental strategies

On the basis of the OSAMTL-DiNS solutions implemented for the two tumour segmentation tasks for breast cancer illustrated in Fig. 2, we conduct extensive experiments to demonstrate the contributions of OSAMTL-DiNS in handling complex noisy labels. In this subsection, we give descriptions about the overall design, data preparation, evaluation metrics and experimental details for conducting the experiments.

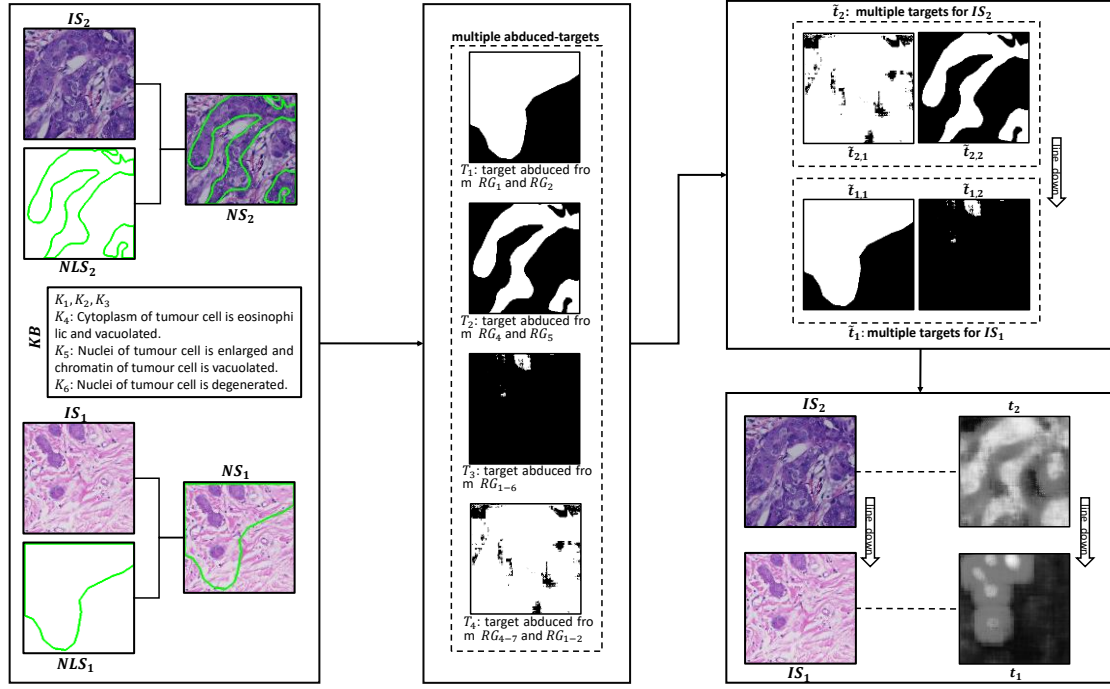


Figure. 6. The simplified outline of the OSAMTL-DiNS solution implemented for residual TSfBC in HE-stained post-treatment surgical resection images based on Fig. 4.

2.4.1 Overall design

Due to the fact that accurate/noisy-free ground-truth labels for the two tumour segmentation tasks for breast cancer illustrated in Fig. 2 (tumour segmentation task in HE-stained pre-treatment biopsy images and tumour segmentation task in HE-stained post-treatment surgical resection images) are quite difficult to collect, we prepare a small noisy-free dataset for each of the two tumour segmentation tasks for usual evaluations with AGTL.

We first respectively conducted experiments of various existing solutions that learn from complex noisy labels and experiments of various existing solutions that introduce OSAMTL-DiNS for enhancement in handling complex noisy labels. Then, to show the contributions of OSAMTL-DiNS in handling complex noisy labels, we also provide some qualitative example results as visualized proofs to show the contributions of OSAMTL-DiNS in handling complex noisy labels.

For all experiments, we first use a training dataset to learn segmentation models, then we use a validation dataset to select the model for testing. The experimental results of segmentation models are averaged on corresponding dataset. The preparation for the training, validation and testing can be found in section 2.4.2.

2.4.2 Dataset preparation

For the tumour segmentation task in HE-stained pre-treatment biopsy images, we collected a total amount of 144 WSIs. Among the collected WSIs, 105 WSIs were used by pathology expert to produce noisy sample one (NS_1 shown in the first row of Fig. 3.A), 20 WSIs were used by pathology expert to produce noisy sample two (NS_2 shown in the second row of Fig. 3.A), and the rest 19 WSIs were used by pathology expert to produce a relatively noisy-free sample ($RNFS$). Both NS_1 and NS_2 were prepared for training without AGTL, and $RNFS$ was prepared for validation and testing with AGTL.

NS_1 contains 992 pairs of images and corresponding noisy labels for training without AGTL. NS_2 contains 142 pairs of images and corresponding noisy labels for training without AGTL. $RNFS$ contains 158 pairs of images and corresponding accurate labels, among which 79 pairs are for validation and 79 pairs are for testing with AGTL.

Similarly, for the tumour segmentation task in HE-stained post-treatment surgical resection images, we collected a total amount of 126 WSIs. Among the collected WSIs, 94 WSIs were used by pathology expert to produce noisy sample one (NS_1 shown in the first row of Fig. 3.B), 20 WSIs were used by pathology expert to produce noisy sample two (NS_2 shown in the second row of Fig. 3.B), and the rest 12 WSIs were used by pathology expert to produce a relatively noisy-free sample ($RNFS$). Both NS_1 and NS_2 were prepared for training without AGTL. NS_1 contains 2944 pairs of images and corresponding noisy labels for training without AGTL. NS_2 contains 1431 pairs of images and corresponding noisy labels for training without AGTL. $RNFS$ contains 242 pairs of images and corresponding accurate labels, among which 121 pairs are for validation and 121 pairs are for testing with AGTL.

The image patches prepared for experiments were cropped at 10 \times magnification of the given WSIs and the size of each cropped image patch was at 256 \times 256 pixels (width \times height) to remain distinguishable morphologies of tumour.

2.4.3 Evaluation metrics

We employed usual metrics for image semantic segmentation evaluation. Let TP (true positive) be the number of pixels correctly predicted to belong to the H. pylori class, FP (false positive) be the number of pixels incorrectly predicted to belong to the H. pylori class, and FN (false negative) be the number of missing pixels predicted to belong to the background class. These metrics are tightly related to the foreground class which we are interested the most. Based on TP, FP and FN, we further employed precision, recall, f1 and foreground intersection over union (fIoU) for evaluation of segmentation.

2.4.4 Experimental details

All of our experiments were performed on an Intel core Xeon E5-2630 v4s with a memory capacity of 128GB and eight NVIDIA GTX 1080Ti GPUs. Our developing environment is based on Tensorflow 1.10.1 and Python 3.5. We started the training procedures of the employed DCNN for the learning model of tumour segmentation with the same initialization and hyperparameters including Adam (Kingma & Ba, 2015) selected as the optimizer, batch size set to 32, learning rate set to 0.0001, and online augmentations involving vertical and horizontal flips and random brightness. Various existing approaches for learning from noisy labels (LfNLs) (Fr  nay & Verleysen, 2014; Karimi et al., 2020; Song et al., 2022), including naively learning from noisy labels (BaseLine), Forward, Backward (Patrini et al., 2017), Boost-Hard, Boost-Soft (Arazo et al., 2019; Reed et al., 2015), D2L (Ma et al., 2018), SCE (Wang et al., 2019), Peer (Liu & Guo, 2020), DT-Forward (Yao et al., 2020), and NCE-SCE (Ma et al., 2020), were chosen for experimental investigations, due to their flexibility to be applied to the situation where no clean dataset is available, the targeted object cannot be clearly defined, and any of the given labels cannot be confidently regarded as clean. We

respectively set the hyper parameters of these approaches as suggested by corresponding papers. In default, we set the weights for the multi-task learning procedure of OSAMTL-DiNS to fifty-fifty in this TSfBC case, considering that both targets are equally important. When calculating the evaluation metrics, we used 0.5 to thresh the logits of the optimized DCNN for segmentation, as it is a default value to separate the predictions into target and non-target which can balance the bias and variance of the optimized DCNN.

3. Results and Discussion

We show the results of various existing methods for learning from noisy labels (LfNLs) and the results of various existing methods with OSAMTL-DiNS introduced for LfNLs respectively on the two tumour segmentation tasks for breast cancer, respectively in sections 3.1 and 3.2. Based on the results presented in sections 3.1 and 3.2, we discuss the contributions of OSAMTL-DiNS in handling complex noisy labels in section 3.3. On the basis of the contents indicated in section 3.3, we discuss the generalization of the contributions of OSAMTL-DiNS from validation to testing in section 3.4. In section 3.5, we show some qualitative testing results as visual proofs to discuss the contributions of OSAMTL-DiNS. Finally in section 3.6, we discuss a released model pretrained with OSAMTL-DiNS for tumour segmentation in HE-stained pre-treatment biopsy images in breast cancer and its application as a pre-processing tool to extract tumour-associated stroma compartment for predicting the pathological complete response to neoadjuvant chemotherapy in breast cancer (F. Li et al., 2022).

3.1 Results of various existing methods for LfNLs

For simplicity, we denote Task1 as the tumour segmentation task in HE-stained pre-treatment biopsy images and Task2 as the tumour segmentation task in HE-stained post-treatment surgical resection images. In this subsection, we respectively employ various existing approaches for LfNLs mentioned in section 5.1.3 on Task1 and Task2.

3.1.1 Evaluations on Task1 with AGTL

We evaluate the results of employing various existing methods for LfNLs on Task1 using usual evaluations with AGTL. Experimental statistics for validation and testing are respectively shown as Table 6 and Table 7.

Table 6. Evaluations of various existing method for validation on Task1

Solution	TP	FP	FN	precision	recall	f1	fIoU
BaseLine	19278	15955	2807	54.72	87.29	67.27	50.68
Forward	20243	16860	1843	54.56	91.66	68.40	51.98
Backward	19069	14239	3016	57.25	86.34	68.85	52.50
Boost-Hard	18806	14959	3279	55.70	85.15	67.34	50.77
Boost-Soft	20138	17912	1948	52.93	91.18	66.97	50.35
D2l	19676	17020	2410	53.62	89.09	66.95	50.31
SCE	19500	15153	2585	56.27	88.30	68.74	52.37
Peer	19775	14660	2310	57.43	89.54	69.98	53.82
DT-Forward	19806	16229	2280	54.96	89.68	68.15	51.69

NCE-SCE	20015	16580	2071	54.69	90.62	68.22	51.76
---------	-------	-------	------	-------	-------	-------	-------

Table 7. Evaluations of various existing method for testing on Task1

Solution	TP	FP	FN	precision	recall	f1	fIoU
BaseLine	22707	13298	3249	63.07	87.48	73.29	57.85
Forward	23494	15160	2462	60.78	90.51	72.73	57.14
Backward	21858	13453	4098	61.90	84.21	71.35	55.46
Boost-Hard	22184	12652	3771	63.68	85.47	72.98	57.46
Boost-Soft	23724	15849	2231	59.95	91.40	72.41	56.75
D2l	23068	14632	2888	61.19	88.87	72.48	56.83
SCE	22753	13499	3203	62.76	87.66	73.15	57.67
Peer	22658	12704	3298	64.07	87.29	73.90	58.61
DT-Forward	23280	14239	2676	62.05	89.69	73.35	57.92
NCE-SCE	23395	14452	2561	61.81	90.13	73.34	57.90

3.1.2 Evaluations on Task2 with AGTL

We evaluate the results of employing various existing methods for LfNLs on Task2 using usual evaluations with AGTL. Experimental statistics for validation and testing are respectively shown as Table 8 and Table 9.

Table 8. Evaluations of various existing method for validation on Task2

Solution	TP	FP	FN	precision	recall	f1	fIoU
BaseLine	18507	12766	11120	59.18	62.47	60.78	43.66
Forward	18176	11995	11451	60.24	61.35	60.79	43.67
Backward	19632	14650	9995	57.27	66.26	61.44	44.34
Boost-Hard	20238	14820	9389	57.73	68.31	62.57	45.53
Boost-Soft	23277	17557	6351	57.00	78.56	66.07	49.33
D2l	19617	12892	10010	60.34	66.21	63.14	46.13
SCE	18807	12118	10821	60.81	63.48	62.12	45.05
Peer	21279	18131	8349	53.99	71.82	61.64	44.55
DT-Forward	18509	13330	11119	58.13	62.47	60.22	43.09
NCE-SCE	19801	14619	9826	57.53	66.83	61.83	44.75

Table 9. Evaluations of various existing method for testing on Task2

Solution	TP	FP	FN	precision	recall	f1	fIoU
BaseLine	15446	13831	8467	52.76	64.59	58.08	40.92
Forward	15129	13409	8783	53.01	63.27	57.69	40.54
Backward	16373	17083	7540	48.94	68.47	57.08	39.94
Boost-Hard	16599	15904	7313	51.07	69.42	58.85	41.69
Boost-Soft	19000	18353	4912	50.87	79.46	62.03	44.95
D2l	16331	14876	7581	52.33	68.30	59.26	42.10
SCE	15604	13286	8309	54.01	65.25	59.10	41.95
Peer	17366	19348	6546	47.30	72.62	57.29	40.14
DT-Forward	15374	15525	8538	49.76	64.29	56.10	38.98
NCE-SCE	16356	16574	7556	49.67	68.40	57.55	40.40

3.2 Results of various existing methods with OSAMTL-DiNS introduced for LfNLs

In this subsection, we respectively introduce OSAMTL-DiNS to various existing approaches for LfNLs mentioned in section 5.1.3 on Task1 and Task2.

3.2.1 Evaluations on Task1

We evaluate the results of employing various existing methods with OSAMTL-DiNS introduced for LfNLs on Task1 using usual evaluations with AGTL. Experimental statistics for validation and testing are respectively shown as Table 10 and Table 11.

Table 10. Evaluations of various existing method with OSAMTL-DiNS introduced for validation on Task1

Solution	TP	FP	FN	precision	recall	f1	fIoU
BaseLine	18026	8651	4059	67.57	81.62	73.93	58.65
Forward	17266	7505	4819	69.70	78.18	73.70	58.35
Backward	17814	8371	4272	68.03	80.66	73.81	58.49
Boost-Hard	17348	7606	4738	69.52	78.55	73.76	58.43
Boost-Soft	17855	8059	4231	68.90	80.84	74.40	59.23
D2l	17597	8128	4489	68.40	79.67	73.61	58.24
SCE	16774	7302	5311	69.67	75.95	72.68	57.08
Peer	17681	8557	4404	67.39	80.06	73.18	57.70
DT-Forward	17218	7393	4868	69.96	77.96	73.74	58.41
NCE-SCE	16305	6562	5781	71.30	73.83	72.54	56.91

Table 11. Evaluations of various existing method with OSAMTL-DiNS introduced for testing on Task1

Solution	TP	FP	FN	precision	recall	f1	fIoU
BaseLine	21010	6381	4946	76.70	80.94	78.77	64.97
Forward	20215	5579	5740	78.37	77.88	78.13	64.11
Backward	20818	6124	5137	77.27	80.21	78.71	64.90
Boost-Hard	20230	5732	5725	77.92	77.94	77.93	63.84
Boost-Soft	20657	5936	5298	77.68	79.59	78.62	64.77
D2l	20348	5981	5608	77.28	78.39	77.83	63.71
SCE	19719	5651	6236	77.73	75.97	76.84	62.39
Peer	20379	6634	5577	75.44	78.51	76.95	62.53
DT-Forward	19958	5347	5998	78.87	76.89	77.87	63.76
NCE-SCE	18712	4594	7244	80.29	72.09	75.97	61.25

3.2.2 Evaluations on Task2

We evaluate the results of various existing methods with OSAMTL-DiNS introduced for LfNLs on Task2 using usual evaluations with AGTL. Experimental statistics for validation and testing are respectively shown as Table 12 and Table 13.

Table 12. Evaluations of various existing method with OSAMTL-DiNS introduced for validation on Task2

Solution	TP	FP	FN	precision	recall	f1	fIoU
----------	----	----	----	-----------	--------	----	------

BaseLine	19291	4878	10337	79.82	65.11	71.72	55.91
Forward	18257	3530	11370	83.80	61.62	71.02	55.06
Backward	18966	4648	10661	80.32	64.02	71.25	55.33
Boost-Hard	18990	3964	10637	82.73	64.10	72.23	56.53
Boost-Soft	18850	5732	10777	76.68	63.62	69.55	53.31
D2l	18438	3154	11190	85.39	62.23	71.99	56.24
SCE	18449	5022	11178	78.60	62.27	69.49	53.24
Peer	20269	6413	9358	75.97	68.41	71.99	56.24
DT-Forward	18371	4117	11256	81.69	62.01	70.50	54.44
NCE-SCE	16177	2620	13451	86.06	54.60	66.81	50.16

Table 13. Evaluations of various existing method with OSAMTL-DiNS introduced for testing on Task2

Solution	TP	FP	FN	precision	recall	f1	fIoU
BaseLine	16000	5649	7912	73.91	66.91	70.24	54.13
Forward	14825	3948	9088	78.97	62.00	69.46	53.21
Backward	15441	5648	8471	73.22	65.57	68.62	52.24
Boost-Hard	15713	4611	8200	77.31	65.71	71.04	55.09
Boost-Soft	15799	6017	8114	72.42	66.07	69.10	52.79
D2l	15109	3599	8803	80.76	63.18	70.90	54.92
SCE	15168	5151	8744	74.65	63.43	68.59	52.19
Peer	16954	7478	6958	69.39	70.90	70.14	54.01
DT-Forward	15175	4483	8737	77.20	63.46	69.66	53.44
NCE-SCE	13101	2749	10811	82.66	54.79	65.90	49.14

3.3 Discussion of contributions of OSAMTL-DiNS in handling complex noisy labels

In this subsection, we respectively show the contributions of OSAMTL-DiNS in handling complex noisy labels on Task1 and Task2.

3.3.1 Discussion of contributions of OSAMTL-DiNS on Task1

We reflect the contributions of OSAMTL-DiNS on Task1 by the differences between Table 6 and Table 10 for validation and the differences between Table 7 and Table 11 for testing, which are respectively shown as Fig. 7 and Fig. 8. More specifically, the contributions of OSAMTL-DiNS on Task1 are quantitatively evaluated by statistics of Table 10 minus statistics of Table 6 for validation and statistics of Table 11 minus statistics of Table 7 for testing, which are respectively shown as Table 14 and Table 15. And the confident intervals for the contributions of OSAMTL-DiNS on Task1 are shown in Table 16.

Table 14. Contributions of OSAMTL-DiNS to various existing method for validation on Task1

Solution	TP	FP	FN	precision	recall	f1	fIoU
BaseLine	-1252	-7304	1252	12.85	-5.67	6.66	7.97
Forward	-2977	-9355	2976	15.14	-13.48	5.3	6.37
Backward	-1255	-5868	1256	10.78	-5.68	4.96	5.99
Boost-Hard	-1458	-7353	1459	13.82	-6.6	6.42	7.66
Boost-Soft	-2283	-9853	2283	15.97	-10.34	7.43	8.88

D2I	-2079	-8892	2079	14.78	-9.42	6.66	7.93
SCE	-2726	-7851	2726	13.4	-12.35	3.94	4.71
Peer	-2094	-6103	2094	9.96	-9.48	3.2	3.88
DT-Forward	-2588	-8836	2588	15	-11.72	5.59	6.72
NCE-SCE	-3710	-10018	3710	16.61	-16.79	4.32	5.15

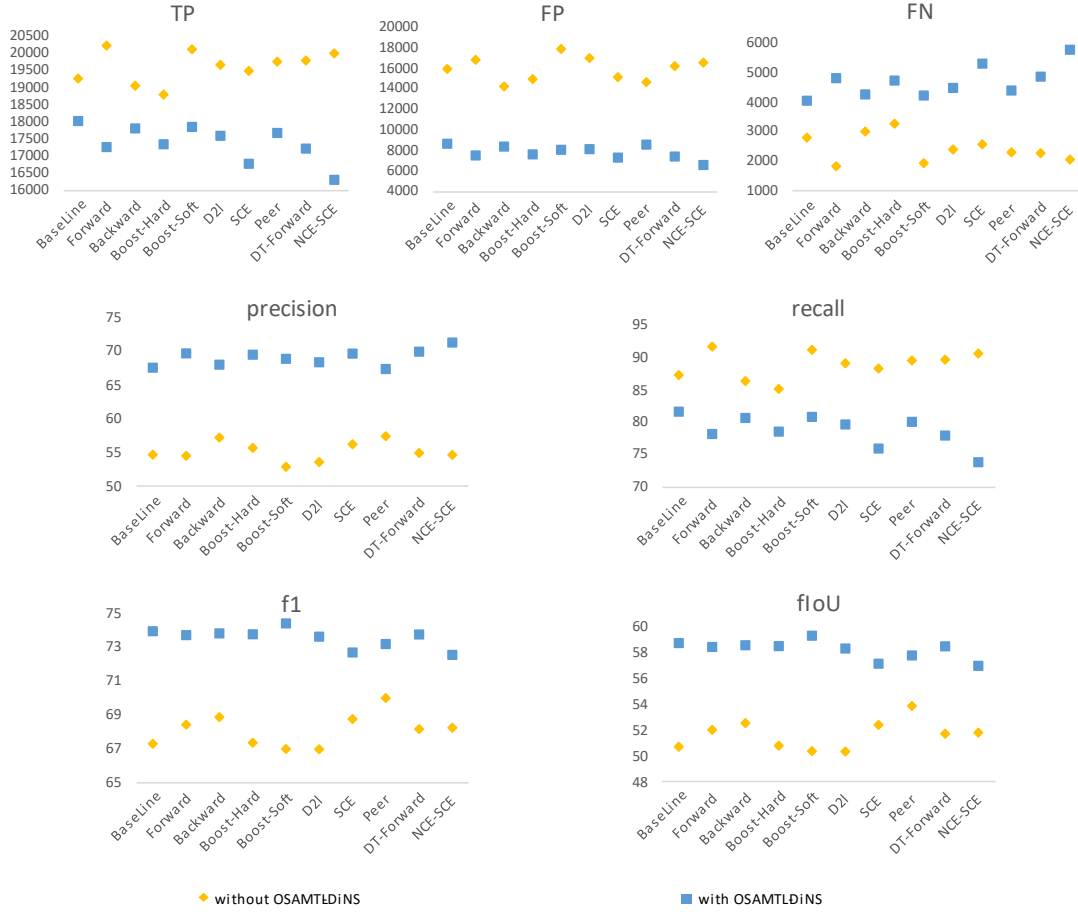


Fig. 7. Differences between Table 6 and Table 10 for validation of Task1.

Table 15. Contributions of OSAMTL-DiNS to various existing method for testing on Task1

Solution	TP	FP	FN	precision	recall	f1	floU
BaseLine	-1697	-6917	1697	13.63	-6.54	5.48	7.12
Forward	-3279	-9581	3278	17.59	-12.63	5.4	6.97
Backward	-1040	-7329	1039	15.37	-4	7.36	9.44
Boost-Hard	-1954	-6920	1954	14.24	-7.53	4.95	6.38
Boost-Soft	-3067	-9913	3067	17.73	-11.81	6.21	8.02
D2I	-2720	-8651	2720	16.09	-10.48	5.35	6.88
SCE	-3034	-7848	3033	14.97	-11.69	3.69	4.72
Peer	-2279	-6070	2279	11.37	-8.78	3.05	3.92
DT-Forward	-3322	-8892	3322	16.82	-12.8	4.52	5.84
NCE-SCE	-4683	-9858	4683	18.48	-18.04	2.63	3.35

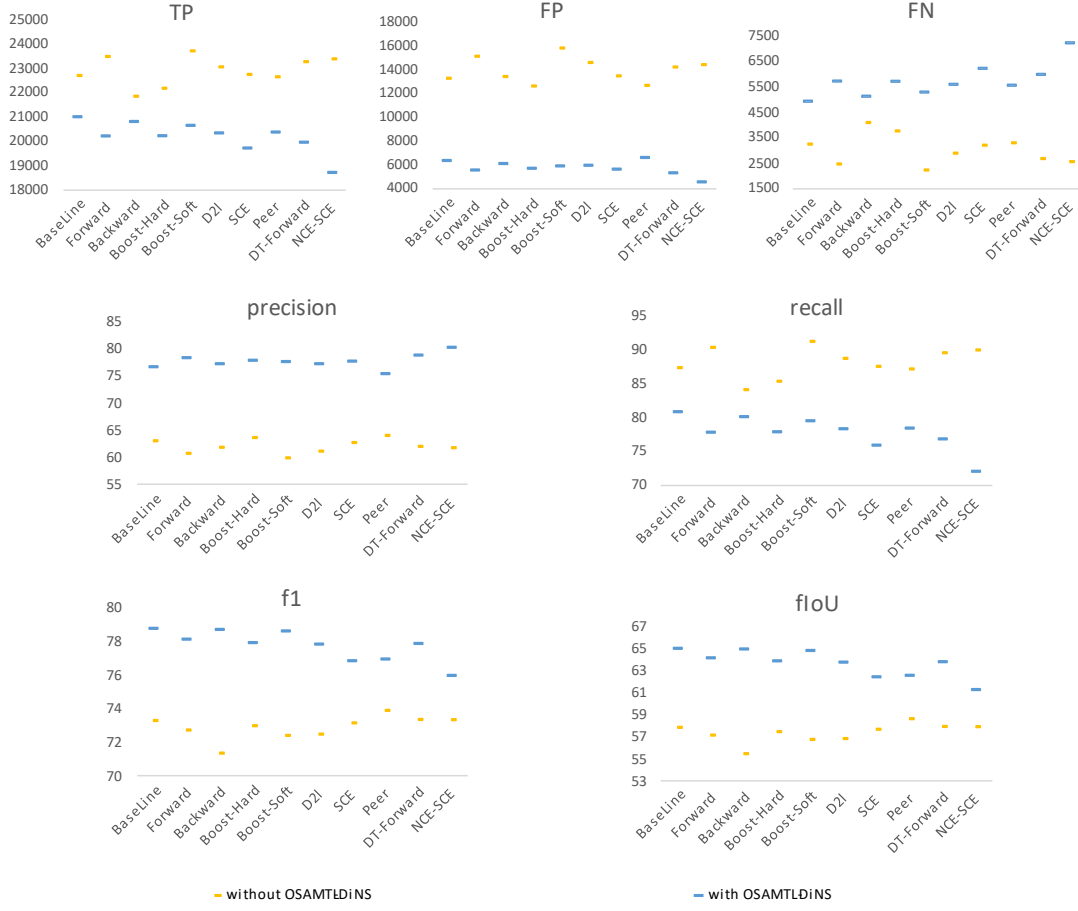


Fig. 8. Differences between Table 7 and Table 11 for testing of Task1.

Table 16. Confident intervals for contributions of OSAMTL-DiNS to various existing method on Task1

Dataset		TP	FP	FN	precision	recall	f1	floU
Validation	lower limit	-2810	-9202	1675	12.29	-12.72	4.47	5.37
	mean	-2242	-8143	2242	13.83	-10.15	5.45	6.53
	upper limit	-1674	-7085	2810	15.37	-7.58	6.42	7.68
Testing	lower limit	-3099	-9027	1876	13.74	-11.94	4.13	5.32
	mean	-2488	-8013	2488	15.31	-9.58	5.11	6.59
	upper limit	-1877	-7000	3099	16.89	-7.23	6.10	7.86

From Fig. 7, Fig. 8, Table 14, Table 15 and Table 16, we can conclude that OSAMTL-DiNS is able to enable various state-of-the-art approaches for handling complex noisy labels to achieve significantly more rational predictions for Task1 on both validation and testing, by appropriately increase the precision performance while reducing the recall performance.

3.3.2 Discussion of contributions of OSAMTL-DiNS on Task2

Similarly, we reflect the contributions of OSAMTL-DiNS on Task2 by the differences between Table 8 and Table 12 for validation and the differences between Table 9 and Table 13 for testing, which are respectively shown as Fig. 9 and Fig. 10. More specifically, the contributions of OSAMTL-DiNS on Task1 are quantitatively

evaluated by statistics of Table 12 minus statistics of Table 8 for validation and statistics of Table 13 minus statistics of Table 9 for testing, which are respectively shown as Table 17 and Table 18. And the confident intervals for the contributions of OSAMTL-DiNS on Task2 are shown in Table 19.

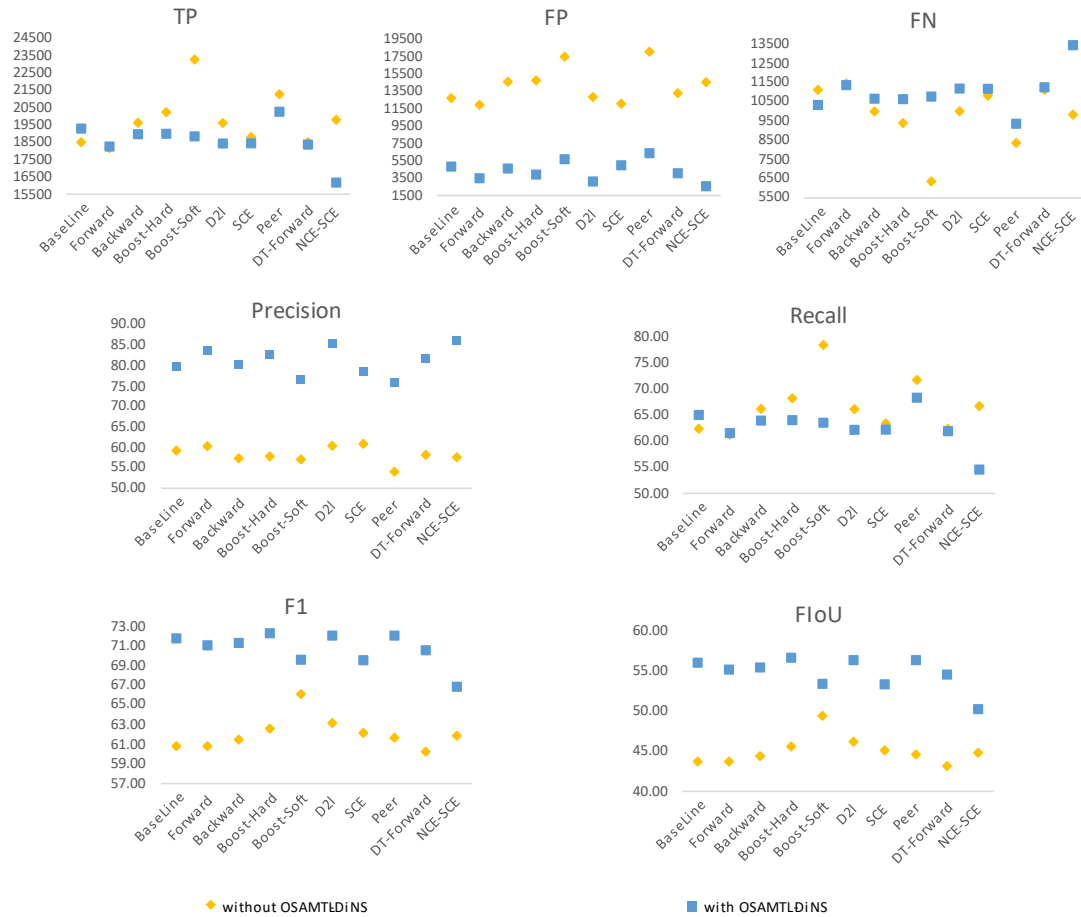


Fig. 9. Differences between Table 8 and Table 12 for validation of Task2.

Table 17. Contributions of OSAMTL-DiNS to various existing method for validation on Task2

Solution	TP	FP	FN	precision	recall	f1	fIoU
BaseLine	784	-7888	-783	20.64	2.64	10.94	12.25
Forward	81	-8465	-81	23.56	0.27	10.23	11.39
Backward	-666	-10002	666	23.05	-2.24	9.81	10.99
Boost-Hard	-1248	-10856	1248	25.00	-4.21	9.66	11.00
Boost-Soft	-4427	-11825	4426	19.68	-14.94	3.48	3.98
D2l	-1179	-9738	1180	25.05	-3.98	8.85	10.11
SCE	-358	-7096	357	17.79	-1.21	7.37	8.19
Peer	-1010	-11718	1009	21.98	-3.41	10.35	11.69
DT-Forward	-138	-9213	137	23.56	-0.46	10.28	11.35
NCE-SCE	-3624	-11999	3625	28.53	-12.23	4.98	5.41

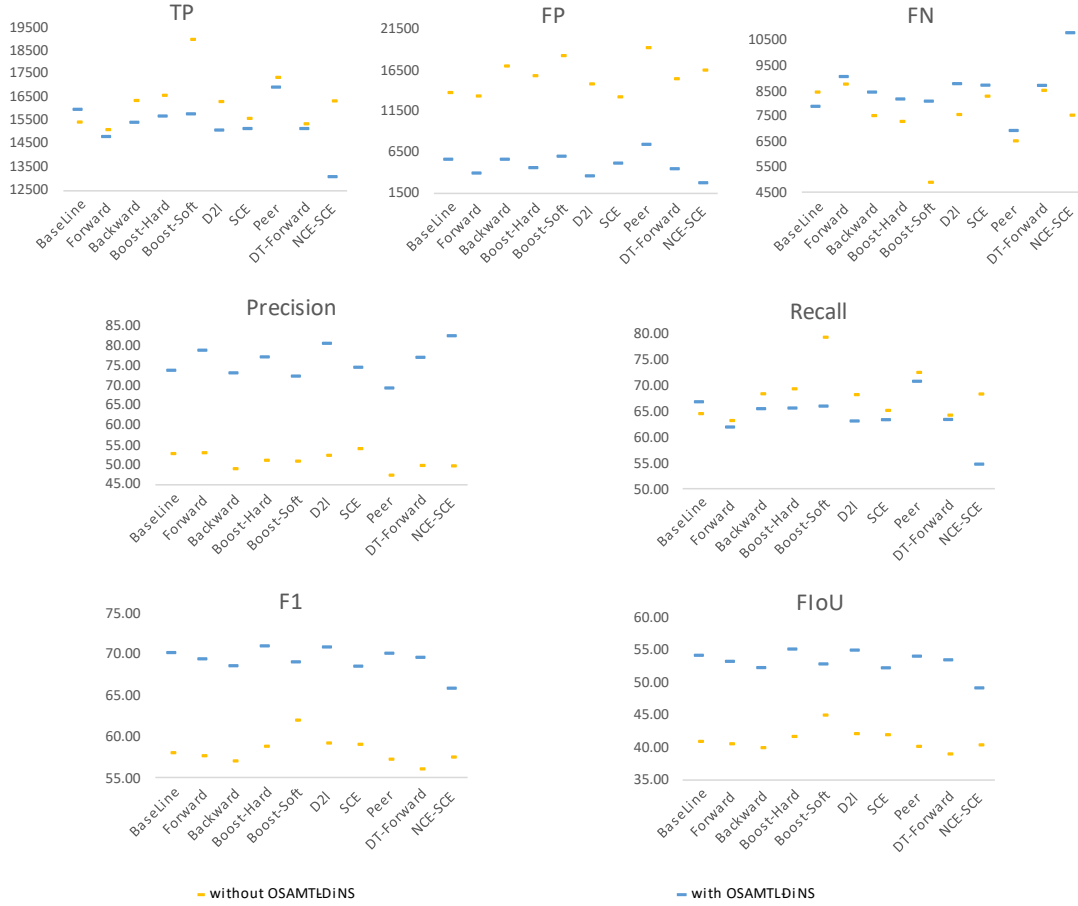


Fig. 10. Differences between Table 9 and Table 13 for testing of Task2.

Table 18. Contributions of OSAMTL-DiNS to various existing method for testing on Task2

Solution	TP	FP	FN	precision	recall	f1	fIoU
BaseLine	554	-8182	-555	21.15	2.32	12.16	13.21
Forward	-304	-9461	305	25.96	-1.27	11.77	12.67
Backward	-932	-11435	931	24.28	-2.90	11.54	12.30
Boost-Hard	-886	-11293	887	26.24	-3.71	12.19	13.40
Boost-Soft	-3201	-12336	3202	21.55	-13.39	7.07	7.84
D2l	-1222	-11277	1222	28.43	-5.12	11.64	12.82
SCE	-436	-8135	435	20.64	-1.82	9.49	10.24
Peer	-412	-11870	412	22.09	-1.72	12.85	13.87
DT-Forward	-199	-11042	199	27.44	-0.83	13.56	14.46
NCE-SCE	-3255	-13825	3255	32.99	-13.61	8.35	8.74

Table 19. Confident intervals for contributions of OSAMTL-DiNS to various existing method on Task2

Dataset		TP	FP	FN	precision	recall	f1	fIoU
Validation	lower limit	-2347	-11115	10	20.70	-7.92	6.79	7.60
	mean	-1179	-9880	1178	22.88	-3.98	8.60	9.64
	upper limit	-10	-8645	2347	25.07	-0.03	10.40	11.67
Testing	lower limit	-1928	-12176	131	22.27	-7.98	9.58	10.35
	mean	-1029	-10886	1029	25.08	-4.21	11.06	11.96

upper limit	-131	-9596	1928	27.89	-0.43	12.55	13.56
-------------	------	-------	------	-------	-------	-------	-------

From Fig. 9, Fig. 10, Table 17, Table 18 and Table 19, we can conclude that OSAMTL-DiNS is able to enable various state-of-the-art approaches for handling complex noisy labels to achieve significantly more rational predictions for Task2 on both validation and testing, by appropriately increase the precision performance while reducing the recall performance.

3.4 Discussion of generalization contributions of OSAMTL-DiNS from validation to testing

In this subsection, we show the generalization of the contributions of OSAMTL-DiNS by statistics between the contributions of OSAMTL-DiNS on validation and the contributions of OSAMTL-DiNS on testing. The results for Task1 and Task2 are respectively shown as Table 20 and Table 21.

Table 20. Statistics between the contributions of OSAMTL-DiNS on validation and the contributions of OSAMTL-DiNS on testing for Task 1

Statistics		TP	FP	FN	precision	recall	f1	fIoU
Mean	validation	-2242	-8143	2242	13.83	-10.15	5.45	6.53
	testing	-2708	-8198	2707	15.63	-10.43	4.86	6.26
P-value		0.270	0.933	0.271	0.080	0.871	0.364	0.741
Similarity		0.960	0.932	0.960	0.862	0.960	0.628	0.645

Table 21. Statistics between the contributions of OSAMTL-DiNS on validation and the contributions of OSAMTL-DiNS on testing for Task 2

Statistics		TP	FP	FN	precision	recall	f1	fIoU
Mean	validation	-1179	-9880	1178	22.88	-3.98	8.60	9.64
	testing	-1029	-10886	1029	25.08	-4.21	11.06	11.96
P-value		0.821	0.219	0.822	0.180	0.926	0.028	0.058
Similarity		0.976	0.936	0.976	0.944	0.979	0.957	0.957

From Table 20 and Table 21, we can observe that significant differences between the contributions of OSAMTL-DiNS from validation to testing for both Task1 and Task2 are quite rare (all P-values are greater than 0.01 and most P-values are greater than 0.05). As a result, the contributions of OSAMTL-DiNS on validation can be well generalized to testing.

3.5 Qualitative results and discussion

Some testing results of various state-of-the-art approaches (respectively without OSAMTL-DiNS introduced and with OSAMTL-DiNS introduced) for handling complex noisy labels on Task1 and Task2 are respectively shown as Fig. 11 and Fig. 12. From Fig. 11 and Fig. 12, we can observe that, with OSAMTL-DiNS introduced, various state-of-the-art approaches can achieve predictions that are visually more consistent with the relatively accurate labels provided by pathology experts for tumour segmentation of breast cancer.

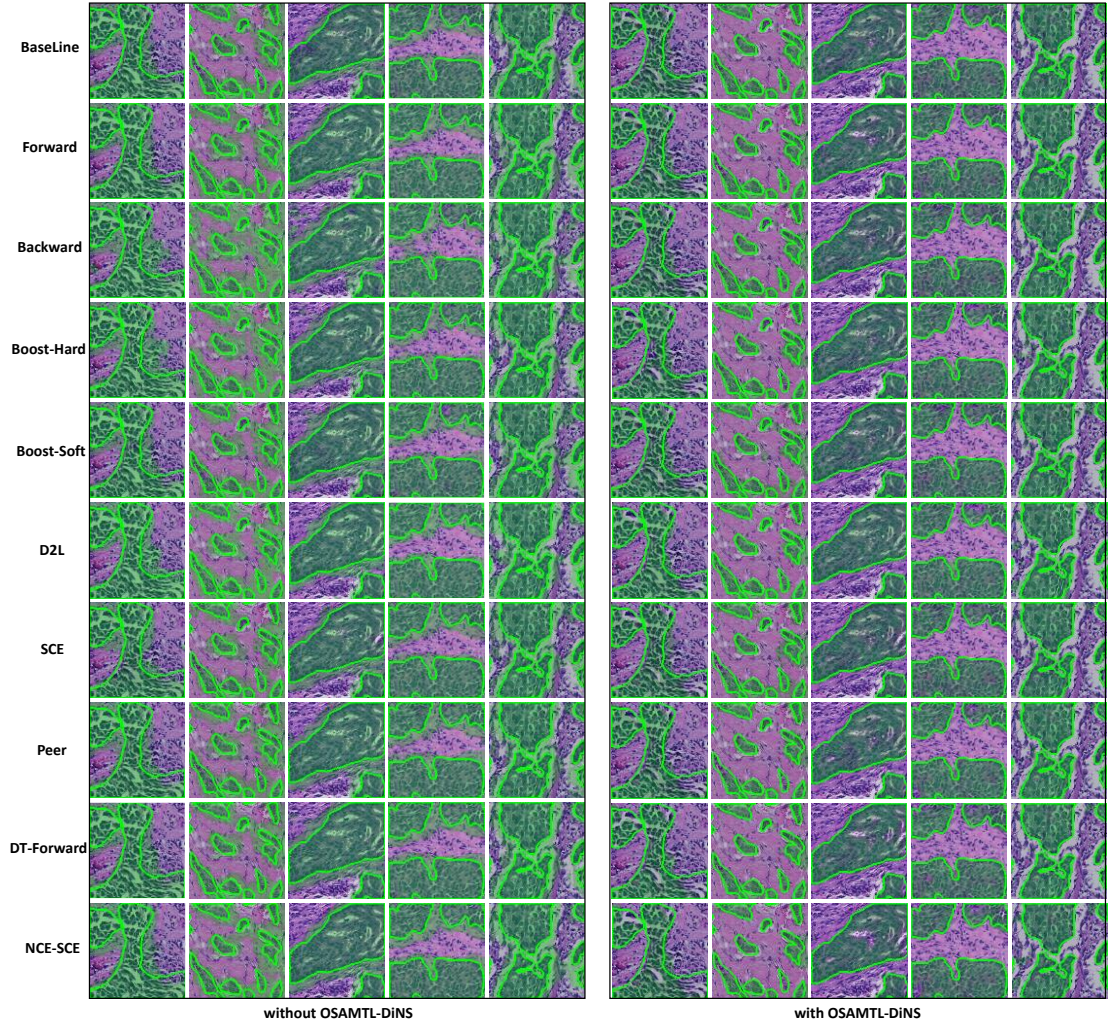


Figure. 11. Some testing results of various state-of-the-art approaches (respectively without OSAMTL-DiNS introduced and with OSAMTL-DiNS introduced) for handling complex noisy labels on Task1. Left: testing results of various state-of-the-art approaches without OSAMTL-DiNS introduced. Right: testing results of state-of-the-art approaches with OSAMTL-DiNS introduced. The green solid polygons are the relatively accurately labelled tumour areas provided by pathology experts and the green transparent masks are the tumour areas predicted by image semantic segmentation models.

3.6 Discussion of released model and its application

We released a model pretrained with OSAMTL-DiNS for tumour segmentation in HE-stained pre-treatment biopsy images in breast cancer (Task 1). The released model was based on the BaseLine solution with OSAMTL-DiNS introduced, since it showed the best generalization performance for Task 1. The release model has also been successfully applied as a pre-processing tool to extract tumour-associated stroma compartment for predicting the pathological complete response to neoadjuvant chemotherapy in breast cancer. For more details about this application, readers can refer to our paper (F. Li et al., 2022). The released model is available at <https://github.com/YongQuanYang/TS-Score>.

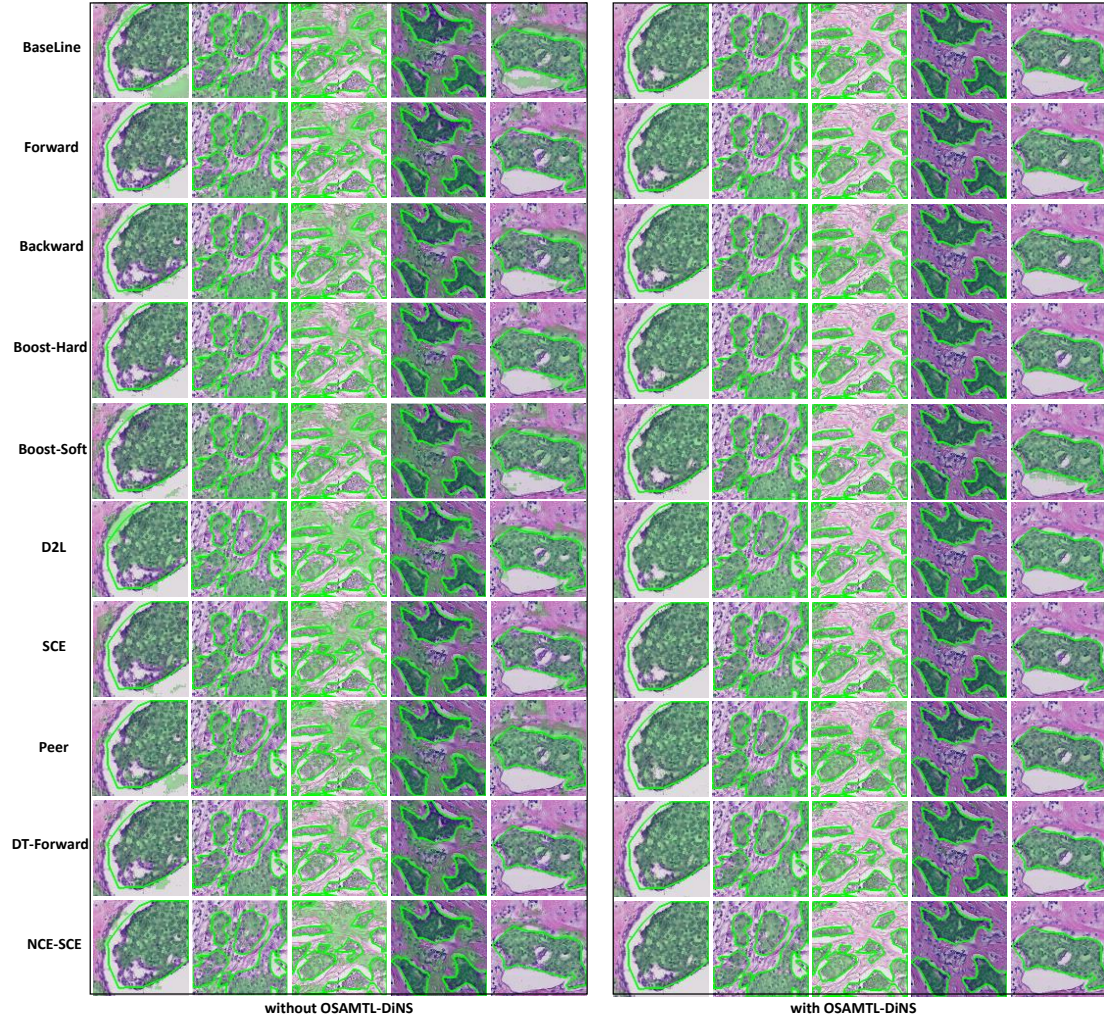


Fig. 12. Some testing results of various state-of-the-art approaches (respectively without OSAMTL-DiNS introduced and with OSAMTL-DiNS introduced) for handling complex noisy labels on Task2. Left: testing results of various state-of-the-art approaches without OSAMTL-DiNS introduced. Right: testing results of state-of-the-art approaches with OSAMTL-DiNS introduced. The green solid polygons are the relatively accurately labelled tumour areas provided by pathology experts and the green transparent masks are the tumour areas predicted by image semantic segmentation models.

4 Conclusions and Future Work

In this paper, giving definition of diverse noisy samples (DiNS), we proposed one-step abductive multi-target learning with DiNS (OSAMTL-DiNS) that expands the original OSAMTL to handle complex noisy labels of DiNS. The major advantage of OSAMTL-DiNS is that it can produce a predictive model based on very inaccurately labelled (complex noisy) data, which makes OSAMTL-DiNS suitable to address some tasks in the field of medical analysis where the problem of complex noisy in data always exists.

Based on the proposed OSAMTL-DiNS, we implemented a solution for tumour segmentation for breast cancer in medical histopathology whole slide image analysis (MHWSIA) and conducted extensive experiments. Experiment results for contributions of OSAMTL-DiNS in handling complex noisy labels show that introducing OSAMTL-DiNS to existing various methods for learning from noisy labels can significantly

enhance the abilities of these methods in handling complex noisy labels. At the meantime, experiment results for the generalization of OSAMTL-DiNS show that the contributions of OSAMTL-DiNS in handling complex noisy labels can be well generalized from validation to testing. Additionally, visualized qualitative results as well show that, with OSAMTL-DiNS introduced, various methods for learning from noisy labels can achieve predictions that are more consistent with the relatively accurate labels provided by experts. These results reflect the potential effectiveness of the proposed OSAMTL-DiNS in handling complex noisy labels in MHWSIA.

We also released a model pretrained with OSAMTL-DiNS for tumour segmentation in HE-stained pre-treatment biopsy images in breast cancer. The released model has been successfully applied as a pre-processing tool to extract tumour-associated stroma compartment for predicting the pathological complete response to neoadjuvant chemotherapy in breast cancer, which reflects the potentials of using OSAMTL-DiNS to help building basic tools for MHWSIA.

Although this work has reflected the potential effectiveness of the proposed OSAMTL-DiNS in handling complex noisy labels in MHWSIA and the potentials of using OSAMTL-DiNS to help building basic tools for MHWSIA, the more rational predictions of OSAMTL-DiNS in TSfBC was achieved by appropriately increase the precision performance while reducing the recall performance to obtain a better overall performance in fIoU. As the recall performance for a target is very important to medical evaluations, in future works, we will continue, with limited annotations, to improve the solution for tumour segmentation of breast cancer to fulfil the goal that increases the recall performance while being able to promote or at least maintain the fIoU performance.

References

- Acuna, D., Kar, A., & Fidler, S. (2019). Devil is in the edges: Learning semantic boundaries from noisy annotations. *Proceedings of the IEEE Computer Society Conference on Computer Vision and Pattern Recognition*. <https://doi.org/10.1109/CVPR.2019.01133>
- Algan, G., & Ulusoy, I. (2021). Image classification with deep learning in the presence of noisy labels: A survey. *Knowledge-Based Systems*. <https://doi.org/10.1016/j.knosys.2021.106771>
- Arazo, E., Ortego, D., Albert, P., O'Connor, N. E., & McGuinness, K. (2019). Unsupervised label noise modeling and loss correction. *36th International Conference on Machine Learning, ICML 2019*.
- Badrinarayanan, V., Kendall, A., & Cipolla, R. (2017). SegNet: A Deep Convolutional Encoder-Decoder Architecture for Image Segmentation. *IEEE Transactions on Pattern Analysis and Machine Intelligence*, 39(12), 2481–2495. <https://doi.org/10.1109/TPAMI.2016.2644615>
- Bhattacharjee, S., Hwang, Y.-B., Kim, H.-C., Choi, H.-K., Kim, D., & Cho, N.-H. (2022). Invasive Region Segmentation using Pre-trained UNet and Prognosis Analysis of Breast Cancer based on Tumor-Stroma Ratio. *2022 International Conference on Electrical, Computer and Energy Technologies (ICECET)*, 1–5. <https://doi.org/10.1109/ICECET55527.2022.9872881>

- Chen, L.-C., Papandreou, G., Kokkinos, I., Murphy, K., & Yuille, A. L. (2018). DeepLab: Semantic Image Segmentation with Deep Convolutional Nets, Atrous Convolution, and Fully Connected CRFs. *IEEE Transactions on Pattern Analysis and Machine Intelligence*, 40(4), 834–848. <https://doi.org/10.1109/TPAMI.2017.2699184>
- D’Amato, C., Bryl, V., & Serafini, L. (2012). Data-driven logical reasoning. *CEUR Workshop Proceedings*.
- Dai, W. Z., Xu, Q., Yu, Y., & Zhou, Z. H. (2019). Bridging machine learning and logical reasoning by abductive learning. *Advances in Neural Information Processing Systems*.
- de Kruijf, E. M., van Nes, J. G. H., van de Velde, C. J. H., Putter, H., Smit, V. T. H. B. M., Liefers, G. J., Kuppen, P. J. K., Tollenaar, R. A. E. M., & Mesker, W. E. (2011). Tumor–stroma ratio in the primary tumor is a prognostic factor in early breast cancer patients, especially in triple-negative carcinoma patients. *Breast Cancer Research and Treatment*, 125(3), 687–696. <https://doi.org/10.1007/s10549-010-0855-6>
- Diao, S., Tian, Y., Hu, W., Hou, J., Lambo, R., Zhang, Z., Xie, Y., Nie, X., Zhang, F., Racoceanu, D., & Qin, W. (2022). Weakly Supervised Framework for Cancer Region Detection of Hepatocellular Carcinoma in Whole-Slide Pathologic Images Based on Multiscale Attention Convolutional Neural Network. *American Journal of Pathology*. <https://doi.org/10.1016/j.ajpath.2021.11.009>
- Falk, T., Mai, D., Bensch, R., Çiçek, Ö., Abdulkadir, A., Marrakchi, Y., Böhm, A., Deubner, J., Jäkel, Z., Seiwald, K., Dovzhenko, A., Tietz, O., Dal Bosco, C., Walsh, S., Saltukoglu, D., Tay, T. L., Prinz, M., Palme, K., Simons, M., ... Ronneberger, O. (2019). U-Net: deep learning for cell counting, detection, and morphometry. *Nature Methods*. <https://doi.org/10.1038/s41592-018-0261-2>
- Frénay, B., & Verleysen, M. (2014). Classification in the presence of label noise: A survey. *IEEE Transactions on Neural Networks and Learning Systems*. <https://doi.org/10.1109/TNNLS.2013.2292894>
- Fu, J., Liu, J., Tian, H., Li, Y., Bao, Y., Fang, Z., & Lu, H. (2019). Dual attention network for scene segmentation. *Proceedings of the IEEE Computer Society Conference on Computer Vision and Pattern Recognition*. <https://doi.org/10.1109/CVPR.2019.00326>
- Hanna, M. G., Parwani, A., & Sirintrapun, S. J. (2020). Whole Slide Imaging: Technology and Applications. In *Advances in Anatomic Pathology*. <https://doi.org/10.1097/PAP.0000000000000273>
- Huang, Y. X., Dai, W. Z., Yang, J., Cai, L. W., Cheng, S., Huang, R., Li, Y. F., & Zhou, Z. H. (2020). Semi-supervised abductive learning and its application to theft judicial sentencing. *Proceedings - IEEE International Conference on Data Mining, ICDM*. <https://doi.org/10.1109/ICDM50108.2020.00127>
- Karimi, D., Dou, H., Warfield, S. K., & Gholipour, A. (2020). Deep learning with noisy labels: Exploring techniques and remedies in medical image analysis. *Medical Image Analysis*, 65, 101759. <https://doi.org/10.1016/j.media.2020.101759>
- Kingma, D. P., & Ba, J. L. (2015). Adam: A method for stochastic gradient descent. *ICLR: International Conference on Learning Representations*.
- LeCun, Y., Bengio, Y., & Hinton, G. (2015). Deep learning. *Nature*, 521(7553), 436–444. <https://doi.org/10.1038/nature14539>
- Li, J., Socher, R., & Hoi, S. C. (2020). Dividemix: Learning with noisy labels as semi-supervised learning. *ICLR*.

- Li, D., Deng, K., Zhao, M., Zhang, S., & Zhu, J. (2020). *Knowledge-Driven Machine Learning: Concept, Model and Case Study on Channel Estimation*. <http://arxiv.org/abs/2012.11178>
- Li, F., Yang, Y., Wei, Y., Zhao, Y., Fu, J., Xiao, X., Zheng, Z., & Bu, H. (2022). Predicting neoadjuvant chemotherapy benefit using deep learning from stromal histology in breast cancer. *Npj Breast Cancer*, 8(1), 124. <https://doi.org/10.1038/s41523-022-00491-1>
- Liu, Y., & Guo, H. (2020). Peer loss functions: Learning from noisy labels without knowing noise rates. *37th International Conference on Machine Learning, ICML 2020*.
- Ma, X., Huang, H., Wang, Y., Erfani, S. R. S., & Bailey, J. (2020). Normalized loss functions for deep learning with noisy labels. *37th International Conference on Machine Learning, ICML 2020*.
- Ma, X., Wang, Y., Houle, M. E., Zhou, S., Erfani, S. M., Xia, S. T., Wijewickrema, S., & Bailey, J. (2018). Dimensionality-Driven learning with noisy labels. *35th International Conference on Machine Learning, ICML 2018*.
- Patrini, G., Rozza, A., Menon, A. K., Nock, R., & Qu, L. (2017). Making deep neural networks robust to label noise: A loss correction approach. *Proceedings - 30th IEEE Conference on Computer Vision and Pattern Recognition, CVPR 2017*. <https://doi.org/10.1109/CVPR.2017.240>
- Priego-Torres, B. M., Lobato-Delgado, B., Atienza-Cuevas, L., & Sanchez-Morillo, D. (2022). Deep learning-based instance segmentation for the precise automated quantification of digital breast cancer immunohistochemistry images. *Expert Systems with Applications*. <https://doi.org/10.1016/j.eswa.2021.116471>
- Priego-Torres, B. M., Sanchez-Morillo, D., Fernandez-Granero, M. A., & Garcia-Rojo, M. (2020). Automatic segmentation of whole-slide H&E stained breast histopathology images using a deep convolutional neural network architecture. *Expert Systems with Applications*. <https://doi.org/10.1016/j.eswa.2020.113387>
- Pu, S., Wang, K., Liu, Y., Liao, X., Chen, H., He, J., & Zhang, J. (2020). Nomogram-derived prediction of pathologic complete response (pCR) in breast cancer patients treated with neoadjuvant chemotherapy (NCT). *BMC Cancer*. <https://doi.org/10.1186/s12885-020-07621-7>
- Reed, S. E., Lee, H., Anguelov, D., Szegedy, C., Erhan, D., & Rabinovich, A. (2015). Training deep neural networks on noisy labels with bootstrapping. *3rd International Conference on Learning Representations, ICLR 2015 - Workshop Track Proceedings*.
- Rips, L. J. (1983). Cognitive processes in propositional reasoning. *Psychological Review*, 90(1), 38–71. <https://doi.org/10.1037/0033-295X.90.1.38>
- Shelhamer, E., Long, J., & Darrell, T. (2017). Fully Convolutional Networks for Semantic Segmentation. *IEEE Transactions on Pattern Analysis and Machine Intelligence*, 39(4), 640–651. <https://doi.org/10.1109/TPAMI.2016.2572683>
- Song, H., Kim, M., Park, D., Shin, Y., & Lee, J.-G. (2022). Learning From Noisy Labels With Deep Neural Networks: A Survey. *IEEE Transactions on Neural Networks and Learning Systems*, 1–19. <https://doi.org/10.1109/TNNLS.2022.3152527>
- Sukhbaatar, S., & Fergus, R. (2014). Learning from Noisy Labels with Deep Neural Networks. *ArXiv Preprint*.
- Wang, Y., Ma, X., Chen, Z., Luo, Y., Yi, J., & Bailey, J. (2019). Symmetric cross entropy for robust learning with noisy labels. *Proceedings of the IEEE International Conference on Computer Vision*. <https://doi.org/10.1109/ICCV.2019.00041>

- Wichmann, F. A., Graf, A. B. A., Simoncelli, E. P., Bülthoff, H. H., & Schölkopf, B. (2005). Machine learning applied to perception: Decision-images for gender classification. *Advances in Neural Information Processing Systems*.
- Xiao, T., Xia, T., Yang, Y., Huang, C., & Wang, X. (2015). Learning from massive noisy labeled data for image classification. *Proceedings of the IEEE Computer Society Conference on Computer Vision and Pattern Recognition*. <https://doi.org/10.1109/CVPR.2015.7298885>
- Xu, G., Song, Z., Sun, Z., Ku, C., Yang, Z., Liu, C., Wang, S., Ma, J., & Xu, W. (2019). CAMEL: A weakly supervised learning framework for histopathology image segmentation. *Proceedings of the IEEE International Conference on Computer Vision*. <https://doi.org/10.1109/ICCV.2019.01078>
- Xu, Y., Zhu, J. Y., Chang, E. I. C., Lai, M., & Tu, Z. (2014). Weakly supervised histopathology cancer image segmentation and classification. *Medical Image Analysis*. <https://doi.org/10.1016/j.media.2014.01.010>
- Yang, Y., Yang, Y., Chen, J., Zheng, J., & Zheng, Z. (2020). *Handling Noisy Labels via One-Step Abductive Multi-Target Learning: An Application to Helicobacter Pylori Segmentation*. <http://arxiv.org/abs/2011.14956>
- Yang, Y., Yang, Y., Yuan, Y., Zheng, J., & Zhongxi, Z. (2020). Detecting helicobacter pylori in whole slide images via weakly supervised multi-task learning. *Multimedia Tools and Applications*, 79(35–36), 26787–26815. <https://doi.org/10.1007/s11042-020-09185-x>
- Yao, Y., Liu, T., Han, B., Gong, M., Deng, J., Niu, G., & Sugiyama, M. (2020). Dual T: Reducing estimation error for transition matrix in label-noise learning. *Advances in Neural Information Processing Systems*.
- Yau, C., Osdoit, M., van der Noordaa, M., Shad, S., Wei, J., de Croze, D., Hamy, A.-S., Laé, M., Rey, F., Sonke, G. S., Steenbruggen, T. G., van Seijen, M., Wesseling, J., Martín, M., del Monte-Millán, M., López-Tarruella, S., Boughey, J. C., Goetz, M. P., Hoskin, T., ... Zeck, J. C. (2022). Residual cancer burden after neoadjuvant chemotherapy and long-term survival outcomes in breast cancer: a multicentre pooled analysis of 5161 patients. *The Lancet Oncology*, 23(1), 149–160. [https://doi.org/10.1016/S1470-2045\(21\)00589-1](https://doi.org/10.1016/S1470-2045(21)00589-1)
- Zhao, H., Shi, J., Qi, X., Wang, X., & Jia, J. (2017). Pyramid Scene Parsing Network. *2017 IEEE Conference on Computer Vision and Pattern Recognition (CVPR)*, 6230–6239. <https://doi.org/10.1109/CVPR.2017.660>
- Zhou, Z. H. (2019). Abductive learning: towards bridging machine learning and logical reasoning. *Science China Information Sciences*. <https://doi.org/10.1007/s11432-018-9801-4>

Supplementary 1

Preliminary of Logical Reasoning

We introduce some propositional connectives and rules for proof of propositional logical reasoning, which are respectively shown as Table 1 and Table 2, for the logical reasonings conducted in this paper.

Table 1. Propositional connectives

Connective	Meaning
\wedge	conjunction
\rightarrow	implication

Table 2. Rules for proof of propositional logical reasoning, \vdash denotes ‘bring out’

Rule	Meaning
$\wedge -$	reductive law of conjunction: $A \wedge B, \vdash A$ or B .
$\wedge +$	additional law of conjunction: $A, B, \vdash A \wedge B$.
MP	modus ponens: $A \rightarrow B, A, \vdash B$.
HS	hypothetical syllogism: $A \rightarrow B, B \rightarrow C, \vdash A \rightarrow C$.

Proof of Reasoning 1

Reasoning 1. *If G_1 is given and KB is given, then inconsistency between the false tumour negatives covered by $G_{1,1}$ and the false tumour negatives covered by KB is low, inconsistency between the false tumour positives covered by $G_{1,2}$ and the false tumour positives covered by KB is high, inconsistency between the true tumour positives covered by $G_{1,2}$ and the true tumour positives covered by KB is low, and inconsistency between the true tumour negatives covered by $G_{1,1}$ and the true tumour negatives covered by KB is high.*

Proof-R1. Firstly, with G_1 and KB, we have following derived preconditions for Reasoning 1.

1. If G_1 is given, then $NS_1 = \{IS_1, NLS_1\}$ exists. (G_1 is associated with NS_1 in Grounding Extract)
2. If $NS_1 = \{IS_1, NLS_1\}$ exists, then NLS_1 can exclude tumour negatives of IS_1 as accurate as possible, and NLS_1 can include many tumour negatives of IS_1 as tumour positives. (facts contained in the existing NS_1)
3. If G_1 is given, then $G_{1,1}$: pixels of IS_1 outside the polygons of NLS_1 are tumour negatives is given, and $G_{1,2}$: pixels of IS_1 inside the polygons of NLS_1 are tumour positives is given. (groundings extracted from NS_1 by Grounding Extract)
4. If $G_{1,1}$: pixels of IS_1 outside the polygons of NLS_1 are tumour negatives is given, and $G_{1,2}$: pixels of IS_1 inside the polygons of NLS_1 are tumour positives is given, then $G_{1,1}$ and $G_{1,2}$ are complementary to each other.

5. If NLS_1 can exclude tumour negatives of IS_1 as accurate as possible, and $G_{1,1}$: pixels of IS_1 outside the polygons of NLS_1 are tumour negatives is given, then false tumour negatives covered by $G_{1,1}$ are rare.
6. If NLS_1 can include many tumour negatives of IS_1 as tumour positives, and $G_{1,2}$: pixels of IS_1 inside the polygons of NLS_1 are tumour positives is given, then false tumour positives covered by $G_{1,2}$ are many.
7. If false tumour negatives covered by $G_{1,1}$ are rare, and $G_{1,1}$ and $G_{1,2}$ are complementary to each other, then $G_{1,2}$ covers almost all true tumour positives.
8. If false tumour positives covered by $G_{1,2}$ are many, and $G_{1,1}$ and $G_{1,2}$ are complementary to each other, then $G_{1,1}$ covers only a part of true tumour negatives.
9. If KB is given, then the information of KB can clearly describe what are the true tumour positives, and the opposite information of KB can clearly describe what are the true tumour negatives. (facts contained in the given KB)
10. If the information of KB can clearly describe what are the true tumour positives, then true tumour positives covered by KB are all-sided, and false tumour negatives covered by KB are none.
11. If the opposite information of KB can clearly describe what are the true tumour negatives, then true tumour negatives covered by KB are all-sided, and false tumour positives covered by KB are none.
12. If false tumour negatives covered by $G_{1,1}$ are rare, and false tumour negatives covered by KB are none, then inconsistency between the false tumour negatives covered by $G_{1,1}$ and the false tumour negatives covered by KB is low.
13. If false tumour positives covered by $G_{1,2}$ are many, and false tumour positives covered by KB are none, then inconsistency between false tumour positives covered by $G_{1,2}$ and the false tumour positives covered by KB is high.
14. If $G_{1,2}$ covers almost all true tumour positives, and true tumour positives covered by KB are all-sided, then inconsistency between the true tumour positives covered by $G_{1,2}$ and the true tumour positives covered by KB is low.
15. If $G_{1,1}$ covers only a part of true tumour negatives, and true tumour negatives covered by KB are all-sided, then inconsistency between true tumour negatives covered by $G_{1,1}$ and the true tumour negatives covered by KB is high.

Secondly, we give the propositional symbols for the above preconditions 1-15 for Reasoning 1, which are shown in Table 3.

Table 3. Propositional symbols of preconditions for Reasoning 1

Symbol	Meaning
a	G_1 is given
b	$NS_1 = \{IS_1, NLS_1\}$ exists
c	NLS_1 can exclude tumour negatives of IS_1 as accurate as possible
d	NLS_1 can include many tumour negatives of IS_1 as tumour positives
e	$G_{1,1}$: pixels of IS_1 outside the polygons of NLS_1 are tumour negatives is given
f	$G_{1,2}$: pixels of IS_1 inside the polygons of NLS_1 are tumour positives is given

<i>g</i>	$G_{1,1}$ and $G_{1,2}$ are complementary to each other
<i>h</i>	false tumour negatives covered by $G_{1,1}$ are rare
<i>i</i>	false tumour positives covered by $G_{1,2}$ are many
<i>j</i>	$G_{1,2}$ covers almost all true tumour positives
<i>k</i>	$G_{1,1}$ covers only a part of true tumour negatives
<i>l</i>	KB is given
<i>m</i>	the information of KB can clearly describe what are the true tumour positives
<i>n</i>	the opposite information of KB can clearly describe what are the true tumour negatives
<i>o</i>	true tumour positives covered by KB are all-sided
<i>p</i>	false tumour negatives covered by KB are none
<i>q</i>	true tumour negatives covered by KB are all-sided
<i>r</i>	false tumour positives covered by KB are none
<i>s</i>	inconsistency between the false tumour negatives covered by $G_{1,1}$ and the false tumour negatives covered by KB is low
<i>t</i>	inconsistency between false tumour positives covered by $G_{1,2}$ and the false tumour positives covered by KB is high
<i>u</i>	inconsistency between the true tumour positives covered by $G_{1,2}$ and the true tumour positives covered by KB is low
<i>v</i>	inconsistency between true tumour negatives covered by $G_{1,1}$ and the true tumour negatives covered by KB is high

Thirdly, referring to Table 3, we signify the propositional formalizations of the preconditions 1-15 for Reasoning 1 and Reasoning 1 via the propositional connectives listed in Table 1 as follows.

1) $a \rightarrow b$	Precondition
2) $b \rightarrow (c \wedge d)$	Precondition
3) $a \rightarrow (e \wedge f)$	Precondition
4) $(e \wedge f) \rightarrow g$	Precondition
5) $(c \wedge e) \rightarrow h$	Precondition
6) $(d \wedge f) \rightarrow i$	Precondition
7) $(h \wedge g) \rightarrow j$	Precondition
8) $(i \wedge g) \rightarrow k$	Precondition
9) $l \rightarrow (m \wedge n)$	Precondition
10) $m \rightarrow (o \wedge p)$	Precondition
11) $n \rightarrow (q \wedge r)$	Precondition
12) $(h \wedge p) \rightarrow s$	Precondition
13) $(i \wedge r) \rightarrow t$	Precondition
14) $(j \wedge o) \rightarrow u$	Precondition
15) $(k \wedge q) \rightarrow v$	Precondition
$(a \wedge l) \rightarrow (s \wedge t \wedge u \wedge v)$	Reasoning 1

Fourthly, we show the validity of Reasoning 1 via the rules for proof of propositional logical reasoning listed in Table 3 as follows.

$\therefore (a \wedge l) \rightarrow (s \wedge t \wedge u \wedge v)$	
16) $a \wedge l$	Hypothesis
17) a	16); $\wedge -$
18) l	16); $\wedge -$
19) $a \rightarrow (c \wedge d)$	1), 2); HS

20) $c \wedge d$	19),17); MP
21) $e \wedge f$	3),17); MP
22) c	20); $\wedge -$
23) d	20); $\wedge -$
24) e	21); $\wedge -$
25) f	21); $\wedge -$
26) $c \wedge e$	22),24); $\wedge +$
27) $d \wedge f$	23),25); $\wedge +$
28) h	5),26); MP
29) i	6),27); MP
30) $a \rightarrow g$	3),4); HS
31) g	30),17); MP
32) $h \wedge g$	28),31); $\wedge +$
33) $i \wedge g$	29),31); $\wedge +$
34) j	7),32); MP
35) k	8),33); MP
36) $m \wedge n$	9),18); MP
37) m	36); $\wedge -$
38) n	36); $\wedge -$
39) $o \wedge p$	10),37); MP
40) $q \wedge r$	11),38); MP
41) o	39); $\wedge -$
42) p	39); $\wedge -$
43) q	40); $\wedge -$
44) r	40); $\wedge -$
45) $h \wedge p$	28),42); $\wedge +$
46) $i \wedge r$	29),44); $\wedge +$
47) $j \wedge o$	34),41); $\wedge +$
48) $k \wedge q$	35),43); $\wedge +$
49) s	12),45); MP
50) t	13),46); MP
51) u	14),47); MP
52) v	15),48); MP
53) $s \wedge t \wedge u \wedge v$	49),50),51),52); $\wedge +$
54) $(a \wedge l) \rightarrow (s \wedge t \wedge u \wedge v)$	16)-53); Conditional Proof

Since the hypothesis $a \wedge l$ of the 16) step can be fulfilled by the input materials of OSAMTL-DiNS applied on tumour segmentation for breast cancer and Grounding Extract, Reasoning 1 is proved to be valid.

Proof of Reasoning 2

Reasoning 2. *If G_2 is given and KB is given, then inconsistency between the false tumour positives covered by $G_{2,1}$ and the false tumour positives covered by KB is low, inconsistency between the false tumour negatives covered by $G_{2,2}$ and the false tumour*

negatives covered by KB is high, inconsistency between the true tumour negatives covered by $G_{2,2}$ and the true tumour negatives covered by KB is low, and inconsistency between the true tumour positives covered by $G_{1,1}$ and the true tumour positives covered by KB is high.

Proof-R2. Firstly, with G_2 and KB , we have following derived preconditions for Reasoning 2.

1. If G_2 is given, then $NS_2 = \{IS_2, NLS_2\}$ exists. (G_2 is associated with NS_2 in Grounding Extract)
2. If $NS_2 = \{IS_2, NLS_2\}$ exists, then NLS_2 can include tumour negatives of IS_2 as accurate as possible, and NLS_2 can exclude many tumour positives of IS_2 as tumour negatives. (facts contained in the existing NS_2)
3. If G_2 is given, then $G_{2,1}$: pixels of IS_2 inside the polygons of NLS_2 are tumour positives is given, and $G_{2,2}$: pixels of IS_2 outside the polygons of NLS_2 are tumour negatives is given. (groundings extracted from NS_2 by Grounding Extract)
4. If $G_{2,1}$: pixels of IS_2 inside the polygons of NLS_2 are tumour positives is given, and $G_{2,2}$: pixels of IS_2 outside the polygons of NLS_2 are tumour negatives is given, then $G_{2,1}$ and $G_{2,2}$ are complementary to each other.
5. If NLS_2 can include tumour negatives of IS_2 as accurate as possible, and $G_{2,1}$: pixels of IS_2 inside the polygons of NLS_2 are tumour positives is given, then false tumour positives covered by $G_{2,1}$ are rare.
6. If NLS_2 can exclude many tumour positives of IS_2 as tumour negatives, and $G_{2,2}$: pixels of IS_2 outside the polygons of NLS_2 are tumour negatives is given, then false tumour negatives covered by $G_{2,2}$ are many.
7. If false tumour positives covered by $G_{2,1}$ are rare, and $G_{2,1}$ and $G_{2,2}$ are complementary to each other, then $G_{2,2}$ covers almost all true tumour negatives.
8. If false tumour negatives covered by $G_{2,2}$ are many, and $G_{2,1}$ and $G_{2,2}$ are complementary to each other, then $G_{2,1}$ covers only a part of true tumour positives.
9. If KB is given, then the information of KB can clearly describe what are the true tumour positives, and the opposite information of KB can clearly describe what are the true tumour negatives. (facts contained in the given KB)
10. If the information of KB can clearly describe what are the true tumour positives, then true tumour positives covered by KB are all-sided, and false tumour negatives covered by KB are none.
11. If the opposite information of KB can clearly describe what are the true tumour negatives, then true tumour negatives covered by KB are all-sided, and false tumour positives covered by KB are none.
12. If false tumour positives covered by $G_{2,1}$ are rare, and false tumour positives covered by KB are none, then inconsistency between the false tumour positives covered by $G_{2,1}$ and the false tumour positives covered by KB is low.

13. If false tumour negatives covered by $G_{2,2}$ are many, and false tumour negatives covered by KB are none, then inconsistency between false tumour negatives covered by $G_{2,2}$ and the false tumour negatives covered by KB is high.
14. If $G_{2,2}$ covers almost all true tumour negatives, and true tumour negatives covered by KB are all-sided, then inconsistency between the true tumour negatives covered by $G_{2,2}$ and the true tumour negatives covered by KB is low.
15. If $G_{2,1}$ covers only a part of true tumour positives, and true tumour positives covered by KB are all-sided, then inconsistency between true tumour positives covered by $G_{2,1}$ and the true tumour positives covered by KB is high.

Secondly, we give the propositional symbols for the above preconditions 1-15 for Reasoning 2, which are shown in Table 3.

Table 3. Propositional symbols of preconditions for Reasoning 2

Symbol	Meaning
a	G_2 is given
b	$NS_2 = \{IS_2, NLS_2\}$ exists
c	NLS_2 can include tumour negatives of IS_2 as accurate as possible
d	NLS_2 can exclude many tumour positives of IS_2 as tumour negatives
e	$G_{2,1}$: pixels of IS_2 inside the polygons of NLS_2 are tumour positives is given
f	$G_{2,2}$: pixels of IS_2 outside the polygons of NLS_2 are tumour negatives is given
g	$G_{2,1}$ and $G_{2,2}$ are complementary to each other
h	false tumour positives covered by $G_{2,1}$ are rare
i	false tumour negatives covered by $G_{2,2}$ are many
j	$G_{2,2}$ covers almost all true tumour negatives
k	$G_{2,1}$ covers only a part of true tumour positives
l	KB is given
m	the information of KB can clearly describe what are the true tumour positives
n	the opposite information of KB can clearly describe what are the true tumour negatives
o	true tumour positives covered by KB are all-sided
p	false tumour negatives covered by KB are none
q	true tumour negatives covered by KB are all-sided
r	false tumour positives covered by KB are none
s	inconsistency between the false tumour positives covered by $G_{2,1}$ and the false tumour positives covered by KB is low
t	inconsistency between false tumour negatives covered by $G_{2,2}$ and the false tumour negatives covered by KB is high
u	inconsistency between the true tumour negatives covered by $G_{2,2}$ and the true tumour negatives covered by KB is low
v	inconsistency between true tumour positives covered by $G_{2,1}$ and the true tumour positives covered by KB is high

Thirdly, referring to Table 3, we signify the propositional formalizations of the preconditions 1-15 for Reasoning 2 and Reasoning 2 via the propositional connectives listed in Table 1 as follows.

- 1) $a \rightarrow b$ Precondition
- 2) $b \rightarrow (c \wedge d)$ Precondition
- 3) $a \rightarrow (e \wedge f)$ Precondition
- 4) $(e \wedge f) \rightarrow g$ Precondition

5) $(c \wedge e) \rightarrow h$	Precondition
6) $(d \wedge f) \rightarrow i$	Precondition
7) $(h \wedge g) \rightarrow j$	Precondition
8) $(i \wedge g) \rightarrow k$	Precondition
9) $l \rightarrow (m \wedge n)$	Precondition
10) $m \rightarrow (o \wedge p)$	Precondition
11) $n \rightarrow (q \wedge r)$	Precondition
12) $(h \wedge r) \rightarrow s$	Precondition
13) $(i \wedge p) \rightarrow t$	Precondition
14) $(j \wedge q) \rightarrow u$	Precondition
15) $(k \wedge o) \rightarrow v$	Precondition
$(a \wedge l) \rightarrow (s \wedge t \wedge u \wedge v)$	Reasoning 2

Fourthly, we show the validity of Reasoning 1 via the rules for proof of propositional logical reasoning listed in Table 3 as follows.

$\therefore (a \wedge l) \rightarrow (s \wedge t \wedge u \wedge v)$

16) $a \wedge l$	Hypothesis
17) a	16); $\wedge -$
18) l	16); $\wedge -$
19) $a \rightarrow (c \wedge d)$	1),2); HS
20) $c \wedge d$	19),17); MP
21) $e \wedge f$	3),17); MP
22) c	20); $\wedge -$
23) d	20); $\wedge -$
24) e	21); $\wedge -$
25) f	21); $\wedge -$
26) $c \wedge e$	22),24); $\wedge +$
27) $d \wedge f$	23),25); $\wedge +$
28) h	5),26); MP
29) i	6),27); MP
30) $a \rightarrow g$	3),4); HS
31) g	30),17); MP
32) $h \wedge g$	28),31); $\wedge +$
33) $i \wedge g$	29),31); $\wedge +$
34) j	7),32); MP
35) k	8),33); MP
36) $m \wedge n$	9),18); MP
37) m	36); $\wedge -$
38) n	36); $\wedge -$
39) $o \wedge p$	10),37); MP
40) $q \wedge r$	11),38); MP
41) o	39); $\wedge -$
42) p	39); $\wedge -$
43) q	40); $\wedge -$

44) r	40); $\wedge -$
45) $h \wedge r$	28),44); $\wedge +$
46) $i \wedge p$	29),42); $\wedge +$
47) $j \wedge q$	34),43); $\wedge +$
48) $k \wedge o$	35),41); $\wedge +$
49) s	12),45); MP
50) t	13),46); MP
51) u	14),47); MP
52) v	15),48); MP
53) $s \wedge t \wedge u \wedge v$	49),50),51),52); $\wedge +$
54) $(a \wedge l) \rightarrow (s \wedge t \wedge u \wedge v)$	16)-53); Conditional Proof

Since the hypothesis $a \wedge l$ of the 16) step can be fulfilled by the input materials of OSAMTL-DiNS applied on tumour segmentation for breast cancer and Grounding Extract, Reasoning 2 is proved to be valid.

Proof of Reasoning 3

Reasoning 3. *If IC_1 is given, then $G_{1,1}$ should not be revised to remain $IC_{1,1}$, $G_{1,2}$ should not be revised to remain $IC_{1,3}$, $G_{1,1}$ should be revised to reduce $IC_{1,4}$, and $G_{1,2}$ should be revised to reduce $IC_{1,2}$.*

Proof-R3. Firstly, with IC_1 , we have following derived preconditions for Reasoning 3.

1. If IC_1 is given, then G_1 exists. (IC_1 is associated with G_1 in Reasoning)
2. If IC_1 is given, then $IC_{1,1}$ is given, $IC_{1,2}$ is given, $IC_{1,3}$ is given, and $IC_{1,4}$ is given.
3. If G_1 exists, then $G_{1,1}$ exists, and $G_{1,2}$ exists.
4. If $IC_{1,1}$ is given, then inconsistency between the false tumour negatives covered by $G_{1,1}$ and the false tumour negatives covered by KB is low. (inconsistency estimated by Reasoning)
5. If $G_{1,1}$ exists, and inconsistency between the false tumour negatives covered by $G_{1,1}$ and the false tumour negatives covered by KB is low, then $G_{1,1}$ should not be revised to remain $IC_{1,1}$.
6. If $IC_{1,3}$ is given, then inconsistency between the true tumour positives covered by $G_{1,2}$ and the true tumour positives covered by KB is low. (inconsistency estimated by Reasoning)
7. If $G_{1,2}$ is given, and inconsistency between the true tumour positives covered by $G_{1,2}$ and the true tumour positives covered by KB is low, then $G_{1,2}$ should not be revised to remain $IC_{1,3}$.
8. If $IC_{1,2}$ is given, then inconsistency between the false tumour positives covered by $G_{1,2}$ and the false tumour positives covered by KB is high. (inconsistency estimated by Reasoning)

9. If $G_{1,2}$ exists, and inconsistency between the false tumour positives covered by $G_{1,2}$ and the false tumour positives covered by KB is high, then $G_{1,2}$ should be revised to reduce $IC_{1,2}$.
10. If $IC_{1,4}$ is given, then inconsistency between the true tumour negatives covered by $G_{1,1}$ and the true tumour negatives covered by KB is high. (inconsistency estimated by Reasoning)
11. If $G_{1,1}$ exists, and inconsistency between the true tumour negatives covered by $G_{1,1}$ and the true tumour negatives covered by KB is high, then $G_{1,1}$ should be revised to reduce $IC_{1,4}$.

Secondly, we give the propositional symbols for the above preconditions 1-11 for Reasoning 3, which are shown in Table 5.

Table 5. Propositional symbols of preconditions for Reasoning 3

Symbol	Meaning
a	IC_1 is given
b	G_1 exists
c	$IC_{1,1}$ is given
d	$IC_{1,2}$ is given
e	$IC_{1,3}$ is given
f	$IC_{1,4}$ is given
g	$G_{1,1}$ exists
h	$G_{1,2}$ exists
i	inconsistency between the false tumour negatives covered by $G_{1,1}$ and the false tumour negatives covered by KB is low
j	$G_{1,1}$ should not be revised to remain $IC_{1,1}$
k	inconsistency between the true tumour positives covered by $G_{1,2}$ and the true tumour positives covered by KB is low
l	$G_{1,2}$ should not be revised to remain $IC_{1,3}$
m	inconsistency between the false tumour positives covered by $G_{1,2}$ and the false tumour positives covered by KB is high
n	then $G_{1,2}$ should be revised to reduce $IC_{1,2}$
o	inconsistency between the true tumour negatives covered by $G_{1,1}$ and the true tumour negatives covered by KB is high
p	$G_{1,1}$ should be revised to reduce $IC_{1,4}$

Thirdly, referring to Table 5, we signify the propositional formalizations of the preconditions 1-11 for Reasoning 3 and Reasoning 3 via the propositional connectives listed in Table 1 as follows.

- | | |
|---|--------------|
| 1) $a \rightarrow b$ | Precondition |
| 2) $a \rightarrow (c \wedge d \wedge e \wedge f)$ | Precondition |
| 3) $b \rightarrow (g \wedge h)$ | Precondition |
| 4) $c \rightarrow i$ | Precondition |
| 5) $(g \wedge i) \rightarrow j$ | Precondition |
| 6) $e \rightarrow k$ | Precondition |
| 7) $(h \wedge k) \rightarrow l$ | Precondition |
| 8) $d \rightarrow m$ | Precondition |

9) $(h \wedge m) \rightarrow n$	Precondition
10) $f \rightarrow o$	Precondition
11) $(g \wedge o) \rightarrow p$	Precondition
$a \rightarrow (j \wedge l \wedge n \wedge p)$	Reasoning 3

Fourthly, we show the validity of Reasoning 3 via the rules for proof of propositional logical reasoning listed in Table 2 as follows.

$\therefore a \rightarrow (j \wedge l \wedge n \wedge p)$	
12) a	Hypothesis
13) $a \rightarrow (g \wedge h)$	1),3); HS
14) $g \wedge h$	13),12); MP
15) g	14); $\wedge -$
16) h	14); $\wedge -$
17) $c \wedge d \wedge e \wedge f$	2),12); MP
18) c	17); $\wedge -$
19) d	17); $\wedge -$
20) e	17); $\wedge -$
21) f	17); $\wedge -$
22) i	4),18); MP
23) $g \wedge i$	15),22); $\wedge +$
24) j	5),23); MP
25) k	6),20); MP
26) $h \wedge k$	16),25); $\wedge +$
27) l	7),26); MP
28) m	8),19); MP
29) $h \wedge m$	16),28); $\wedge +$
30) n	9),29); MP
31) o	10),21); MP
32) $g \wedge o$	15),31); $\wedge +$
33) p	11),32); MP
34) $j \wedge l \wedge n \wedge p$	24),27),30),33); $\wedge +$
35) $a \rightarrow j \wedge l \wedge n \wedge p$	12)-34); Conditional Proof

Since the hypothesis a of the 17) step can be fulfilled by the Reasoning step, Reasoning 3 is proved to be valid.

Proof of Reasoning 4

Reasoning 4. If IC_2 is given, then $G_{2,1}$ should not be revised to remain $IC_{2,1}$, then $G_{2,2}$ should not be revised to remain $IC_{2,3}$, $G_{2,1}$ should be revised to reduce $IC_{2,2}$, and $G_{2,2}$ should be revised to reduce $IC_{2,4}$.

Proof-R4. Firstly, with IC_2 , we have following derived preconditions for Reasoning 4.

1. If IC_2 is given, then G_2 exists. (IC_2 is associated with G_2 in Reasoning)
2. If IC_2 is given, then $IC_{2,1}$ is given, $IC_{2,2}$ is given, $IC_{2,3}$ is given, and $IC_{2,4}$ is given.

3. If G_2 exists, then $G_{2,1}$ exists, and $G_{2,2}$ exists.
4. If $IC_{2,1}$ is given, then inconsistency between the false tumour positives covered by $G_{2,1}$ and the false tumour positives covered by KB is low. (inconsistency estimated by Reasoning)
5. If $G_{2,1}$ exists, and inconsistency between the false tumour positives covered by $G_{2,1}$ and the false tumour positives covered by KB is low, then $G_{2,1}$ should not be revised to remain $IC_{2,1}$.
6. If $IC_{2,3}$ is given, then inconsistency between the true tumour negatives covered by $G_{2,2}$ and the true tumour negatives covered by KB is low. (inconsistency estimated by Reasoning)
7. If $G_{2,2}$ is given, and inconsistency between the true tumour negatives covered by $G_{2,2}$ and the true tumour negatives covered by KB is low, then $G_{2,2}$ should not be revised to remain $IC_{2,3}$.
8. If $IC_{2,2}$ is given, then inconsistency between the false tumour negatives covered by $G_{2,2}$ and the false tumour negatives covered by KB is high. (inconsistency estimated by Reasoning)
9. If $G_{2,2}$ exists, and inconsistency between the false tumour negatives covered by $G_{2,2}$ and the false tumour negatives covered by KB is high, then $G_{2,2}$ should be revised to reduce $IC_{2,2}$.
10. If $IC_{2,4}$ is given, then inconsistency between the true tumour positives covered by $G_{2,1}$ and the true tumour positives covered by KB is high. (inconsistency estimated by Reasoning)
11. If $G_{2,1}$ exists, and inconsistency between the true tumour positives covered by $G_{2,1}$ and the true tumour negatives covered by KB is high, then $G_{2,1}$ should be revised to reduce $IC_{2,4}$.

Secondly, we give the propositional symbols for the above preconditions 1-11 for Reasoning 4, which are shown in Table 6.

Table 6. Propositional symbols of preconditions for Reasoning 4

Symbol	Meaning
a	IC_2 is given
b	G_2 exists
c	$IC_{2,1}$ is given
d	$IC_{2,2}$ is given
e	$IC_{2,3}$ is given
f	$IC_{2,4}$ is given
g	$G_{2,1}$ exists
h	$G_{2,2}$ exists
i	inconsistency between the false tumour positives covered by $G_{2,1}$ and the false tumour positives covered by KB is low
j	$G_{2,1}$ should not be revised to remain $IC_{2,1}$
k	inconsistency between the true tumour negatives covered by $G_{2,2}$ and the true tumour negatives covered by KB is low
l	$G_{2,2}$ should not be revised to remain $IC_{2,3}$

m	inconsistency between the false tumour negatives covered by $G_{2,2}$ and the false tumour negatives covered by KB is high
n	then $G_{2,2}$ should be revised to reduce $IC_{2,2}$
o	inconsistency between the true tumour positives covered by $G_{2,1}$ and the true tumour positives covered by KB is high
p	$G_{2,1}$ should be revised to reduce $IC_{2,4}$

Thirdly, referring to Table 6, we signify the propositional formalizations of the preconditions 1-11 for Reasoning 4 and Reasoning 4 via the propositional connectives listed in Table 1 as follows.

1) $a \rightarrow b$	Precondition
2) $a \rightarrow (c \wedge d \wedge e \wedge f)$	Precondition
3) $b \rightarrow (g \wedge h)$	Precondition
4) $c \rightarrow i$	Precondition
5) $(g \wedge i) \rightarrow j$	Precondition
6) $e \rightarrow k$	Precondition
7) $(h \wedge k) \rightarrow l$	Precondition
8) $d \rightarrow m$	Precondition
9) $(h \wedge m) \rightarrow n$	Precondition
10) $f \rightarrow o$	Precondition
11) $(g \wedge o) \rightarrow p$	Precondition
$a \rightarrow (j \wedge l \wedge n \wedge p)$	Reasoning 3

Fourthly, we show the validity of Reasoning 3 via the rules for proof of propositional logical reasoning listed in Table 2 as follows.

$\therefore a \rightarrow (j \wedge l \wedge n \wedge p)$	
12) a	Hypothesis
13) $a \rightarrow (g \wedge h)$	1),3); HS
14) $g \wedge h$	13),12); MP
15) g	14); $\wedge -$
16) h	14); $\wedge -$
17) $c \wedge d \wedge e \wedge f$	2),12); MP
18) c	17); $\wedge -$
19) d	17); $\wedge -$
20) e	17); $\wedge -$
21) f	17); $\wedge -$
22) i	4),18); MP
23) $g \wedge i$	15),22); $\wedge +$
24) j	5),23); MP
25) k	6),20); MP
26) $h \wedge k$	16),25); $\wedge +$
27) l	7),26); MP
28) m	8),19); MP
29) $h \wedge m$	16),28); $\wedge +$
30) n	9),29); MP

31) o	10),21); MP
32) $g \wedge o$	15),31); $\wedge +$
33) p	11),32); MP
34) $j \wedge l \wedge n \wedge p$	24),27),30),33); $\wedge +$
35) $a \rightarrow j \wedge l \wedge n \wedge p$	12)-34); Conditional Proof

Since the hypothesis a of the 17) step can be fulfilled by the Reasoning step, Reasoning 4 is proved to be valid.

Proof of Reasoning 5

Reasoning 5. *If RG_1 is given and RG_2 is given, then a target (T_1) can be abduced from the union of RG_1 and RG_2 , and T_1 has a high recall of true tumour positives and a high precision of true tumour negatives.*

Proof-R5. Firstly, with RG_1 and RG_2 , we have following derived preconditions for Reasoning 5.

1. If RG_1 is given, then RG_1 is equivalent to $G_{1,1}$: pixels of IS_1 outside the polygons of NLS_1 are tumour negatives. (revised grounding produced by Abduction)
2. If RG_2 is given, then RG_2 is equivalent to $G_{1,2}$: pixels of IS_1 inside the polygons of NLS_1 are tumour positives. (revised grounding produced by Abduction)
3. If RG_1 is equivalent to $G_{1,1}$: pixels of IS_1 outside the polygons of NLS_1 are tumour negatives and RG_2 is equivalent to $G_{1,2}$: pixels of IS_1 inside the polygons of NLS_1 are tumour positives, then RG_1 indicates where are tumour negatives of IS_1 and RG_2 indicates where are tumour positives of IS_1 .
4. If RG_1 indicates where are tumour negatives of IS_1 and RG_2 indicates where are tumour positives of IS_1 , then a target (T_1) can be abduced from the union of RG_1 and RG_2 .
5. If T_1 can be abduced from the union of RG_1 and RG_2 , RG_1 is equivalent to $G_{1,1}$: pixels of IS_1 outside the polygons of NLS_1 are tumour negatives, and RG_2 is equivalent to $G_{1,2}$ pixels of IS_1 inside the polygons of NLS_1 are tumour positives, then the recall of T_1 for true tumour positives can be denoted by true tumour positives covered by $G_{1,2}$ ($TP(G_{1,2})$) dividing the sum of $TP(G_{1,2})$ and false tumour negatives covered by $G_{1,1}$ ($FN(G_{1,1})$), i.e., $TP(G_{1,2}) / (TP(G_{1,2}) + FN(G_{1,1}))$; and the precision of T_1 for true tumour negatives can be denoted by true tumor negatives covered by $G_{1,1}$ ($TN(G_{1,1})$) dividing the sum of $TN(G_{1,1})$ and $FN(G_{1,1})$, i.e., $TN(G_{1,1}) / (TN(G_{1,1}) + FN(G_{1,1}))$.
6. If RG_1 is given, then $G_{1,1}$ should not be revised to remain $IC_{1,1}$. (revised grounding produced by Abduction is only associated with corresponding grounding revision in Abduction)
7. If $G_{1,1}$ should not be revised to remain $IC_{1,1}$, then $G_{1,1}$ should not be revised to remain the fact that inconsistency between $FN(G_{1,1})$ and false tumour negatives covered by KB ($FN(KB)$) is low. (fact contained in $IC_{1,1}$)

8. If $G_{1,1}$ is not revised to remain the fact that inconsistency between $FN(G_{1,1})$ and $FN(KB)$ is low, then $FN(G_{1,1})$ can be regarded as close to $FN(KB)$.
9. If $FN(G_{1,1})$ can be regarded as close to $FN(KB)$, then $FN(G_{1,1})$ can be regarded as close to 0.
10. If $FN(G_{1,1})$ can be regarded as close to 0, then tumour negatives covered by $G_{1,1}$ can be regarded as true tumor negatives.
11. If tumour negatives covered by $G_{1,1}$ can be regarded as true tumor negatives, then $TN(G_{1,1})$ can be regarded as a constant positive integer.
12. If RG_2 is given, then $G_{1,2}$ should not be revised to remain $IC_{1,3}$. (revised grounding produced by Abduction is only associated with corresponding grounding revision in Abduction)
13. If $G_{1,2}$ should not be revised to remain $IC_{1,3}$, then $G_{1,2}$ should not be revised to remain the fact that inconsistency between $TP(G_{1,2})$ and true tumour positives covered by KB ($TP(KB)$) is low.
14. If $G_{1,2}$ should not be revised to remain the fact that inconsistency between $TP(G_{1,2})$ and $TP(KB)$ is low, then $TP(G_{1,2})$ can be regarded as close to $TP(KB)$.
15. If $TP(G_{1,2})$ can be regarded as close to $TP(KB)$, $TP(G_{1,2})$ can be regarded as a constant positive integer.
16. If $TP(G_{1,2})$ can be regarded as a constant positive integer and $FN(G_{1,1})$ can be regarded as close to 0, and the recall of T_1 for true tumour positives can be denoted by $TP(G_{1,2}) / (TP(G_{1,2}) + FN(G_{1,1}))$, then the recall of T_1 for true tumour positives is close to 1.
17. If $TN(G_{1,1})$ can be regarded as a constant positive integer, $FN(G_{1,1})$ can be regarded as close to 0, and the precision of T_1 for true tumour negatives can be denoted by $TN(G_{1,1}) / (TN(G_{1,1}) + FN(G_{1,1}))$, then the precision of T_1 for true tumour negatives is close to 1.
18. If the recall of T_1 for true tumour positives is close to 1 and the precision of T_1 for true tumour negatives is close to 1, then T_1 has a high recall of true tumour positives and a high precision of true tumour negatives.

Secondly, we give the propositional symbols for the above preconditions 1-18 for Reasoning 5, which are shown in Table 7.

Table 7. Propositional symbols of preconditions for Reasoning 5

Symbol	Meaning
a	RG_1 is given
b	RG_1 is equivalent to $G_{1,1}$: pixels of IS_1 outside the polygons of NLS_1 are tumour negatives
c	RG_2 is given
d	RG_2 is equivalent to $G_{1,2}$ pixels of IS_1 inside the polygons of NLS_1 are tumour positives
e	RG_1 indicates where are tumour negatives of IS_1
f	RG_2 indicates where are tumour positives of IS_1
g	a target (T_1) can be abducted from the union of RG_1 and RG_2

<i>h</i>	the recall of T_1 for true tumour positives can be denoted by true tumour positives covered by $G_{1,2}$ ($TP(G_{1,2})$) dividing the sum of $TP(G_{1,2})$ and false tumour negatives covered by $G_{1,1}$ ($FN(G_{1,1})$), i.e., $TP(G_{1,2})/(TP(G_{1,2})+FN(G_{1,1}))$
<i>i</i>	the precision of T_1 for true tumour negatives can be denoted by true tumor negatives covered by $G_{1,1}$ ($TN(G_{1,1})$) dividing the sum of $TN(G_{1,1})$ and $FN(G_{1,1})$, i.e., $TN(G_{1,1})/(TN(G_{1,1})+FN(G_{1,1}))$
<i>j</i>	$G_{1,1}$ should not be revised to remain $IC_{1,1}$
<i>k</i>	$G_{1,1}$ should not be revised to remain the fact that inconsistency between $FN(G_{1,1})$ and false tumour negatives covered by KB ($FN(KB)$) is low
<i>l</i>	$FN(G_{1,1})$ can be regarded as close to $FN(KB)$
<i>m</i>	$FN(G_{1,1})$ can be regarded as close to 0
<i>n</i>	tumour negatives covered by $G_{1,1}$ can be regarded as true tumor negatives
<i>o</i>	$TN(G_{1,1})$ can be regarded as a constant positive integer
<i>p</i>	$G_{1,2}$ should not be revised to remain $IC_{1,3}$
<i>q</i>	$G_{1,2}$ should not be revised to remain the fact that inconsistency between $TP(G_{1,2})$ and true tumour positives covered by KB ($TP(KB)$) is low
<i>r</i>	$TP(G_{1,2})$ can be regarded as close to $TP(KB)$
<i>s</i>	$TP(G_{1,2})$ can be regarded as a constant positive integer
<i>t</i>	the recall of T_1 ($TP(G_{1,2})/(TP(G_{1,2})+FN(G_{1,1}))$) for true tumour positives is close to 1
<i>u</i>	the precision of T_1 ($TN(G_{1,1})/(TN(G_{1,1})+FN(G_{1,1}))$) for true tumour negatives is close to 1
<i>v</i>	T_1 has a high recall of true tumour positives and a high precision of true tumour negatives

Thirdly, referring to Table 7, we signify the propositional formalizations of the preconditions 1-18 for Reasoning 5 and Reasoning 5 via the propositional connectives listed in Table 1 as follows.

1) $a \rightarrow b$	Precondition
2) $c \rightarrow d$	Precondition
3) $(b \wedge d) \rightarrow (e \wedge f)$	Precondition
4) $(e \wedge f) \rightarrow g$	Precondition
5) $(g \wedge b \wedge d) \rightarrow (h \wedge i)$	Precondition
6) $a \rightarrow j$	Precondition
7) $j \rightarrow k$	Precondition
8) $k \rightarrow l$	Precondition
9) $l \rightarrow m$	Precondition
10) $m \rightarrow n$	Precondition
11) $n \rightarrow o$	Precondition
12) $b \rightarrow p$	Precondition
13) $p \rightarrow q$	Precondition
14) $q \rightarrow r$	Precondition
15) $r \rightarrow s$	Precondition
16) $(s \wedge m \wedge h) \rightarrow t$	Precondition
17) $(o \wedge m \wedge i) \rightarrow u$	Precondition
18) $(t \wedge u) \rightarrow v$	Precondition
$(a \wedge c) \rightarrow (g \wedge v)$	Reasoning 5

Fourthly, we show the validity of Reasoning 5 via the rules for proof of propositional logical reasoning listed in Table 2 as follows.

$\therefore (a \wedge c) \rightarrow (g \wedge v)$

19) $a \wedge c$	Hypothesis
20) a	19); $\wedge -$
21) c	19); $\wedge -$
22) b	1),20); MP
23) d	2),21); MP
24) $b \wedge d$	22),23); $\wedge +$
25) $(b \wedge d) \rightarrow g$	3),24); HS
26) g	25),24); MP
27) $g \wedge b \wedge d$	26),24); $\wedge +$
28) $h \wedge i$	5),27); MP
29) h	28); $\wedge -$
30) i	28); $\wedge -$
31) $a \rightarrow m$	6),7),8),9); HS
32) m	31),20); MP
33) $m \rightarrow o$	10),11); HS
34) o	33),32); MP
35) $b \rightarrow s$	12),13),14),15); HS
36) s	35),22); MP
37) $s \wedge m \wedge h$	36),32),29); $\wedge +$
38) $o \wedge m \wedge i$	34),32),30); $\wedge +$
39) t	16),37); MP
40) u	17),38); MP
41) $t \wedge u$	39),40); $\wedge +$
42) v	18),41); MP
43) $g \wedge v$	26),42); $\wedge +$
48) $(a \wedge c) \rightarrow (g \wedge v)$	19)-43); Conditional Proof

Since the hypothesis $a \wedge c$ of the 19) step can be fulfilled by the Abduction step, Reasoning 5 is proved to be valid.

Proof of Reasoning 6

Reasoning 6. *If RG_5 is given and RG_6 is given, then a target (T_2) can be abduced from the union of RG_5 and RG_6 , and T_2 has a high precision of true tumour positives and a high recall of true tumour negatives.*

Proof-R6. Firstly, with RG_5 and RG_6 , we have following derived preconditions for Reasoning 6.

1. If RG_5 is given, then RG_5 is equivalent to $G_{2,1}$: pixels of IS_2 inside the polygons of NLS_2 are tumour positives. (revised grounding produced by Abduction)
2. If RG_6 is given, then RG_6 is equivalent to $G_{2,2}$: pixels of IS_2 outside the polygons of NLS_2 are tumour negatives. (revised grounding produced by Abduction)

3. If RG_5 is equivalent to $G_{2,1}$: pixels of IS_2 inside the polygons of NLS_2 are tumour positives and RG_6 is equivalent to $G_{2,2}$: pixels of IS_2 outside the polygons of NLS_2 are tumour negatives, then RG_5 indicates where are tumour positives of IS_2 and RG_6 indicates where are tumour negatives of IS_2 .
4. If RG_5 indicates where are tumour positives of IS_2 and RG_6 indicates where are tumour negatives of IS_2 , then a target (T_2) can be abduced from the union of RG_5 and RG_6 .
5. If T_2 can be abduced from the union of RG_5 and RG_6 , RG_5 is equivalent to $G_{2,1}$: pixels of IS_2 inside the polygons of NLS_2 are tumour positives, and RG_6 is equivalent to $G_{2,2}$ pixels of IS_2 outside the polygons of NLS_2 are tumour negatives, then the precision of T_2 for true tumour positives can be denoted by true tumour positives covered by $G_{2,1}$ ($TP(G_{2,1})$) dividing the sum of $TP(G_{2,1})$ and false tumour positives covered by $G_{2,1}$ ($FP(G_{2,1})$), i.e., $TP(G_{2,1}) / (TP(G_{2,1}) + FP(G_{2,1}))$; and the recall of T_2 for true tumour negatives can be denoted by true tumor negatives covered by $G_{2,2}$ ($TN(G_{2,2})$) dividing the sum of $TN(G_{2,2})$ and $FP(G_{2,1})$, i.e., $TN(G_{2,2}) / (TN(G_{2,2}) + FP(G_{2,1}))$.
6. If RG_5 is given, then $G_{2,1}$ should not be revised to remain $IC_{2,1}$. (revised grounding produced by Abduction is only associated with corresponding grounding revision in Abduction)
7. If $G_{2,1}$ should not be revised to remain $IC_{2,1}$, then $G_{2,1}$ should not be revised to remain the fact that inconsistency between $FP(G_{2,1})$ and false tumour positives covered by KB ($FP(KB)$) is low. (fact contained in $IC_{2,1}$)
8. If $G_{2,1}$ should not be revised to remain the fact that inconsistency between $FP(G_{2,1})$ and $FP(KB)$ is low, then $FP(G_{2,1})$ can be regarded as close to $FP(KB)$.
9. If $FP(G_{2,1})$ can be regarded as close to $FP(KB)$, then $FP(G_{2,1})$ can be regarded as close to 0.
10. If $FP(G_{2,1})$ can be regarded as close to 0, then tumour positives covered by $G_{2,1}$ can be regarded as true tumor positives.
11. If tumour positives covered by $G_{2,1}$ can be regarded as true tumor positives, then $TP(G_{2,1})$ can be regarded as a constant positive integer.
12. If RG_6 is given, then $G_{2,2}$ should not be revised to remain $IC_{2,3}$. (revised grounding produced by Abduction is only associated with corresponding grounding revision in Abduction)
13. If $G_{2,2}$ should not be revised to remain $IC_{2,3}$, then $G_{2,2}$ should not be revised to remain the fact that inconsistency between $TN(G_{2,2})$ and true tumour negatives covered by KB ($TN(KB)$) is low.
14. If $G_{2,2}$ should not be revised to remain the fact that inconsistency between $TN(G_{2,2})$ and $TN(KB)$ is low, then $TN(G_{2,2})$ can be regarded as close to $TN(KB)$.
15. If $TN(G_{2,2})$ can be regarded as close to $TN(KB)$, $TN(G_{2,2})$ can be regarded as a constant positive integer.

16. If $TP(G_{2,1})$ can be regarded as a constant positive integer, $FP(G_{2,1})$ can be regarded as close to 0, and the precision of T_2 for true tumour positives can be denoted by $TP(G_{2,1})/(TP(G_{2,1})+FP(G_{2,1}))$, then the precision of T_2 for true tumour positives is close to 1.
17. If $TN(G_{2,2})$ can be regarded as a constant positive integer, $FP(G_{2,1})$ can be regarded as close to 0, and the recall of T_2 for true tumour negatives can be denoted by $TN(G_{2,2})/(TN(G_{2,2})+FP(G_{2,1}))$, then the recall of T_2 for true tumour negatives is close to 1.
18. If the precision of T_2 for true tumour positives is close to 1 and the precision of T_2 for true tumour negatives is close to 1, then T_2 has a high precision of true tumour positives and a high recall of true tumour negatives.

Secondly, we give the propositional symbols for the above preconditions 1-18 for Reasoning 6, which are shown in Table 8.

Table 8. Propositional symbols of preconditions for Reasoning 6

Symbol	Meaning
a	RG_5 is given
b	RG_5 is equivalent to $G_{2,1}$: pixels of IS_2 inside the polygons of NLS_2 are tumour positives
c	RG_6 is given
d	RG_6 is equivalent to $G_{2,2}$: pixels of IS_2 outside the polygons of NLS_2 are tumour negatives
e	RG_5 indicates where are tumour positives of IS_2
f	RG_6 indicates where are tumour negatives of IS_2
g	a target (T_2) can be abducted from the union of RG_5 and RG_6
h	the precision of T_2 for true tumour positives can be denoted by true tumour positives covered by $G_{2,1}$ ($TP(G_{2,1})$) dividing the sum of $TP(G_{2,1})$ and false tumour positives covered by $G_{2,1}$ ($FP(G_{2,1})$), i.e., $TP(G_{2,1})/(TP(G_{2,1})+FP(G_{2,1}))$
i	the recall of T_2 for true tumour negatives can be denoted by true tumor negatives covered by $G_{2,2}$ ($TN(G_{2,2})$) dividing the sum of $TN(G_{2,2})$ and $FP(G_{2,1})$, i.e., $TN(G_{2,2})/(TN(G_{2,2})+FP(G_{2,1}))$
j	$G_{2,1}$ should not be revised to remain $IC_{2,1}$
k	$G_{2,1}$ should not be revised to remain the fact that inconsistency between $FP(G_{2,1})$ and false tumour positives covered by KB ($FP(KB)$) is low
l	$FP(G_{2,1})$ can be regarded as close to $FP(KB)$
m	$FP(G_{2,1})$ can be regarded as close to 0
n	tumour positives covered by $G_{2,1}$ can be regarded as true tumor positives
o	$TP(G_{2,1})$ can be regarded as a constant positive integer
p	$G_{2,2}$ should not be revised to remain $IC_{2,3}$
q	$G_{2,2}$ should not be revised to remain the fact that inconsistency between $TN(G_{2,2})$ and true tumour negatives covered by KB ($TN(KB)$) is low
r	$TN(G_{2,2})$ can be regarded as close to $TN(KB)$
s	$TN(G_{2,2})$ can be regarded as a constant positive integer
t	the precision of T_2 for true tumour positives is close to 1
u	the recall of T_2 for true tumour negatives is close to 1
v	T_2 has a high precision of true tumour positives and a high recall of true tumour negatives

Thirdly, referring to Table 8, we signify the propositional formalizations of the preconditions 1-18 for Reasoning 6 and Reasoning 6 via the propositional connectives listed in Table 1 as follows.

1) $a \rightarrow b$	Precondition
2) $c \rightarrow d$	Precondition
3) $(b \wedge d) \rightarrow (e \wedge f)$	Precondition
4) $(e \wedge f) \rightarrow g$	Precondition
5) $(g \wedge b \wedge d) \rightarrow (h \wedge i)$	Precondition
6) $a \rightarrow j$	Precondition
7) $j \rightarrow k$	Precondition
8) $k \rightarrow l$	Precondition
9) $l \rightarrow m$	Precondition
10) $m \rightarrow n$	Precondition
11) $n \rightarrow o$	Precondition
12) $b \rightarrow p$	Precondition
13) $p \rightarrow q$	Precondition
14) $q \rightarrow r$	Precondition
15) $r \rightarrow s$	Precondition
16) $(o \wedge m \wedge h) \rightarrow t$	Precondition
17) $(s \wedge m \wedge i) \rightarrow u$	Precondition
18) $(t \wedge u) \rightarrow v$	Precondition
$(a \wedge c) \rightarrow (g \wedge v)$	Reasoning 6

Fourthly, we show the validity of Reasoning 6 via the rules for proof of propositional logical reasoning listed in Table 2 as follows.

$\therefore (a \wedge c) \rightarrow (g \wedge v)$	
19) $a \wedge c$	Hypothesis
20) a	19); $\wedge -$
21) c	19); $\wedge -$
22) b	1),20); MP
23) d	2),21); MP
24) $b \wedge d$	22),23); $\wedge +$
25) $(b \wedge d) \rightarrow g$	3),24); HS
26) g	25),24); MP
27) $g \wedge b \wedge d$	26),24); $\wedge +$
28) $h \wedge i$	5),27); MP
29) h	28); $\wedge -$
30) i	28); $\wedge -$
31) $a \rightarrow m$	6),7),8),9); HS
32) m	31),20); MP
33) $m \rightarrow o$	10),11); HS
34) o	33),32); MP
35) $b \rightarrow s$	12),13),14),15); HS
36) s	35),22); MP

37) $o \wedge m \wedge h$	36),32),29); $\wedge +$
38) $s \wedge m \wedge i$	34),32),30); $\wedge +$
39) t	16),37); MP
40) u	17),38); MP
41) $t \wedge u$	39),40); $\wedge +$
42) v	18),41); MP
43) $g \wedge v$	26),42); $\wedge +$
48) $(a \wedge c) \rightarrow (g \wedge v)$	19)-43); Conditional Proof

Since the hypothesis $a \wedge c$ of the 19) step can be fulfilled by the Abduction step, Reasoning 6 is proved to be valid.

Proof of Reasoning 7

Reasoning 7. *If the target (T_1) abducted from the union of RG_1 and RG_2 is given, RG_3 is given and RG_4 is given, then T_1 has a low precision of true tumour positives and a low recall of true tumour negatives.*

Proof-R7. Firstly, with T_1 , RG_3 and RG_4 , we have following derived preconditions for Reasoning 7.

1. If the target (T_1) abducted from the union of RG_1 and RG_2 is given, then T_1 is abducted based on $G_{1,1}$: pixels of IS_1 outside the polygons of NLS_1 are tumour negatives and $G_{1,2}$: pixels of IS_1 inside the polygons of NLS_1 are tumour positives. (revised grounding produced by Abduction)
2. If the target (T_1) abducted from the union of RG_1 and RG_2 is given, then the fact that T_1 has a high recall of true tumour positives and a high precision of true tumour negatives exists. (Reasoning 5)
3. If RG_3 is given, then RG_3 is equivalent to the fact that pixels of IS_1 outside the polygons of NLS_1 are not exactly true tumour negatives. (revised grounding produced by Abduction)
4. If RG_4 is given, then RG_4 is equivalent to the fact that pixels of IS_1 inside the polygons of NLS_1 are not exactly true tumour positives. (revised grounding produced by Abduction)
5. If T_1 is abducted based on $G_{1,1}$: pixels of IS_1 outside the polygons of NLS_1 are tumour negatives and $G_{1,2}$: pixels of IS_1 inside the polygons of NLS_1 are tumour positives, the fact that T_1 has a high recall of true tumour positives and a high precision of true tumour negatives exists, RG_3 is equivalent to the fact that pixels of IS_1 outside the polygons of NLS_1 are not exactly true tumour negatives, and RG_4 is equivalent to the fact that pixels of IS_1 inside the polygons of NLS_1 are not exactly true tumour positives, then many true tumour negatives are taken as as tumour positives by $G_{1,2}$.
6. If many true tumour negatives are taken as tumour positives by $G_{1,2}$, then false tumour positives are covered by $G_{1,2}$ ($FP(G_{1,2})$) can be regarded as large.
7. If $FP(G_{1,2})$ can be regarded as large, and then T_1 has a low precision of true tumour positives and a low recall of true tumour negatives.

Secondly, we give the propositional symbols for the above preconditions 1-7 for Reasoning 7, which are shown in Table 9.

Table 9. Propositional symbols of preconditions for Reasoning 7

Symbol	Meaning
a	the target (T_1) abducted from the union of RG_1 and RG_2 is given
b	RG_3 is given
c	RG_4 is given
d	T_1 is abducted based on $G_{1,1}$: pixels of IS_1 outside the polygons of NLS_1 are tumour negatives and $G_{1,2}$: pixels of IS_1 inside the polygons of NLS_1 are tumour positives
e	the fact that T_1 has a high recall of true tumour positives and a high precision of true tumour negatives exists
f	RG_3 is equivalent to the fact that pixels of IS_1 outside the polygons of NLS_1 are not exactly true tumour negatives
g	RG_4 is equivalent to the fact that pixels of IS_1 inside the polygons of NLS_1 are not exactly true tumour positives
h	many true tumour negatives are taken as as tumour positives by $G_{1,2}$
i	false tumour positives are covered by $G_{1,2}$ ($FP(G_{1,2})$) can be regarded as large
v	T_1 has a low precision of true tumour positives and a low recall of true tumour negatives

Thirdly, referring to Table 9, we signify the propositional formalizations of the preconditions 1-7 for Reasoning 7 and Reasoning 7 via the propositional connectives listed in Table 1 as follows.

- | | |
|---|--------------|
| 1) $a \rightarrow d$ | Precondition |
| 2) $a \rightarrow e$ | Precondition |
| 3) $b \rightarrow f$ | Precondition |
| 4) $c \rightarrow g$ | Precondition |
| 5) $(d \wedge e \wedge f \wedge g) \rightarrow h$ | Precondition |
| 6) $h \rightarrow i$ | Precondition |
| 7) $i \rightarrow v$ | Precondition |
| $(a \wedge b \wedge c) \rightarrow v$ | Reasoning 7 |

Fourthly, we show the validity of Reasoning 7 via the rules for proof of propositional logical reasoning listed in Table 2 as follows.

$\therefore (a \wedge b \wedge c) \rightarrow v$

- | | |
|------------------------------------|-----------------------------|
| 8) $a \wedge b \wedge c$ | Hypothesis |
| 9) a | 8); $\wedge -$ |
| 10) b | 8); $\wedge -$ |
| 11) c | 8); $\wedge -$ |
| 12) d | 1),9); MP |
| 13) e | 2),9); MP |
| 14) f | 3),10); MP |
| 15) g | 4),11); MP |
| 16) $d \wedge e \wedge f \wedge g$ | 12),13),14),15); $\wedge +$ |
| 17) h | 5),16); MP |
| 18) $h \rightarrow v$ | 6),7); HS |

- 19) v 18),17); MP
 20) $(a \wedge b \wedge c) \rightarrow v$ 8)-19); Conditional Proof

Since the hypothesis $a \wedge b \wedge c$ of the 8) step can be fulfilled by Reasoning 5 and the Abduction step, Reasoning 7 is proved to be valid.

Proof of Reasoning 8

Reasoning 8. *If the target (T_2) abducted from the union of RG_5 and RG_6 is given, RG_7 is given and RG_8 is given, then T_2 has a low recall of true tumour positives and a low precision of true tumour negatives.*

Proof-R8. Firstly, with T_2 , RG_7 and RG_8 , we have following derived preconditions for Reasoning 8.

1. If the target (T_2) abducted from the union of RG_5 and RG_6 is given, then T_2 is abducted based on $G_{2,1}$: pixels of IS_2 inside the polygons of NLS_2 are tumour positives and $G_{2,2}$: pixels of IS_2 outside the polygons of NLS_2 are tumour negatives. (revised grounding produced by Abduction)
2. If the target (T_2) abducted from the union of RG_5 and RG_6 is given, then the fact that T_2 has a high precision of true tumour positives and a high recall of true tumour negatives exists. (Reasoning 6)
3. If RG_7 is given, then RG_7 is equivalent to the fact that pixels of IS_1 inside the polygons of NLS_1 are not exactly true tumour positives. (revised grounding produced by Abduction)
4. If RG_8 is given, then RG_8 is equivalent to the fact that pixels of IS_1 outside the polygons of NLS_1 are not exactly true tumour negatives. (revised grounding produced by Abduction)
5. If T_2 is abducted based on $G_{2,1}$: pixels of IS_2 inside the polygons of NLS_2 are tumour positives and $G_{2,2}$: pixels of IS_2 outside the polygons of NLS_2 are tumour negatives, the fact that T_2 has a high precision of true tumour positives and a high recall of true tumour negatives exists, RG_7 is equivalent to the fact that pixels of IS_1 inside the polygons of NLS_1 are not exactly true tumour positives, and RG_8 is equivalent to the fact that pixels of IS_1 outside the polygons of NLS_1 are not exactly true tumour negatives, then many true tumour positives are taken as as tumour negatives by $G_{2,2}$.
6. If many true tumour positives are taken as as tumour negatives by $G_{2,2}$, then false tumour negatives are covered by $G_{2,2}$ ($FN(G_{2,2})$) can be regarded as large.
7. If $FN(G_{2,2})$ can be regarded as large, and then T_2 has a low recall of true tumour positives and a low precision of true tumour negatives.

Secondly, we give the propositional symbols for the above preconditions 1-7 for Reasoning 8, which are shown in Table 10.

Table 10. Propositional symbols of preconditions for Reasoning 8

Symbol	Meaning
a	the target (T_2) abducted from the union of RG_5 and RG_6 is given
b	RG_7 is given

<i>c</i>	RG_8 is given
<i>d</i>	T_2 is abducted based on $G_{2,1}$: pixels of IS_2 inside the polygons of NLS_2 are tumour positives and $G_{2,2}$: pixels of IS_2 outside the polygons of NLS_2 are tumour negatives
<i>e</i>	the fact that T_2 has a high precision of true tumour positives and a high recall of true tumour negatives exists
<i>f</i>	RG_7 is equivalent to the fact that pixels of IS_1 inside the polygons of NLS_1 are not exactly true tumour positives
<i>g</i>	If RG_8 is given, then RG_8 is equivalent to the fact that pixels of IS_1 outside the polygons of NLS_1 are not exactly true tumour negatives
<i>h</i>	many true tumour positives are taken as as tumour negatives by $G_{2,2}$
<i>i</i>	false tumour negatives are covered by $G_{2,2}$ ($FN(G_{2,2})$) can be regarded as large
<i>j</i>	T_2 has a low recall of true tumour positives and a low precision of true tumour negatives

Thirdly, referring to Table 10, we signify the propositional formalizations of the preconditions 1-7 for Reasoning 8 and Reasoning 8 via the propositional connectives listed in Table 1 as follows.

1) $a \rightarrow d$	Precondition
2) $a \rightarrow e$	Precondition
3) $b \rightarrow f$	Precondition
4) $c \rightarrow g$	Precondition
5) $(d \wedge e \wedge f \wedge g) \rightarrow h$	Precondition
6) $h \rightarrow i$	Precondition
7) $i \rightarrow j$	Precondition
$(a \wedge b \wedge c) \rightarrow j$	Reasoning 8

Fourthly, we show the validity of Reasoning 8 via the rules for proof of propositional logical reasoning listed in Table 2 as follows.

$\therefore (a \wedge b \wedge c) \rightarrow j$	
8) $a \wedge b \wedge c$	Hypothesis
9) a	8); $\wedge -$
10) b	8); $\wedge -$
11) c	8); $\wedge -$
12) d	1),9); MP
13) e	2),9); MP
14) f	3),10); MP
15) g	4),11); MP
16) $d \wedge e \wedge f \wedge g$	12),13),14),15); $\wedge +$
17) h	5),16); MP
18) $h \rightarrow j$	6),7); HS
19) j	18),17); MP
20) $(a \wedge b \wedge c) \rightarrow j$	8)-19); Conditional Proof

Since the hypothesis $a \wedge b \wedge c$ of the 8) step can be fulfilled by Reasoning 5 and the Abduction step, Reasoning 8 is proved to be valid.

Proof of Reasoning 9

Reasoning 9. *If the target (T_1) abduced from the union of RG_1 and RG_2 is given and the target (T_2) abduced from the union of RG_5 and RG_6 is given, then a target (T_3) can be abduced by improving T_1 with T_2 , a target (T_4) can be abduced by improving T_2 with T_1 , T_3 can have a relatively higher precision of true tumour positives than T_1 and a relatively higher recall of true tumour negatives than T_1 , and T_4 can have a relatively higher recall of true tumour positives than T_2 and a relatively higher precision of true tumour negatives than T_2 .*

Proof-R9. Firstly, with T_1 and T_2 , we have following derived preconditions for Reasoning 9.

1. If the target (T_1) abduced from the union of RG_1 and RG_2 is given, then T_1 has a high recall of true tumour positives and a high precision of true tumour negatives and T_1 has a low precision of true tumour positives and a low recall of true tumour negatives. (Reasoning 5 and Reasoning 7)
2. If the target (T_2) abduced from the union of RG_5 and RG_6 is given, T_2 has a high precision of true tumour positives and a high recall of true tumour negatives and T_2 has a low recall of true tumour positives and a low precision of true tumour negatives. (Reasoning 6 and Reasoning 8)
3. If T_1 has a low precision of true tumour positives and a low recall of true tumour negatives and T_2 has a high precision of true tumour positives and a high recall of true tumour negatives, then T_2 is complementary to T_1 to represent the true target.
4. If T_2 is complementary to T_1 to represent the true target, then a target (T_3) can be abduced by improving T_1 with T_2 .
5. If T_3 can be abduced by improving T_1 with T_2 , T_2 has a high precision of true tumour positives and a high recall of true tumour negatives, and T_1 has a low precision of true tumour positives and a low recall of true tumour negatives, then T_3 can have a relatively higher precision of true tumour positives than T_1 and a relatively higher recall of true tumour negatives than T_1 .
6. If T_2 has a low recall of true tumour positives and a low precision of true tumour negatives and T_1 has a high recall of true tumour positives and a high precision of true tumour negatives, then T_1 is complementary to T_2 to represent the true target.
7. If T_1 is complementary to T_2 to represent the true target, then a target (T_4) can be abduced by improving T_2 with T_1 .
8. If T_4 can be abduced by improving T_2 with T_1 , T_1 has a high recall of true tumour positives and a high precision of true tumour negatives, and T_2 has a low recall of true tumour positives and a low precision of true tumour negatives, then T_4 can have a relatively higher recall of true tumour positives than T_2 and a relatively higher precision of true tumour negatives than T_2 .

Secondly, we give the propositional symbols for the above preconditions 1-8 for Reasoning 9, which are shown in Table 11.

Table 11. Propositional symbols of preconditions for Reasoning 9

Symbol	Meaning
<i>a</i>	the target (T_1) abduced from the union of RG_1 and RG_2 is given
<i>b</i>	the target (T_2) abduced from the union of RG_5 and RG_6 is given
<i>c</i>	T_1 has a high recall of true tumour positives and a high precision of true tumour negatives
<i>d</i>	T_1 has a low precision of true tumour positives and a low recall of true tumour negatives
<i>e</i>	T_2 has a high precision of true tumour positives and a high recall of true tumour negatives
<i>f</i>	T_2 has a low recall of true tumour positives and a low precision of true tumour negatives
<i>g</i>	T_2 is complementary to T_1 to represent the true target
<i>h</i>	a target (T_3) can be abduced by improving T_1 with T_2
<i>i</i>	T_3 can have a relatively higher precision of true tumour positives than T_1 and a relatively higher recall of true tumour negatives than T_1
<i>j</i>	T_1 is complementary to T_2 to represent the true target
<i>k</i>	a target (T_4) can be abduced by improving T_2 with T_1
<i>l</i>	T_4 can have a relatively higher recall of true tumour positives than T_2 and a relatively higher precision of true tumour negatives than T_2

Thirdly, referring to Table 11, we signify the propositional formalizations of the preconditions 1-8 for Reasoning 9 and Reasoning 9 via the propositional connectives listed in Table 1 as follows.

1) $a \rightarrow (c \wedge d)$	Precondition
2) $b \rightarrow (e \wedge f)$	Precondition
3) $(d \wedge e) \rightarrow g$	Precondition
4) $g \rightarrow h$	Precondition
5) $(g \wedge e \wedge d) \rightarrow i$	Precondition
6) $(f \wedge c) \rightarrow j$	Precondition
7) $j \rightarrow k$	Precondition
8) $(k \wedge c \wedge f) \rightarrow l$	Precondition
$(a \wedge b) \rightarrow (h \wedge k \wedge i \wedge l)$	Reasoning 9

Fourthly, we show the validity of Reasoning 9 via the rules for proof of propositional logical reasoning listed in Table 2 as follows.

$\therefore (a \wedge b) \rightarrow (h \wedge k \wedge i \wedge l)$	
9) $a \wedge b$	Hypothesis
10) a	9); $\wedge -$
11) b	9); $\wedge -$
12) $c \wedge d$	1),10); MP
13) $e \wedge f$	2),11); MP
14) c	12); $\wedge -$
15) d	12); $\wedge -$
16) e	13); $\wedge -$
17) f	13); $\wedge -$
18) $d \wedge e$	15),16); $\wedge +$
19) g	3),18); MP
20) h	4),19); MP

21) $g \wedge e \wedge d$	19),16),15); $\wedge +$
22) i	21),5); MP
23) $f \wedge c$	17),14); $\wedge +$
24) j	6),23); MP
25) k	7),24); MP
26) $k \wedge c \wedge f$	25),14),17); $\wedge +$
27) l	8),26); MP
28) $h \wedge k \wedge i \wedge l$	20),25),22),27); $\wedge +$
29) $(a \wedge b) \rightarrow (h \wedge k \wedge i \wedge l)$	9)-28); Conditional Proof

Since the hypothesis $a \wedge b$ of the 9) step can be fulfilled by Reasoning 5 and Reasoning 6, Reasoning 9 is proved to be valid.

Proof of Reasoning 10

Reasoning 10. *If T_1 is given and T_3 is given, then T_1 and T_3 can be combined to approximate the true target for IS_1 .*

Proof-R10. Firstly, with T_1 and T_3 , we have following derived preconditions for Reasoning 10.

1. If T_1 is given and T_3 is given, then T_1 and T_3 are both corresponding to IS_1 .
2. If T_1 is given, then T_1 has a high recall of true tumour positives and a high precision of true tumour negatives and T_1 has a low precision of true tumour positives and a low recall of true tumour negatives. (Reasoning 5 and Reasoning 7)
3. If T_3 is given, then T_3 can have a relatively higher precision of true tumour positives than T_1 and a relatively higher recall of true tumour negatives than T_1 . (Reasoning 9)
4. If T_1 has a high recall of true tumour positives and a high precision of true tumour negatives and T_3 can have a relatively higher precision of true tumour positives than T_1 and a relatively higher recall of true tumour negatives than T_1 , then T_1 and T_3 can be combined to possess a high recall of true tumour positives and a high precision of true tumour negatives while having a relatively higher precision of true tumour positives and a relatively higher recall of true tumour negatives.
5. If T_1 and T_3 can be combined to possess a high recall of true tumour positives and a high precision of true tumour negatives while having a relatively higher precision of true tumour positives and a relatively higher recall of true tumour negatives, and T_1 and T_3 are both corresponding to IS_1 , then T_1 and T_3 can be combined to approximate the true target for IS_1 .

Secondly, we give the propositional symbols for the above preconditions 1-5 for Reasoning 10, which are shown in Table 12.

Table 12. Propositional symbols of preconditions for Reasoning 10

Symbol	Meaning
a	T_1 is given

<i>b</i>	T_3 is given
<i>c</i>	T_1 and T_3 are both corresponding to IS_1
<i>d</i>	T_1 has a high recall of true tumour positives and a high precision of true tumour negatives and T_1 has a low precision of true tumour positives and a low recall of true tumour negatives
<i>e</i>	T_3 can have a relatively higher precision of true tumour positives than T_1 and a relatively higher recall of true tumour negatives than T_1
<i>f</i>	T_1 and T_3 can be combined to possess a high recall of true tumour positives and a high precision of true tumour negatives while having a relatively higher precision of true tumour positives and a relatively higher recall of true tumour negatives
<i>g</i>	T_1 and T_3 can be combined to approximate the true target for IS_1

Thirdly, referring to Table 12, we signify the propositional formalizations of the preconditions 1-5 for Reasoning 10 and Reasoning 10 via the propositional connectives listed in Table 1 as follows.

1) $(a \wedge b) \rightarrow c$	Precondition
2) $a \rightarrow d$	Precondition
3) $b \rightarrow e$	Precondition
4) $(d \wedge e) \rightarrow f$	Precondition
5) $(f \wedge c) \rightarrow g$	Precondition
$(a \wedge b) \rightarrow g$	Reasoning 10

Fourthly, we show the validity of Reasoning 10 via the rules for proof of propositional logical reasoning listed in Table 2 as follows.

$\therefore (a \wedge b) \rightarrow g$	
6) $a \wedge b$	Hypothesis
7) a	6); $\wedge -$
8) b	6); $\wedge -$
9) c	1),6); MP
10) d	2),7); MP
11) e	3),8); MP
12) $d \wedge e$	10),11); $\wedge +$
13) f	4),12); MP
14) $f \wedge c$	13),9); $\wedge +$
15) g	5),14); MP
16) $(a \wedge b) \rightarrow g$	6)-15); Conditional Proof

Since the hypothesis $a \wedge b$ of the 6) step can be fulfilled by the Target Abduce step, Reasoning 10 is proved to be valid.

Proof of Reasoning 11

Reasoning 11. If T_2 is given and T_4 is given, then T_2 and T_4 can be combined to approximate the true target for NS_2 .

Proof-R11. Firstly, with T_2 and T_4 , we have following derived preconditions for Reasoning 11.

1. If T_2 is given and T_4 is given, then T_2 and T_4 are both corresponding to IS_2 .

2. If T_2 is given, then T_2 has a high precision of true tumour positives and a high recall of true tumour negatives and T_2 has a low recall of true tumour positives and a low precision of true tumour negatives. (Reasoning 6 and Reasoning 8)
3. If T_4 is given, then T_4 can have a relatively higher recall of true tumour positives than T_2 and a relatively higher precision of true tumour negatives than T_2 . (Reasoning 9)
4. If T_2 has a high precision of true tumour positives and a high recall of true tumour negatives and T_2 has a low recall of true tumour positives and a low precision of true tumour negatives, and T_4 can have a relatively higher recall of true tumour positives than T_2 and a relatively higher precision of true tumour negatives than T_2 , then T_2 and T_4 can be combined to possess a high precision of true tumour positives and a high recall of true tumour negatives while having a relatively higher recall of true tumour positives and a relatively higher precision of true tumour negatives.
5. If T_2 and T_4 can be combined to possess a high precision of true tumour positives and a high recall of true tumour negatives while having a relatively higher recall of true tumour positives and a relatively higher precision of true tumour negatives, and T_2 and T_4 are both corresponding to IS_2 , then T_2 and T_4 can be combined to approximate the true target for IS_2 .

Secondly, we give the propositional symbols for the above preconditions 1-5 for Reasoning 11, which are shown in Table 13.

Table 13. Propositional symbols of preconditions for Reasoning 11

Symbol	Meaning
a	T_2 is given
b	T_4 is given
c	T_2 and T_4 are both corresponding to IS_2
d	T_2 has a high precision of true tumour positives and a high recall of true tumour negatives and T_2 has a low recall of true tumour positives and a low precision of true tumour negatives
e	T_4 can have a relatively higher recall of true tumour positives than T_2 and a relatively higher precision of true tumour negatives than T_2
f	T_2 and T_4 can be combined to possess a high precision of true tumour positives and a high recall of true tumour negatives while having a relatively higher recall of true tumour positives and a relatively higher precision of true tumour negatives
g	T_2 and T_4 can be combined to approximate the true target for IS_2

Thirdly, referring to Table 13, we signify the propositional formalizations of the preconditions 1-5 for Reasoning 11 and Reasoning 11 via the propositional connectives listed in Table 1 as follows.

- | | |
|---------------------------------|--------------|
| 1) $(a \wedge b) \rightarrow c$ | Precondition |
| 2) $a \rightarrow d$ | Precondition |
| 3) $b \rightarrow e$ | Precondition |
| 4) $(d \wedge e) \rightarrow f$ | Precondition |
| 5) $(f \wedge c) \rightarrow g$ | Precondition |
| $(a \wedge b) \rightarrow g$ | Reasoning 10 |

Fourthly, we show the validity of Reasoning 11 via the rules for proof of propositional logical reasoning listed in Table 2 as follows.

$\therefore (a \wedge b) \rightarrow g$

6) $a \wedge b$	Hypothesis
7) a	6); $\wedge -$
8) b	6); $\wedge -$
9) c	1),6); MP
10) d	2),7); MP
11) e	3),8); MP
12) $d \wedge e$	10),11); $\wedge +$
13) f	4),12); MP
14) $f \wedge c$	13),9); $\wedge +$
15) g	5),14); MP
16) $(a \wedge b) \rightarrow g$	6)-15); Conditional Proof

Since the hypothesis $a \wedge b$ of the 6) step can be fulfilled by the Target Abduce step, Reasoning 11 is proved to be valid.

Supplementary 2

Multiple Targets Abduced from DiNS

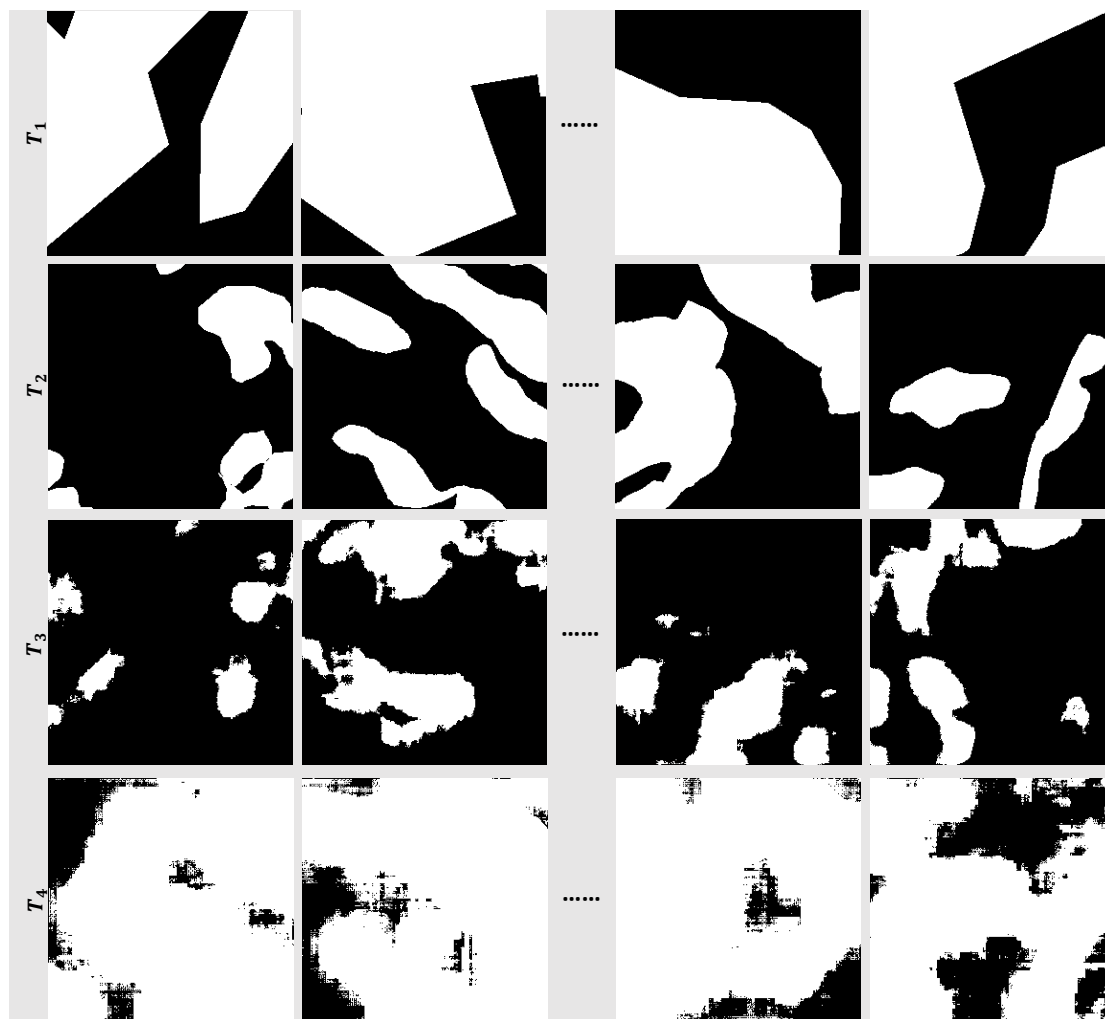


Fig. 1. Examples of multiple targets abduced from the diverse noisy samples provided for tumour segmentation in HE-stained pre-treatment biopsy images.

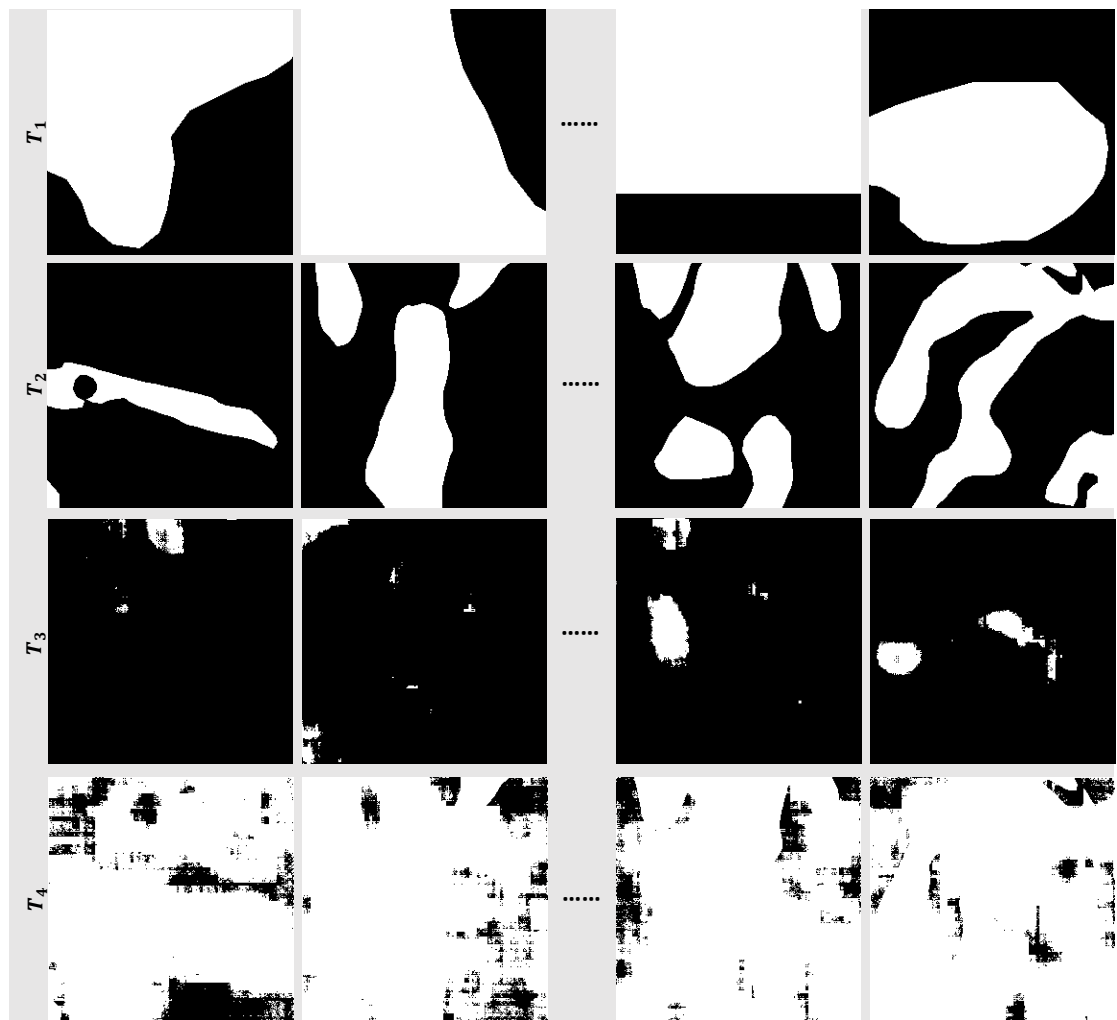


Fig. 2. Examples of multiple targets abducted from the diverse noisy samples provided for tumour segmentation in HE-stained post-treatment surgical resection images.

Rearranged Multiple Targets

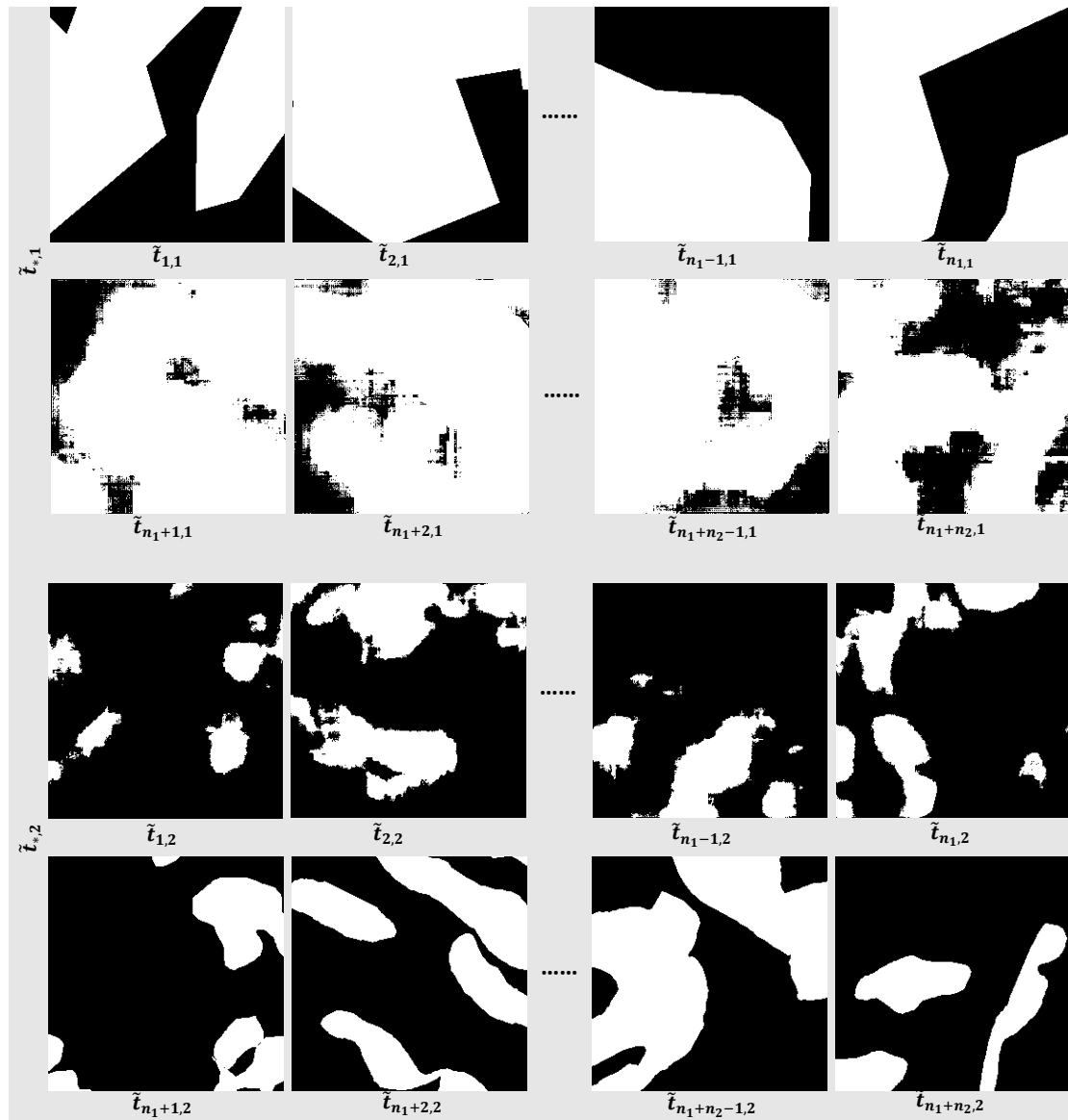


Fig. 3. Examples of rearranged multiple targets corresponding to Fig. 1.

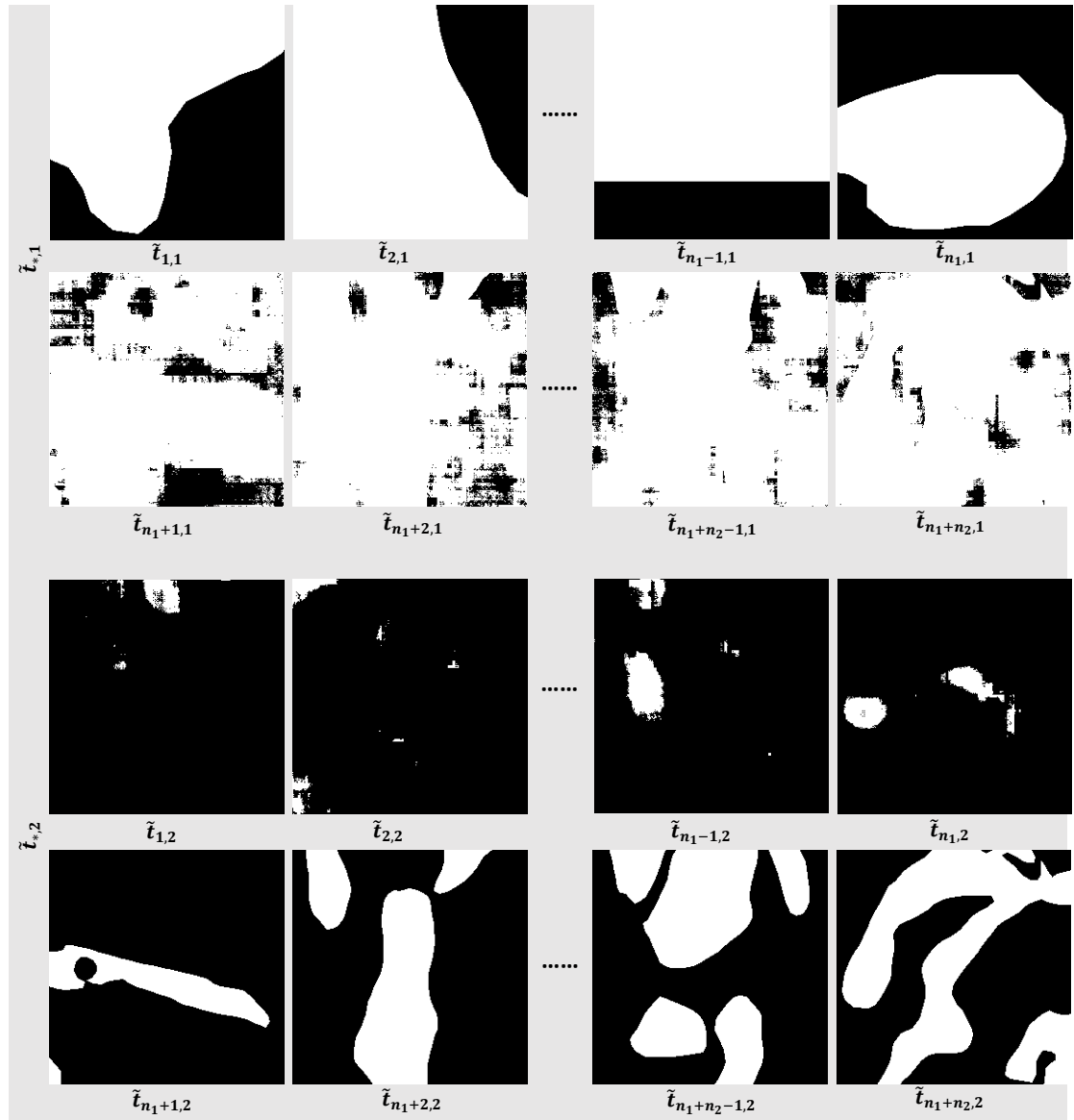


Fig. 4. Examples of rearranged multiple targets corresponding to Fig. 2.